HAND2 FUNCTION WITHIN NON-CARDIOMYOCYTES REGULATES CARDIAC MORPHOGENESIS AND PERFORMANCE

Nathan J. VanDusen

Submitted to the faculty of the University Graduate School
in partial fulfillment of the requirements
for the degree
Doctor of Philosophy
in the Department of Medical and Molecular Genetics,
Indiana University

August 2014

Accepted by the Graduate Faculty, Indiana University, in partial fulfillment of the requirements for the degree of Doctor of Philosophy.

Anthony B. Firulli, Ph.D., Chair

Brittney-Shea Herbert, Ph.D.

Doctoral Committee

Lindsey D. Mayo, Ph.D.

May 28, 2014

Weinian Shou, Ph.D.

ACKNOWLEDGEMENTS

During my tenure as a graduate student numerous people have invested time, energy, and resources into my training. I would first like to thank Dr. Anthony Firulli for his substantial efforts to foster my development as a scientist. His insights have greatly contributed to the success of my studies, and the lessons I've learned under his mentorship will be integral to my success in future endeavors. Additionally, I am thankful for the advice and constructive criticisms received from my committee members: Dr. Brittney-Shea Herbert, Dr. Lindsey Mayo, and Dr. Weinian Shou. The Wells Center Cardiac Group has also provided helpful discussion and feedback on several occasions. I would like to thank all past and present members of the Firulli lab, particularly Dr. Josh Vincentz, Beth Firulli, and Dr. Ralston Barnes, who all played a large role in my training. Their technical expertise and wealth of experience spared me countless hours of troubleshooting and frustration. Similarly, I thank Danny Carney for consistently providing a wide range of supporting services. Dr. Michael Rubart provided valuable technical assistance with heart rate measurements, while Dr. Bin Zhou generously provided *Nfatc1*^{Cre} mice. Similarly, Dr. Thomas Coate provided EfnB2 flox mice, while Dr. Jose Luis De La Pompa and Dr. Joaquim Grego-Bessa provided Hand2 expression data in *RBPJk* knockout embryos. This work was funded by a pre-doctoral fellowship from the American Heart Association (12PRE11700006).

On a more personal note, I would also like to acknowledge my family, who have provided constant love, inspiration, and encouragement. Without them I

would never have been in a position to pursue this degree, much less complete it. Furthermore, I am very thankful for the love, patience, and support received from my amazing wife, Natalie. She is always there to celebrate with me when things are going well, and to listen and encourage when things are not. Perhaps more importantly, she constantly reminds me of what is most important in life, helping me view my academic struggles and successes from a greater perspective. I have been blessed to have many others in my life who, in one way or another, have aided and supported me on my journey to this degree. While not mentioned here, your contributions are very much appreciated.

Nathan J. VanDusen

HAND2 FUNCTION WITHIN NON-CARDIOMYOCYTES REGULATES CARDIAC MORPHOGENESIS AND PERFORMANCE

The heart is a complex organ that is composed of numerous cell types, which must integrate their programs for proper specification, differentiation, and cardiac morphogenesis. During cardiac development the basic helix-loop-helix transcription factor Hand2 is dynamically expressed within the endocardium and extra-cardiac lineages such as the epicardium, cardiac neural crest cells (cNCCs), and NCC derived components of the autonomic nervous system. To investigate Hand2 function within these populations we utilized multiple murine *Hand2* Conditional Knockout (*H2CKO*) genetic models. These studies establish for the first time a functional requirement for Hand2 within the endocardium, as several distinct phenotypes including hypotrabeculation, tricuspid atresia, aberrant septation, and precocious coronary development are observed in endocardial *H2CKOs*. Molecular analyses reveal that endocardial Hand2 functions within the Notch signaling pathway to regulate expression of *Nrg1*, which encodes a crucial secreted growth factor. Furthermore, we demonstrate that Notch signaling regulates coronary angiogenesis via Hand2 mediated modulation of Vegf signaling.

Hand2 is strongly expressed within midgestation NCC and endocardium derived cardiac cushion mesenchyme. To ascertain the function of Hand2 within these cells we employed the *Periostin Cre* (*Postn-Cre*), which marks cushion mesenchyme, a small subset of the epicardium, and components of the

autonomic nervous system, to conditionally ablate *Hand2.* We find that *Postn-Cre H2CKOs* die shortly after birth despite a lack of cardiac structural defects. Gene expression analyses demonstrate that *Postn-Cre* ablates *Hand2* from the adrenal medulla, causing downregulation of *Dopamine Beta Hydroxylase* (*Dbh*), a gene encoding a crucial catecholaminergic biosynthetic enzyme. Electrocardiograms demonstrate that 3-day postnatal *Postn-Cre H2CKO* pups exhibit significantly slower heart rates than control littermates. In conjunction with the aforementioned gene expression analyses, these results indicate that loss of Hand2 function within the adrenal medulla results in a catecholamine deficiency and subsequent heart failure.

Anthony B. Firulli, Ph.D., Chair

TABLE OF CONTENTS

Chapter I

Heart Development Overview

A. Introduction to Cardiogenesis and bHLH Transcription Factors

The heart is a complex organ whose origins initiate from several mesodermal progenitor populations during early stages of embryonic development. The complete organ is composed of a number of cell types, which include an endothelial lining of the lumen (the endocardium), cardiomyocytes which provide the mechanical function of the pump, an outer epicardial layer, and neural crest cells (NCCs) which form the great arteries connecting the pump to systemic and pulmonary components of the vasculature. What follows is an overview of the cell types, developmental paradigms, and molecular mechanisms which underlie mammalian cardiogenesis.

The complex process of cardiac development begins with the specification of the anterior lateral mesoderm, termed the cardiac crescent, which contributes to the first heart field (FHF) myocardium and a portion of the endocardium (Brand, 2003; Lyons, 1996; Olson and Srivastava, 1996; Prall et al., 2007; Sucov, 1998). These cells first undergo migration to the embryo midline to form a linear heart tube (Fig. 1). This heart tube is composed of two cell layers, an inner layer composed of endocardial (endothelial) cells and the outer being cardiomyocytes. The space between the layers is filled with extracellular matrix (ECM) commonly referred to as cardiac jelly. This substance is primarily composed of secreted molecules such as proteoglycans and glycosaminoglycans which provide structural support and facilitate cell-cell

communication (DeLaughter et al., 2011). After initial heart tube formation, pharyngeal mesoderm that lies anterior to the cardiac crescent, which is termed the second heart field (SHF; yellow in Fig. 1 marks tissues that receive a SHF contribution), migrates into the heart tube from both the rostral and caudal ends, adding endocardium and myocardium to the now expanding heart (for review see Kelly, 2005; Nakajima, 2010; Vincent and Buckingham, 2010). As a consequence of the SHF cell contribution, the tube loops to the right and balloons to form common atrial and ventricular chambers, adjoined by a single common atrioventricular canal (AVC). Further expansion and remodeling (accompanied by atrial, ventricular, and AVC septation) results in a four chambered heart complete with two distinct AVCs; the right AVC contains the tricuspid valve and the left the mitral valve. Similarly, cardiac outflow tract (OFT) cushions are invaded by migratory NCCs. Once populated, these cushions will septate the OFT and remodel into pulmonary and aortic valves.

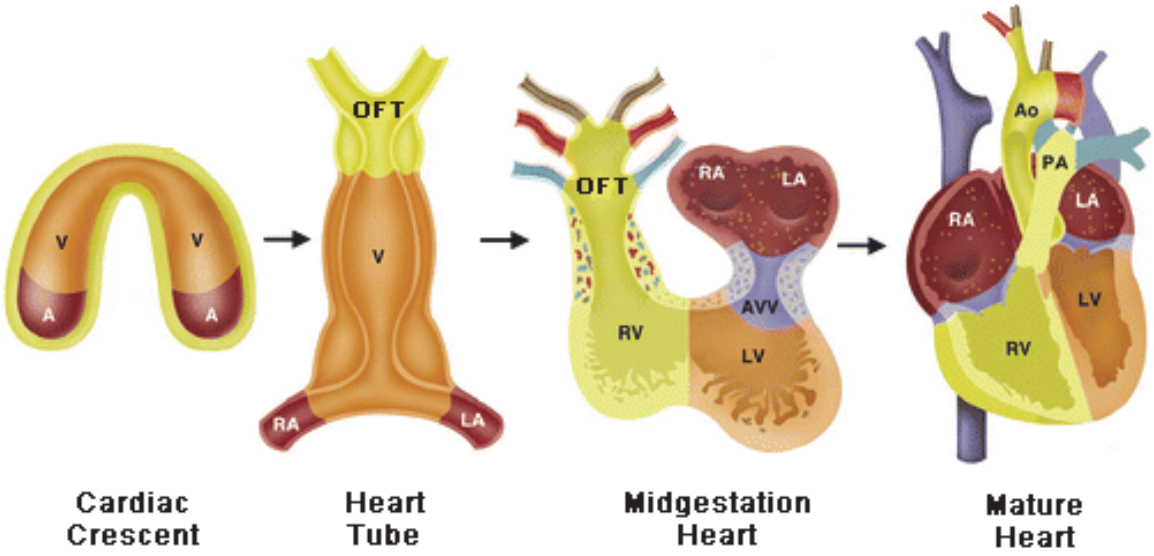

Figure 1: Cardiac Development

Diagram of cardiac development. Ventricle, V; atria, A; right atria, RA; left atria, LA; outflow tract, OFT; atrioventricular valve, AVV; aorta, Ao; pulmonary artery, PA. FHF derived structures are colored in orange; tissues that the SHF contributes to are colored in yellow.

(Adapted from Srivastava, 2006)

B. Endocardium

The endocardium and myocardium both derive from the anterior lateral splanchnic mesoderm which forms the cardiac crescent (Fig. 1; Srivastava, 2006; Smith and Bader, 2007), and second heart field progenitors. The heart tube will grow and expand due to SHF and cardiac NCC (cNCC) contributions. Paracrine signaling originating from the myocardium induces endocardial cells in the future AV canal and outflow tract (OFT) to increase ECM synthesis, producing local swelling. These protrusions, termed cardiac cushions, are populated when a subset of endocardial cells undergo epithelial-to-mesenchymal transition (EMT) and invade. Conditional gene deletion studies, in addition to *in vitro* data, suggest that myocardial Bone Morphogenetic Protein (Bmp) production is the primary initiator of cardiac cushion formation. Mice lacking myocardial *Bmp2* or endocardial *Bmp receptor-1a* expression exhibit defective EMT (Ma et al., 2005). Additional factors demonstrated to be necessary for endocardial EMT, including *Notch1*, *Msx2*, and members of the *Tgfβ* signaling pathway, are downregulated in models of aberrant Bmp signaling (Combs and Yutzey, 2009; Ma et al., 2005). Notch1 encodes a transmembrane receptor that acts as a crucial signaling component in a wide variety of cell types and organ systems. Genetic deletion of *Notch1* or its functional partner *RBPJk* does not affect initial ECM deposition, but results in EMT failure (Timmerman et al., 2004). Endothelial deletion of cell-cell adhesion regulator β-catenin also results in EMT failure, implicating Wnt signaling in murine cardiac cushion formation. Post-EMT, the ECM and mesenchymal cells of the cushions are remodeled from their unorganized

primitive state into the highly ordered structures that constitute mature heart valves (Combs and Yutzey, 2009). Given the complex combination of EMT, ECM secretion, and remodeling that must occur in a precise spatiotemporal manner for correct valve development, it is not surprising that valve related deficiencies are present in a majority of all heart defects (Barnett and Desgrosellier, 2003).

As the endocardial subset of cells undergoing EMT invades the cardiac cushions, signaling factors originating from the endocardium cue expansion and proper patterning of the myocardium. These factors operate within Vegf, Notch, Ephrin, Bmp, Wnt, and Neuregulin signaling (Armstrong, 2004), with extensive cross-talk between pathways. Current models suggest that activated Vegf receptors (VegfRs) initiate Notch signaling via upregulation of the Notch ligand Dll4 (Wythe et al., 2013). Endocardial Notch1 then activates endocardial production of the secreted growth factor Neuregulin1 (*Nrg1*) via direct regulation of EphrinB2 (*EfnB2*), a transmembrane ligand (Grego-Bessa et al., 2007). Significantly, specific mechanisms of *Nrg1* regulation by Ephrin signaling have not been proposed. In addition to *Nrg1* regulation, endocardial Notch1 also activates expression of myocardial *Bmp10* through a poorly understood independent mechanism. Recent studies demonstrate that *Nrg1* and *Bmp10* have unique but equally important roles in the process of trabeculation. Nrg1 induces specification of the trabecular myocardium, and upon specification Bmp10 drives proliferation (Fig. 2). Genetic deletion of *Notch1*, *EfnB2*, *Nrg1*, or *Bmp10* all result in loss of cardiac trabeculation (Chen et al., 2004; Grego-Bessa et al., 2007).

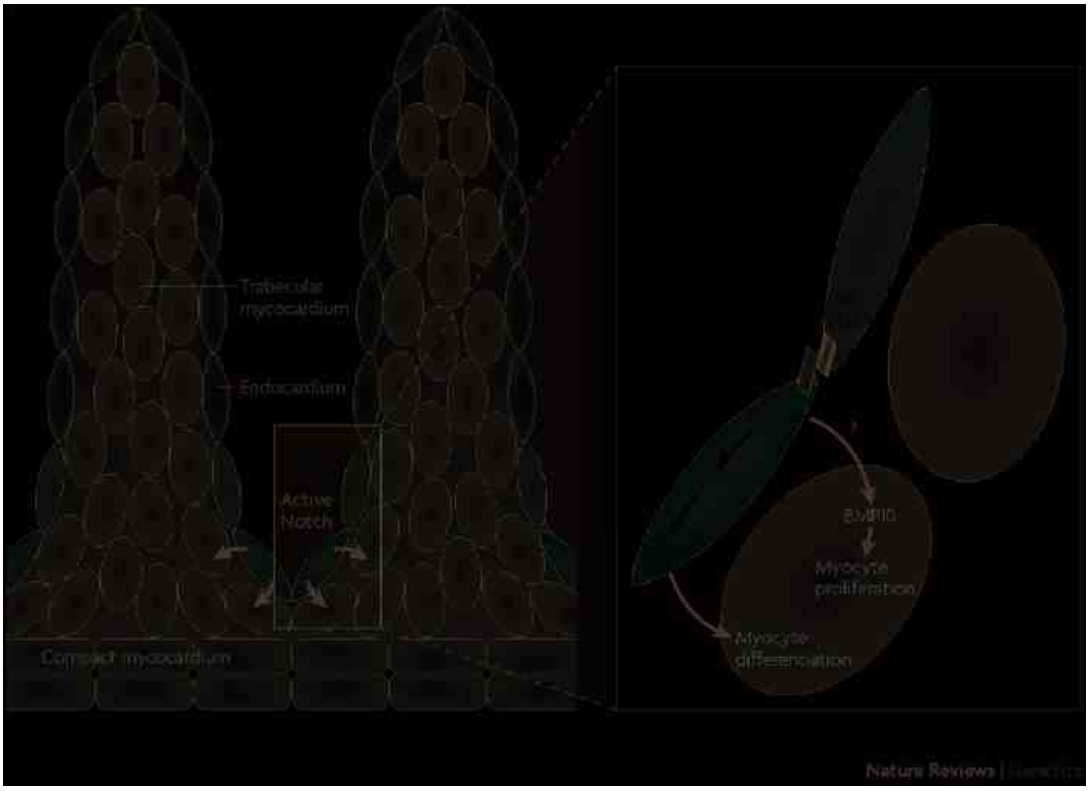

Figure 2: Notch signaling and trabeculation

Schematic showing endocardial signaling events that direct myocardial trabeculation.

(High and Epstein, 2008)

C. Neural Crest Cells

NCCs arise from ectoderm at the lateral edge of the neural plate, and extend along the dorsal aspect of the neural tube from the mid-diencephalon through the caudal portion of the developing embryo (Creazzo et al., 1998; Huang and Saint-Jeannet, 2004). These ectodermal cells are induced to undergo EMT by a combination of Wnt, Bmp, and Fgf signaling, resulting in delamination from the neuroepithelium and migration into the caudal pharyngeal arches (Huang and Saint-Jeannet, 2004). The cNCCs are a small vagal subpopulation of NCC which migrate into the heart (Stoller and Epstein, 2005). During heart development, cNCC populations make essential contributions via migration into the third, fourth, and sixth pharyngeal arches, where they will contribute to remodeling of the aortic arch arteries and cardiac outflow tract (Stoller and Epstein, 2005). Upon arrival, cNCC differentiate into smooth muscle cells and pericytes, which participate in septation of the embryonic OFT tract into pulmonary and aortic components (Kirby et al., 1983; Nelms and Labosky, 2010; Snider et al., 2007). Subsequently, the majority of neural crest derived cells in the aorticopulmonary septum undergo apoptosis (Poelmann and Gittenberger-de Groot, 1999). The remodeling of the aortic arch arteries is a complex programmed process involving the regression of some arterial structures and the persistence of others. Initially, each pharyngeal arch contains a symmetrically branched artery originating from the single vessel of the early OFT. Through the action of cNCC, this symmetrical arterial network is remodeled into the predominantly left sided vascular pattern seen in adults (Snider et al., 2007). This

coordinated regression has been associated with Tgfβ2 signaling, as Tgfβ2$^{-/-}$ mice display aberrant apoptosis in both fourth arch arteries, while lacking normal apoptosis in the right dorsal aorta (Molin et al., 2002).

If a significant portion of the cNCC fail to reach the OFT, as a result of cell death or a defect in migration, a common congenital abnormality known as persistent truncus arteriosus (PTA) results. In PTA, the OFT fails to septate and results in a single large common vessel. The high incidence of PTA in congenital disorders such as Di George Syndrome implicates NCC dysfunction in the pathology of these diseases (Van Mierop and Kutsche, 1986). Other NCC-related OFT abnormalities include double outlet right ventricle (DORV) and overriding aorta. These defects result from the incorrect alignment of the aorta with the left ventricle (LV). During proper alignment, the cardiac tube loops to bring the OFT (distal end) into close proximity with the inflow tract (proximal end). The OFT undergoes septation such that the newly formed aorta gets placed between the left and right AVC in a process called wedging, which ultimately results in correct alignment of the aorta over the developing LV and the pulmonary artery over the right ventricle (Allwork and Anderson, 1978; Kirby and Waldo, 1995). If wedging occurs incorrectly, the aorta is often displaced to the right, resulting in either DORV, where both the pulmonary artery and aorta are connected to the right ventricle, or in overriding aorta, where the aorta partially connects to each ventricle. Experimental evidence suggests that OFT septation must occur properly to avoid looping defects which result in improper wedging (Yelbuz et al., 2002). Indeed, the OFT septum in genetic models of cNCC

ablation is often either misaligned with the ventricular septum or incompletely developed (Creazzo et al., 1998).

Although the processes of aortic arch artery and OFT remodeling are still not well understood, genetic loss-of-function models have revealed a number of proteins that are involved in the regulation of cNCC. These include the transcription factor Pax3, which is thought to play a role in NCC progenitor formation (Olaopa et al., 2011), the Wnt/Dvl downstream effector Pitx2 (Kioussi et al., 2002), and winged helix-turn-helix factor Ets1 (Gao et al., 2010). Loss of these factors results in aortic arch artery and OFT defects such as DORV, PTA, and transposition of the great arteries (TGA). While transcriptional regulation of the genes discussed above clearly affects cNCC movement and function, many other proteins in the surrounding environment have a non-cell autonomous role to play. For instance *Tbx1*, which is affected by a chromosomal deletion of 22q11.2 causing Di George Syndrome, is not expressed in NCC, but can be found in tissue of the pharyngeal arches adjacent to NCC (Snider et al., 2007). Despite this fact, haploinsufficient mice display major defects in the development of the aortic arch arteries, indicating that cNCC take important cues relating to migration and morphogenesis from their environment (Garg et al., 2001; Hutson and Kirby, 2003; Snider et al., 2007). Indeed, the forkhead/winged helix transcription factors Foxc1 and Foxc2 are expressed in endothelial tissues surrounding NCCs and have been shown to be essential for proper OFT and arch artery morphogenesis (Hutson and Kirby, 2003). These factors most likely act through transcriptional regulation of secreted molecules, such as Endothelin-

1, which is produced by endothelial cells neighboring NCCs (Kurihara et al., 1995). Additional factors that mediate cell-cell signaling within NCC populations include the gap junction protein Connexin43 (*Cx43*; Reaume et al., 1995), the secreted ligand Semaphorin3c (*Sema3C*; Feiner et al., 2001), and its receptor Plexin A2 (Brown et al., 2001; Hutson and Kirby, 2003). Research on these factors has demonstrated the critical nature of cell-cell interactions and communication during cNCC development. While this fact is well appreciated, future studies are still needed to fully reveal and define regulatory mechanisms.

Many cell types and structures including facial bones, the peripheral nervous system (PNS), and endocrine system receive heavy contributions from NCC and have been extensively reviewed (Creuzet, 2009; Gross and Hanken, 2008; Heude et al., 2010; Wang et al., 2011). The autonomic nervous system (ANS), a branch of the PNS, is of particular importance, as its components have been demonstrated to regulate cardiac function (Kishi, 2012). The ANS is composed of sympathetic and parasympathetic neurons, as well as medullary cells of the adrenal gland. NCC sympathoadrenal precursors migrate ventrally from the neural tube towards the dorsal aorta, which coordinates NCC migration through the release of Bmp. Bmp in turn activates production of additional cytokines and growth factors, such as Stromal Cell-Derived Factor-1 (*Sdf1*) and Neuregulin1 (*Nrg1*), which regulate sympathoadrenal cell morphogenesis (Saito et al., 2012). This molecular cascade guides NCC migration, but also activates a poorly defined transcriptional program that drives the specification of the adrenal and sympathetic lineages. Once specified, neurons of the sympathetic ganglia

and cells of the adrenal medulla produce enzymes necessary for catecholamine biosynthesis. These include Tyrosine Hydroxylase (*Th*), the enzyme responsible for conversion of L-tyrosine to a dopamine precursor, Dopamine Beta Hydroxylase (*Dbh*), responsible for conversion of dopamine to norepinephrine, and Phenylethanolamine N-Methyltransferase (*Pnmt)*, which converts norepinephrine to epinephrine. The catecholamines epinephrine and norepinephrine are then released into the bloodstream to regulate heart rate, blood pressure, blood vessel constriction, and other critical aspects of cardiovascular function (Axelrod and Reisine, 1984; Fung et al., 2008).

D. Epicardium

The epicardium originates from a cluster of cells at the venous pole of the heart termed the proepicardial organ (PEO). Due to a combination of Fibroblast Growth Factor (Fgf) and Bmp signaling, aggregates of cells from within the PEO's mesothelial projections undergo an EMT event and migrate to the surface of the developing ventricles, ultimately covering the entire surface of the heart in a caudal to cranial fashion (Lie-Venema et al., 2007). In mice, this process is initiated by E9.0 and is complete by approximately E11.0 (Komiyama et al., 1987). Once the epicardial cells have enveloped the heart, multiple waves of epicardial cells undergo a secondary EMT and migrate into the adjacent myocardium. Similar to cNCC EMT, this event is regulated by a combination of paracrine growth factors and proteins such as Slug, Snail, and E-cadherin, with good evidence for Ets1, Ets2, α4 integrin, and WT1 involvement (Lie-Venema et

al., 2007). Growth factors implicated in epicardial cell EMT include Fgf, Pdgf, Tgfβ, and Vegf (Morabito et al., 2001). Upon entering the myocardium, epicardial progenitor derived cells (EPDCs) are guided to their final destinations by signaling mechanisms that are not yet well understood, but are known to involve Pdgf-β, Pdgfrβ, Tbx5, Thymosin β4, and the Ets transcription factors. EPDCs will ultimately take up position in interstitial spaces of the ventricles and atria, contributing to the cardiac fibroblast lineage, smooth muscle of the coronary vasculature, and cardiac cushions (Lie-Venema et al., 2007). In chick, there is good evidence for EPDC contribution to the coronary endothelium (Perez-Pomares et al., 2002), although this has not been substantiated in mice. While controversial, evidence also exists for limited EPDC contribution to the myocardium (Zhou et al., 2008).

E. Twist Family bHLH Factors

In humans, the bHLH superfamily is known to contain over 100 factors, which play crucial roles both during and after embryonic development, and in the etiology of many diseases (Jones, 2004). bHLH transcription factors share two common domains. The first is a motif consisting of basic residues that facilitate DNA binding to a canonical consensus sequence. Many variations in the consensus sequence have been demonstrated, depending on the specific bHLH factor, but CANNTG is a commonly bound sequence, and is termed an E-box. The second is the helix-loop-helix domain, which contains two amphipathic α-helices separated by a loop of variable length. The HLH domains facilitate

dimerization via juxtaposition of the hydrophobic faces of the α-helices from two different bHLH proteins. Dimer formation allows for correct positioning of the two basic domains that directly bind DNA (for extensive bHLH review see Massari and Murre 2000). Of the hundreds of proteins which contain a bHLH motif (Atchley and Fitch, 1997) the Twist subclass of bHLH proteins is a small group of transcription factors that contain high amino acid identity, with particularly high conservation within the bHLH domain (Castanon and Baylies, 2002). In mammals, the Twist family of bHLH transcription factors is composed of six members: *Twist1*, *Twist2*, *Hand1*, *Hand2*, *Paraxis*, and *Scleraxis;* although homologs of these factors can also be found in phylogenetically distant species such as flies, flatworms, and jellyfish (Barnes and Firulli, 2009; Gitelman, 2007). While Twist proteins show great diversity in their expression profiles, and thus in the developmental processes they regulate, Twist family members have several key characteristics in common. It is has been well established that Twist bHLH proteins functionally operate either as homodimers or heterodimers with other bHLH factors (Barnes and Firulli, 2009; Castanon and Baylies, 2002; Castanon et al., 2001; Firulli et al., 2000; Tapanes-Castillo and Baylies, 2004). Heterodimerization can occur with other Twist members, but also commonly involves non-Twist bHLH proteins, such as the ubiquitously expressed E-proteins. Dimer partner choice has been shown to dictate factor function (Castanon et al., 2001; Firulli et al., 2003; Firulli et al., 2005; Firulli et al., 2007) and is affected by elements such as gene dosage, which can alter the ratio of Twist family proteins present within the transcription factor pool inside each cell.

Phosphoregulation also plays multiple roles in the regulatory process. The phosphorylation of conserved threonine and serine residues within the first α-helix of Twist family bHLH factors has been demonstrated to affect dimerization partner choice and therefore function. Phosphoregulation can also alter intracellular localization of Twist factors thus modifying dimer capacity (Barnes and Firulli, 2009; Firulli et al., 2003; Firulli et al., 2005; Firulli et al., 2007). In order to understand the role Twist proteins play in developmental pathways such as cardiogenesis, these observations establish that one must define not only where and when the protein is expressed, but also understand the potential partners and post-translational modifications that collectively drive the formation of tissue-specific transcriptional complexes.

Twist1

Twist1 is a dynamic member of the Twist bHLH family, which is broadly expressed during development and marks the extra-embryonic, somitic, limb, and pharyngeal mesenchyme (Chen and Behringer, 1995; Fuchtbauer, 1995; Vincentz et al., 2008). Given this expression pattern, it is not surprising that genetic models reveal a role for *Twist1* in regulating specification and differentiation in developing mesenchyme. Systemic deletion of *Twist1* in mice results in embryonic lethality at E11.5 due to a spectrum of defects that include failure of the neural tube to close, defects in cranial mesenchyme, pharyngeal arches, somites, and limb buds (Chen and Behringer, 1995). This phenotype is consistent with a role for *Twist1* in regulating mesenchyme morphology and

behavior during NCC migration and development. Furthermore, this correlates well with what is known about *Twist1* function in neoplastic diseases, where a direct connection between elevated *Twist1* expression and EMT has been found (Hoek et al., 2004). During EMT, epithelial cells lose polarity and take on an invasive phenotype via loss of cell adhesion due in part to a loss of the calcium dependent transmembrane protein E-cadherin, which is regulated by Twist1 as well as Snail and Zeb1 (Smit and Peeper, 2008). In the context of migratory cNCC, current evidence points to N-cadherin as a major mediator of EMT with Snail, Slug, Id2, and Pinch1 expression specifying EMT competence (Duband et al., 1995; Martinsen and Bronner-Fraser, 1998; Snider et al., 2007). It is not currently clear what role, if any, *Twist1* plays in cNCC EMT.

Upon close examination of *Twist1*$^{-/-}$ mice, it was discovered that the OFT cushions contain amorphic cellular nodules (Vincentz et al., 2008). Molecular analyses demonstrate that these nodules are of NCC origin and molecularly resemble ectodermal sympathetic ganglia. Further investigation subsequently revealed a role for Twist1 in the repression of pro-neural factors, such that Twist1 regulates cell fate determination between ectodermal and mesodermal lineages within post-migratory NCC (Vincentz et al., 2013). In addition, *Twist1* null mice are reported to exhibit a delay in colonization of the OFT cushions, as well as aberrant placement of NCC derivatives in the pericardium and endocardium. These data are consistent with research on Saethre Chotzen Syndrome (SCS), which is caused by *TWIST1* mutations (Howard et al., 1997). These data

demonstrate that appropriate *Twist1* dosage is essential for correct differentiation of cNCC, and suggest a role in guiding cNCC migration and cell adhesion.

Twist1 is expressed in EPDCs undergoing EMT, but is not expressed within the epicardium (Zhou et al., 2010), and no epicardial functions have been reported. While not detectable in ventricular endocardium, *Twist1* is robustly expressed in endocardial cushions of the AVC during murine mid-gestation, although this expression is down-regulated as the cushions are remodeled into valves. Indeed, by E17.5 *Twist1* expression is either completely absent, or nearly so (Chakraborty et al., 2010). Loss-of-function and gain-of-function experiments in transduced chick endocardial cushion explants have revealed multiple roles for *Twist1* during cushion formation and subsequent valve development. *Twist1* can induce cell proliferation in these cushion explants, promote cushion migration, and affect differentiation marker genes (Shelton and Yutzey, 2008). These proposed functions correlate well with information gathered from persistent and overexpression of *Twist1* in mice. In these studies a *CAG-CAT-Twist1* transgene was induced by the endothelial specific *Tie2-Cre*, resulting in stable and persistent overexpression of *Twist1* in the endocardium, and endocardium derived cushions (Chakraborty et al., 2010). Despite increases in area, length, and thickness of AV and OFT valve leaflets, double transgenic animals were viable. Detailed phenotypic analysis revealed abnormally high levels of proliferation in these valves, possibly due to a significant increase in *Tbx20* expression. Indeed, *Tbx20* has previously been associated with proliferation via induction of *N-myc* (Cai et al., 2005). *Twist1* overexpression was shown to affect

several ECM related genes, possibly accounting for phenotypic abnormalities in cushion remodeling and migration. Dysregulated genes include *Col2a1*, *Mmp2*, and *Mmp13,* and *Postn* – all of which are significantly upregulated (Chakraborty et al., 2010). Furthermore, a *Col2a1* regulatory element is bound by *Twist1 in vivo*, and can be transactivated *in vitro*. This binding occurs at a conserved E-box in the *Col2a1* first intron. Similarly, *Twist1* has been demonstrated to be capable of binding an E-box in the *Postn* promoter and *trans*-activating a reporter construct (Oshima et al., 2002). This information correlates well with the increased levels of *Postn* expression observed at E17.5 in Twist1 overexpressing mice. Together, these results support a role for endocardial Twist1 in promoting proliferation of cardiac valve progenitors, and subsequently guiding their organization as the endocardial cushions remodel, through regulation of critical ECM proteins.

Hand1

As the heart loops rightward, expression of Twist family member *Hand1* is observed in the outer curvature of the left ventricle myocardium, as well as in the pericardium and septum transversum (Barnes et al., 2010; Cserjesi et al., 1995b; Firulli et al., 1998). During mid-gestation, *Hand1* is expressed within the left ventricular myocardium, medial cNCC populating the caudal pharyngeal arches, and approximately 50% of the cNCC mesenchyme within the OFT cushions (Vincentz et al., 2011). *Hand1* null mice die in utero at E9.5, due to defects in the yolk sac, placenta, vasculature, and heart (Firulli et al., 1998; Morikawa and

Cserjesi, 2004; Riley et al., 1998). Cardiac defects include failure of complete heart tube fusion and hypoplastic LV, which are likely secondary to placental, yolk sac and vascular defects. Conditional ablation of *Hand1* within NCC does not reveal any developmental defects and may reflect a true functional redundancy with Hand2 in these cells (Barbosa et al., 2007). Indeed, NCC specific loss of *Hand1* in *Hand2*$^{+/-}$ mice results in a dysregulation of *Msx2*, *Pax9*, and *Prrx2* expression, as well as hypoplasia of certain pharyngeal arch derived structures such as the mandible. This again demonstrates the critical nature of gene dosage for the Twist family of bHLH factors (Barbosa et al., 2007). Given this data, it seems likely that interactions and redundancy with additional transcription factors may be masking an unknown role for *Hand1* in cNCC development.

Hand1 is not expressed within the PEO or epicardium but is expressed within the septum transversum that is directly caudal to the PEO. Interestingly, experiments using the *Hand1*^{eGFPCre} allele in conjunction with *R26R* lineage mapping shows that the permanently-marked *Hand1* expressing cells within the septum transversum migrate into the forming PEO and subsequently mark the entire epicardium, as well as secondary EMT epicardial-derived cell types such as the coronary smooth muscle, and cardiac fibroblasts (Barnes et al., 2010). Collectively, these experiments identify Hand1 as one of the earliest transcription factors that defines the epicardial lineage. Given the transitory expression of *Hand1* in the early precursors of the PEO, it will be interesting to see what role, if any, it plays in the early specification and or migration of the epicardium. As a

tool, the *Hand1*^{eGFPCre} allele allows for conditional gene recombination within the early epicardial lineage (Fig. 3). When this tool was employed to interrogate epicardial Hand2 function, several intriguing phenotypes were observed. These phenotypes included defective epicardialization, altered ECM secretion, and failure to form coronary arteries. For a detailed description of this study, as well as similar analyses utilizing both a tamoxifen inducible *WT1*^{ERT2Cre}, and a transgenic *WT1-Cre* allele, see Appendix I.

Hand1 is not expressed in the endocardium or endocardial cushions, and Hand1-lineage analysis shows no endocardial contributions of any cells that have expressed *Hand1* (Barnes et al., 2010; Vincentz et al., 2011). However, myocardial specific ablation of *Hand1* surprisingly results in hyperplastic endocardial cushions that mature into abnormally thick AV valves (McFadden et al., 2005). This would suggest that Hand1 is involved in a myocardium derived signaling pathway that regulates endocardial cushion cells. However, *Bmp2*, *Bmp4*, *Smad6*, *Smad7*, and *Tgfβ* expression levels are all normal in *Hand1* myocardial specific conditional knock outs (CKOs), leaving the details of such a pathway undiscovered (McFadden et al., 2005).

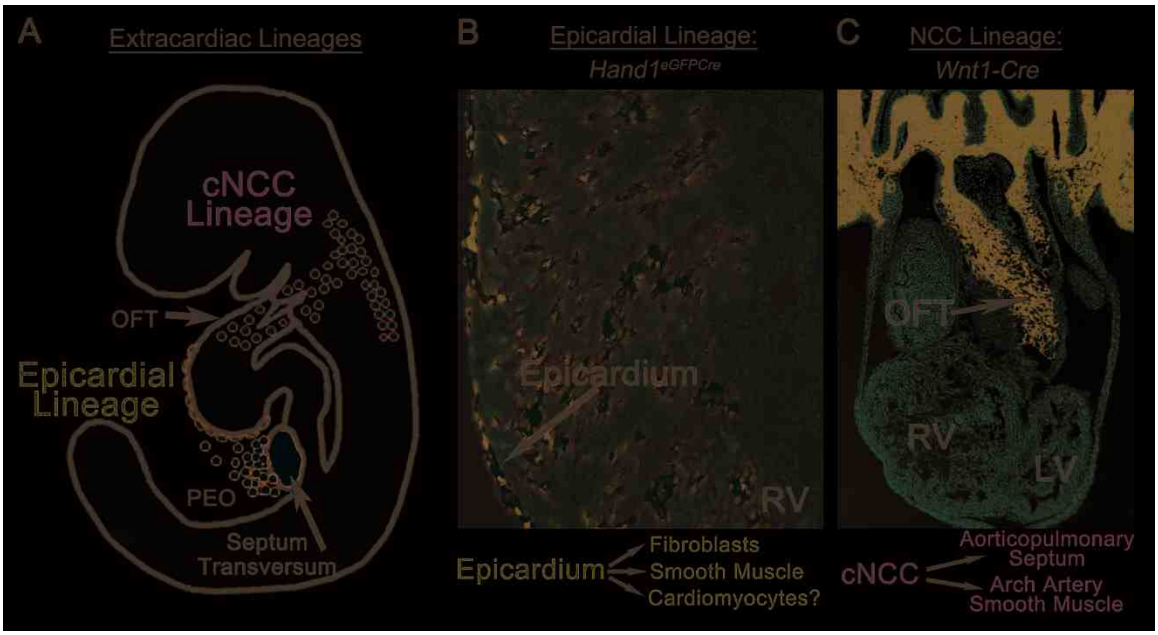

Figure 3: **Extracardiac Lineages**

Diagram of epicardial and cNCC lineage contributions to heart development (A). Epicardial lineage shown by lacZ staining of *Hand1*^{eGFPCre} *R26R*$^{Z/Z}$ activation in right ventricle at E15.5 (B). Neural crest cell lineage, shown by lacZ staining of *Wnt1-Cre; R26R*$^{Z/Z}$ activation in OFT at E11.5 (C). PEO, proepicardial organ; OFT, outflow tract; RV, right ventricle; LV, left ventricle; cNCC, cardiac neural crest cell (VanDusen and Firulli, 2012).

Paraxis, Scleraxis, and Twist2

While *Twist1* and Hand1 are established regulators of cardiac morphogenesis, less is known regarding the Twist family members *Paraxis*, Scleraxis (*Scx),* and *Twist2*. Although *Paraxis* is not expressed within the developing heart (Burgess et al., 1995), recent studies demonstrate that *Scx* plays an integral role in remodeling of the endocardium derived mesenchyme of the primitive valves. *Scx* is first expressed in mice at E9.5 in somites and mesenchyme of the body wall and limb buds. As the embryo matures this expression becomes restricted to areas of developing cartilage and connective tissue, including heart valves (Cserjesi et al., 1995a). Indeed, *Scx*$^{-/-}$ mouse embryos have thickened valve structures, increased expression of cartilage-associated genes such as *Sox9*, *Msx1*, and *Snail*, and a disruption of ECM and collagen fiber organization. Conversely, overexpression of *Scx* in avian valve precursor cells and porcine adult valve interstitial cells results in increased secretion of chondroitin sulfate proteoglycans (Barnette et al., 2013). Further analyses revealed that *Scx* transcription is positively regulated by Tgfβ2 signaling, while Mapk activity attenuates this activation. These observations have lead researchers to conclude that *Scx* is involved in valve precursor cell differentiation and ECM organization (Barnette et al., 2013; Levay et al., 2008). However, few direct transcriptional targets of Scleraxis have been identified (Espira et al., 2009; Liu et al., 1997), and the extent of its role in cardiogenesis is not well defined. Additional investigation will be required to extend our current understanding. Twist2 is expressed within AV cushion mesenchyme during

midgestation cardiogenesis, and this expression is ectopically expanded to ventricular endocardium in mice that overexpress the Notch1 intracellular domain within the endothelial lineage. Twist2 function in cardiac development has not been described, but is commonly thought to considerably overlap with Twist1 function.

Chapter II

Hand2 Function within the Endocardium

A. Introduction

Hand2 is strongly expressed within ventricular endocardium and mesenchymal cells of the endocardial cushions during midgestation. However, no endocardial *Hand2* functions have currently been defined. In *Mef2c-Cre H2CKOs Hand2* is ablated from SHF cardiac progenitors, which contribute to both myocardium and endocardium. *Mef2c-Cre H2CKO* embryos display OFT septation defects, hypoplastic RV, and atresia of the tricuspid valve (tricuspid atresia, TA; Fig. 4), resulting in death at E13.5 (Tsuchihashi et al., 2011). As TA is not observed in myocardial *H2CKOs* (Morikawa and Cserjesi, 2008), and mesenchyme of the tricuspid valve is derived from the endocardium, these data suggest an important endocardial role for Hand2. We therefore hypothesized that loss of Hand2 function within the endocardium could be causative of a TA phenotype. Indeed, this study shows that conditional deletion of *Hand2* (*H2CKO*) using both the endothelial specific *Tie2-Cre* and endocardial-specific *Nfatc1-Cre* results in loss of the tricuspid valve, hypotrabeculation, and altered septation which collectively resemble TA phenotypes. We show that endocardium to myocardium signaling is disrupted as *Neuregulin1* (*Nrg1*) is dramatically downregulated within the endocardium of *H2CKOs*. Since *Nrg1* is a known downstream component of *Notch1* signaling, we examined additional components of the Notch pathway for expression level alterations. Our results show that Hand2 endocardial expression is Notch-dependent and that Hand2 is

downstream of both Notch1 and its direct target *EphrinB2*. Collectively, these data support a model whereby Notch signaling via Hand2 function within the endocardium allows for endocardial-myocardial cell communication that directly influences trabeculation and septal positioning/outgrowth. Subsequently, endocardial loss of *Hand2* results in a consistently misplaced interventricular septum (IVS) that interferes with tricuspid valve development. As a consequence of this alteration in IVS position the RA and RV fail to make a direct connection, resulting in a TA phenotype.

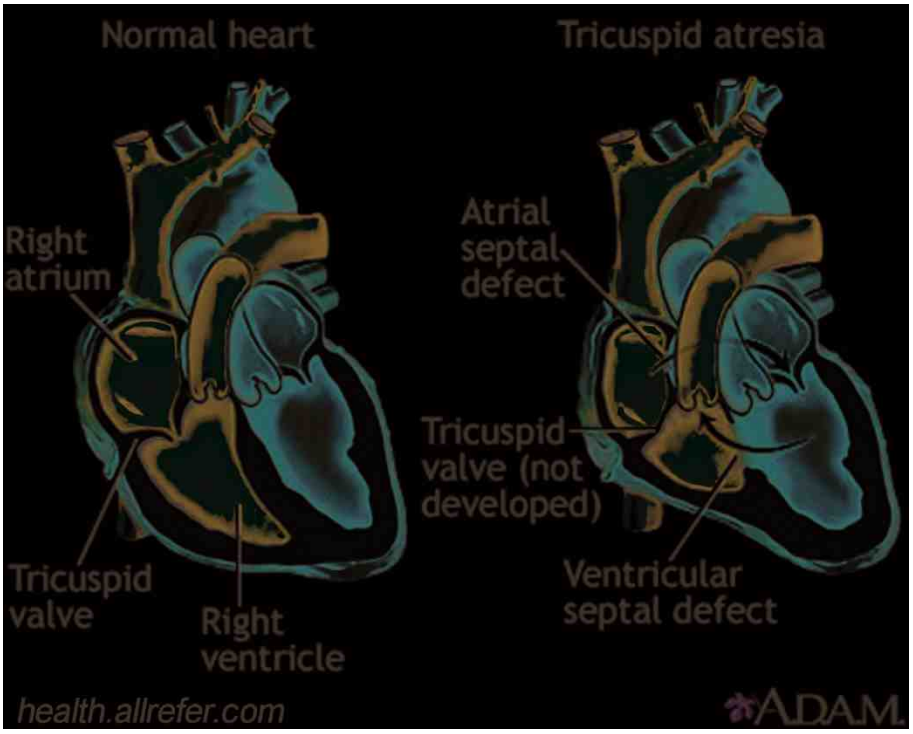

Figure 4: Tricuspid Atresia

Diagram showing a normal heart at left, and tricuspid atresia heart at right.

B. Methods

Mice and Genotyping

Tie2-Cre(+) and *Nfatc1-Cre(+)* mice were crossed with *Hand2*$^{+/-}$ mice to generate *Tie2-Cre(+);Hand2*$^{+/-}$ and *Nfatc1-Cre(+);Hand2*$^{+/-}$ males (germline activation of *Tie2-Cre* occurs in females; de Lange et al., 2008). These males were then crossed with *Hand2*$^{fx/fx}$*;ROSA26R* reporter mice (*lacZ* or *eYFP*) to generate conditional null *Hand2* embryos. *Tie2-Cre(+)* females were crossed with *EfnB2*$^{fx/fx}$ males to generate *Tie2-Cre(+);EfnB2*$^{fx/+}$ males. These males were then crossed with *EfnB2*$^{fx/fx}$ females to generate conditional null *EfnB2* embryos. *Twist1+/−* and *Wnt1-Cre* mice were obtained from the Jackson Laboratory. *Postn-Cre(+)* mice (Lindsley et al., 2007) were crossed with *Hand2*$^{fx/fx}$ (Morikawa et al., 2007) mice to generate *Postn-Cre(+);Hand2*$^{fx/+}$ males. These males were then crossed with *Hand2*$^{fx/fx}$*;ROSA26R lacZ* (*R26R*$^{z/z}$) reporter mice to generate conditionally null *Hand2* embryos.

For embryo generation female mice were checked daily for a semen plug, with the morning of detection being considered E0.5. Pregnant females were sacrificed at the desired stage, and embryos dissected out in cold PBS. Yolk sacs were collected for embryo genotyping. The cre-activatable transgene *CAG-CAT-Hand2* was constructed by replacing the *Myc-Twist1* cDNA of *CAG-CAT-Twist1* (Connerney et al., 2006) with the murine *Myc-Hand2* cDNA. This construct was used for microinjection to establish a transgenic line. *CAGCAT-Hand2* and *Cre* genotyping of adult mice was achieved by southern blot on tail genomic DNA using a probe corresponding to the appropriate cDNA. For *Hand2*^{flox}, *Hand2* systemic,

EphrinB2^{flox}, and *Rosa* genotyping, southern probes corresponding to the appropriate loci were utilized (Barnes et al., 2011; Gerety and Anderson, 2002). Genotyping for *CAGCAT-Hand2(+)* embryos was conducted by PCR using the Hand2 specific oligo 5'GGGATCCATCTGCCCAAGGACGACCAG 3' and SV40PA(R). These primers were used with a denaturing temperature of 95°C for 30 seconds, annealing temperature of 55°C for 60 seconds, and extension at 72°C for 60 seconds, for 35 cycles. Mouse maintenance and experimentation was performed according to protocols approved by the Indiana University School of Medicine Institutional Animal Care and Use Committee.

Histological Preparations

For X-gal staining, embryos were dissected in PBS, fixed in 2% PFA plus 0.2% glutaraldehyde for 20 minutes, rinsed in PBS, and incubated in X-gal staining solution overnight. Embryos were then post-fixed with 4% PFA for one hour, rinsed, and dehydrated through a graded series of ethanol dilutions, with 10 minutes in each dilution (50%, 70%, 90%, 95%, and 100% ethanol). Dehydrated embryos were incubated in a 1:1 citrosolv ethanol solution for 10 minutes, rinsed with 100% citrosolv twice for 10 minutes each, and embedded in paraffin for sectioning. Sections were counterstained with nuclear fast red. For alcian blue staining, embryos were dissected in PBS, fixed in 4% PFA for one hour, rinsed with PBT, and dehydrated through a graded series of methanol dilutions (25%, 50%, 75%, 100%) for 10 minutes in each dilution. Dehydrated embryos were rinsed in a 1:1 xylene methanol solution for 10 minutes, cleared with 100% xylene, and embedded in

paraffin. Paraffin was removed from sections using citrosolv. Sections were rehydrated, and stained with 0.15mg/ml Alcian Blue in 5% glacial acetic acid for 30 minutes. Stained sections were rinsed with H_2O, counterstained with nuclear fast red, and dehydrated with ethanol. Dehydrated sections were incubated in citrosolv for 15 minutes, and cover-slipped.

Section RNA *In Situ* Hybridization

This protocol was performed essentially as previously described (Vincentz et al., 2008). Embryos were dissected and embedded as for Alcian Blue staining. Embryos were sectioned at 10 microns, and paraffin was removed from sections using xylene. Sections were then rehydrated, digested in 10µg/mL Proteinase K for eight minutes, briefly rinsed in 0.2% glycine, and post-fixed for 10 minutes. Sections were then rinsed, incubated in 0.1M triethanolamine plus 1:400 acetic anhydride for 20 minutes, and rinsed with PBS. Sections were then dehydrated with ethanol, and hybridized with antisense digoxygenin labeled riboprobes overnight at 70°C. Riboprobes were transcribed with T7, SP6, or T3 (Roche). After hybridization slides were washed in a 50% formamide, 1x SSC, 1% SDS solution for 1.25 hours at 65°C. Slides were next washed with an STE solution containing 4x SSC, 20mM Tris-Cl (pH 7.5), 1mM EDTA for 10 minutes. Slides were then washed in STE again, with the addition of 0.02mg/mL RNAse (Life Technologies) for 30 minutes. After this incubation slides were rinsed once more with STE (no RNAse) for 10 minutes. All STE washes were conducted at 37°C. Slides were then rinsed twice in a maleic acid buffer solution (MABT) containing 0.1M maleic acid, 0.15M NaCl, and 0.1% Tween-

20 (pH 7.5) for 30 minutes each, at room temperature. Slides were then placed in blocking solution composed of 0.08M maleic acid, 2% Boehringer Blocking Reagent, 10% heat inactivated sheep serum, and 0.1% Tween-20 (pH 7.5) for two hours at room temperature. After blocking, slides were incubated with anti-DIG antibody (Roche) at a dilution of 1:2000 overnight at room temperature. Slides were than washed five times in MABT plus 2mM levamisole for 30 minutes each at room temperature. Slides were then washed for 5 minutes in a solution containing 0.1M NaCl, 0.1M TrisCl (pH 9.5), 0.05M $MgCl_2$, and 0.1% Tween-20 at room temperature. Slides were then incubated in BM Purple AP substrate (Roche) until appropriate staining was achieved (generally 1-3 days).

RNA Isolation and Quantitative RT-PCR

Total RNA was isolated from individual flash-frozen E10.5 or E13.5 ventricles (AV canal to OFT), using the High Pure RNA Isolation Kit (Roche). Briefly, tissue is lysed, debris removed by centrifugation, RNA is purified by column, and DNA removed by DNase digestion. This RNA served as a template to generate cDNA using the Transcriptor First Strand cDNA Synthesis Kit (Roche). For quantitative RT-PCR (qRT-PCR), cDNA was amplified using Taqman Probe-Based Gene Expression Assays (Applied Biosystems). Relative gene expression was determined after normalization to GAPDH. At least four samples were assayed per genotype at each time point. The Student's t-test was used to detect significant differences between sample groups, with P-values ≤ 0.05 considered significant.

Immunohistochemistry

Embryos were fixed in 2% PFA overnight, infused with 30% sucrose, cryoprotected, and sectioned at 10μm on a cryostat. Frozen sections were washed in PBS, blocked in 1.5% normal serum for one hour, and incubated with primary antibody overnight at 4˚C. Antibody staining for phospho-Histone H3 (pHistone H3; Abcam 47297), activated-Caspase 3 (aCaspase; Promega G748A), and Green Fluorescent Protein (GFP; Aves 1020) was conducted at a 1:500 dilution. Flk1 immunostaining was conducted at a 1:50 dilution (Abcam 10972), while c-Myc immunostaining was conducted at a 1:200 dilution (Sigma C3956). Secondary antibodies were conjugated with Alexa 488 or 594 (Molecular probes). Images were collected on a Leica CTR 5000 microscope at standardized conditions with Leica Application Suite software. Cell-autonomous proliferation/death was calculated by counting cells displaying colocalization of GFP and pHistone H3/aCaspase, divided by total number of GFP(+) cells. Non cell-autonomous proliferation/death was calculated by counting all cells displaying pHistone H3/aCaspase expression, divided by total number of GFP(+) cells. All death and proliferation counts were generated from a minimum of 12 pairs of sections, obtained from two control embryos and two somite matched littermate *H2CKO* embryos.

Electrophoretic mobility shift assays, luciferase assays, and chromatin immunoprecipitation

Hand2 and E12 were *in vitro* translated using the Promega Reticulocyte Lysate System. 5μl of translated protein was incubated with radio-labeled oligos

corresponding to conserved E-boxes and D-boxes, in binding buffer for 30 minutes at room temperature (Firulli et al., 2007). The following oligos and their compliments were utilized: Nrg1.D1, 5'-GCGAAGGAGG**CGCCTG**CGTCCAACT-3'; Nrg1.D1m, 5'-GCGAAGGAGG**GCACTG**CGTCCAACT-3'; Nrg1.E2, 5'-AACTT GCGGG**CAATTG**AAAAAGAGC-3'; Nrg1.E2m, 5'-AACTTGCGGG**GCATTG**AAA AAGAGC-3'; Nrg1.E3, 5'-GCAGCGGCGG**CAGCTG**CCGGGAGAT-3'; Nrg1.E3m, 5'-GCAGCGGCGG**GCACTG**CCGGGAGAT-3'. Bold type signifies E/Dbox or corresponding mutagenized region. Transcription factor/oligo complexes were run out on a non-denaturing 6% polyacrylamide gel and assessed on a phospho-imager. For luciferase assays, HeLa cells were transfected using X-tremeGENE HP (Roche) at a ratio of 3:1 with *Nrg1-500bp+pGL4.10* (luciferase), *pGL4.73* (renilla), *Pcs2+Myc-Hand2*, *Pcs2+Myc-E12*, *pcDNA+Myc-ΔBasic-Hand2* (kindly provided by Eric Olson), or *pcDNA3.1* and cultured for 48 hours. Cultures were harvested by scraping off cells in cold PBS and pelleting. Pellets were resuspended in 10x volume of passive lysis buffer (provided in Promega Dual Reporter Luciferase kit), frozen in liquid nitrogen, and thawed at 37°C. Luciferase and renilla reporter activity was assessed in 50ul of cell lysate using Luminoskan Ascent software and a ThermoLabsystems luminometer. Luciferase results were normalized to renilla (Holler et al., 2010), or protein lysate concentration. For chromatin immunoprecipitation (ChIP) of the *Nrg1* promoter, HeLA cells were again transfected using X-tremeGENE HP at a ratio of 3:1. After culturing for 48 hours, cells were processed as previously described (Holler et al., 2010; Vincentz et al.,

2012). Equal amounts of sheered chomatin were immunoprecipitated overnight at 4°C with 50µl of αMyc-conjugated agarose beads (Sigma), or beads without antibody for a negative control. After reversing crosslinks, eluted immunoprecipitated DNA was phenol chlorophorm extracted, resuspended in ddH_2O, and used for subsequent PCR reactions. After 37 cycles of PCR amplification, product was analyzed on an agarose gel. ChIP primer pairs were as follows (forward, F; reverse, R): Nrg1-426F, 5'-GAGTTCCCCGAAACTTGT TG-3'; Nrg1-324R, 5'-AGGTTATCACCGTCCTGCTC-3'; GAPDH(F), 5-CTG CACCACCAACTGCTTAG-3; GAPDH(R), 5-CAGTGAGCTTCCCGTTCAG-3. Transfection constructs used for ChIP included *Pcs2+Myc-Hand2*, *Pcs2+E12*, and *Pcs2+Myc*.

C. Results

Ablation of *Hand2* within the endocardium

To test the hypothesis that loss of endocardial *Hand2* results in TA, we first utilized the endothelial cell-specific *Tie2-Cre* allele (Kisanuki et al., 2001). Intercrossing *Tie2-Cre* with mice carrying the *Hand2* conditional allele ($Hand2^{fx}$) deletes *Hand2* within the *Cre*-expressing cells and their descendants. *Tie2-Cre* is expressed in all endothelial cells, including cells of the endocardium, and mesenchymal cells of the atrioventricular cushions (Kisanuki et al., 2001). *Tie2-Cre* expression initiates at E8.5 in a fraction of endothelial cells, and by E9.5 virtually all are *Tie2-Cre* lineage positive (Kisanuki et al., 2001). Its activation proceeds the onset of endocardial *Hand2* expression, which marks all endocardial cells by E8.5 (Barnes et al., 2011).

Hand2$^{fx/fx}$;*R26R*$^{Z/Z}$ females were mated with *Tie2-Cre(+);Hand2*$^{+/-}$ males, and neonates were genotyped. No *H2CKO* mice were observed (n=58, Table 1). We therefore set up timed matings and collected embryos at E14.5. Live *Tie2-Cre H2CKO* embryos were identified at less than Mendalian ratios (Table 1), while most were dead and beginning to be resorbed (data not shown).

	E10.5	E12.5	E14.5	Postnatal
Total	199	75	53	58
Cre(+)	98	38	20	26
Mutants	38 (41)	18 (16)	2 (9)	0 (11)

Table 1: *Tie2-Cre H2CKOs* die at E14.5

Genotypic frequencies of embryos obtained from ♂*Tie2-Cre; H2*$^{+/-}$ x ♀*Hand2*$^{fx/fx}$*;R26R*$^{Z/Z}$ intercrosses. Expected number in parentheses.

Hand2 deletion within the endothelium was first verified by *in situ* hybridization (*ISH*) at E10.5 (Fig. 5A, B). Subsequent examination of *Tie2-Cre H2CKO* whole mount (Fig. 5D, E) and section histology (Fig. 5G, H) revealed hypotrabeculation and a highly penetrant TA phenotype comparable to that observed in the SHF *Mef2c-Cre Hand2* mutants (Tsuchihashi et al., 2011). At E12.5 we observe hypotrabeculation, ventricular septal defects (VSDs), and varying degrees of RV hypoplasticity in *Tie2-Cre H2CKO* hearts. Rightward septal

displacement and, occasionally (~20%), a double inlet left ventricle (DILV) phenotype was also observed (Fig. 5J). DILV is a CHD that closely resembles TA (Kim et al., 2001).

To examine atrioventricular (AV) cushion formation, cell density, and extracellular matrix (ECM) deposition, tissue sections were stained with alcian blue. Although comparison of *H2CKO* cushions with those of controls reveals no difference in general size, or amount of ECM (Fig. 5K, L), there does appear to be a minor cushion positioning defect (asterisk in Fig. 5L). Despite normal AV cushion size and ECM deposition, no direct connection between the RA and RV is detected in any plane of section, resulting in a single left sided AV canal in most *H2CKOs* (Fig. 5H).

We recently have shown that the *Hand1*-lineage contributes to caudle vascular endothelium (Barnes et al., 2010). While no defects were observed in the yolk sac vasculature of *Tie2-Cre H2CKOs* (Fig. 6A-B), Hand2 may play critical roles in vascular endothelium that could contribute to the observed embryonic lethality of *Tie2-Cre H2CKO* embryos. Therefore, we used the endocardial-specific *Nfatc1*^{Cre} allele (Wu et al., 2012) to generate *H2CKOs* (Fig. 5C, F, N). Similar to the *Tie2-Cre*, the *Nfatc1*^{Cre} initiates expression throughout the endocardium at E9.0 (Wu et al., 2012).

Nfatc1^{Cre} *H2CKOs* showed dramatic defects in trabeculation, malformed IVS, and in most cases (~70%), atresia of the tricuspid valve (Fig. 5F, H, N). Interestingly, in some cases IVS malformations included abnormally large protrusions of myocardium that appear to indicate the formation of multiple IVSs (Fig. 5N).

Together, these data confirm that conditional deletion of *Hand2* within the endocardium is critical for normal trabeculation and septation. Given that these phenotypes are myocardial in nature, this suggests that endocardial Hand2 plays a crucial role in endocardium to myocardium signaling.

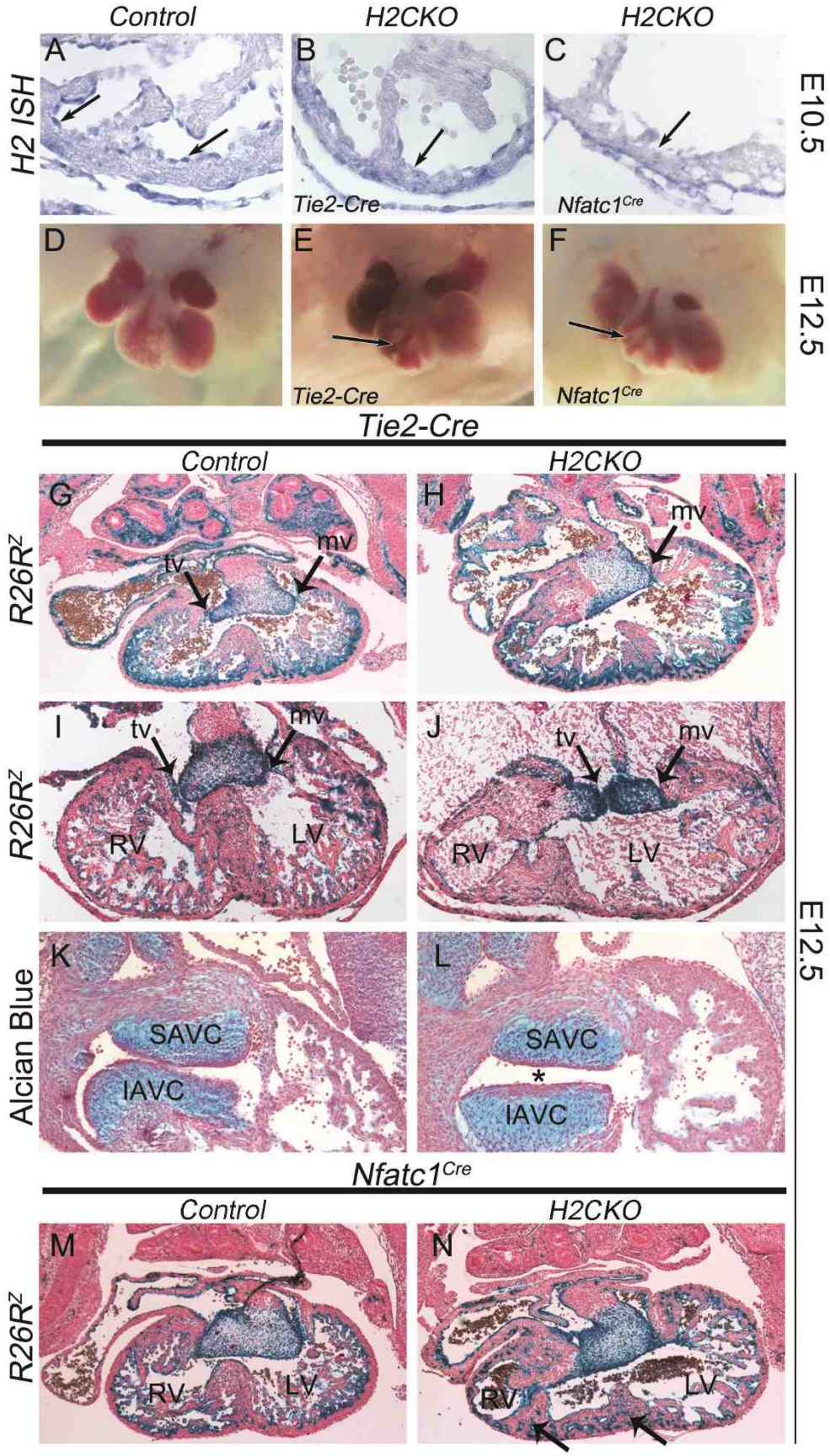
Control
H2CKO
H2CKO
H2 ISH
A
B
C
E10.5
Tie2-Cre
Nfatc1Cre
D
E
F
E12.5
Tie2-Cre
Control
H2CKO
R26RZ
G
H
tv
mv
I
J
RV
LV
E12.5
Alcian Blue
K
L
SAVC
IAVC
*
Nfatc1Cre
Control
H2CKO
M
N

Figure 5: Endocardial deletion of *Hand2* results in a VSD, hypotrabeculation, hypoplastic RV, and tricuspid valve abnormalities akin to the human CHD tricuspid atresia.

Hand2 ISH of RV section from E10.5 control, *Tie2-Cre H2CKO,* and *Nfatc1^{Cre} H2CKO*, respectively (A-C). Wholemount view of E12.5 control heart, *Tie2-Cre H2CKO*, and *Nfatc1^{Cre} H2CKO*, respectively (D-F). *R26R* lacZ stained sections from E12.5 *Tie2-Cre(+)* control embryo (G), *Tie2-Cre H2CKO* with tricuspid atresia (H). *R26R lacZ* stained E12.5 *Tie2-Cre(+)* control embryo (I), and *Tie2-Cre H2CKO* with double inlet left ventricle (J). *R26R* lacZ stained sections from E12.5 *Nfatc1^{Cre}* control embryo (M), and *Nfatc1^{Cre} H2CKO* (N). Alcian blue staining of E12.5 *Tie2-Cre(+)* control AV cushions (K), and *Tie2-Cre H2CKO* (L). Asterisk denotes abnormalities in AV cushion shape and position. SAVC, superior atrioventricular cushion; IAVC, inferior atrioventricular cushion;
tv, tricuspid valve; mv, mitral valve.

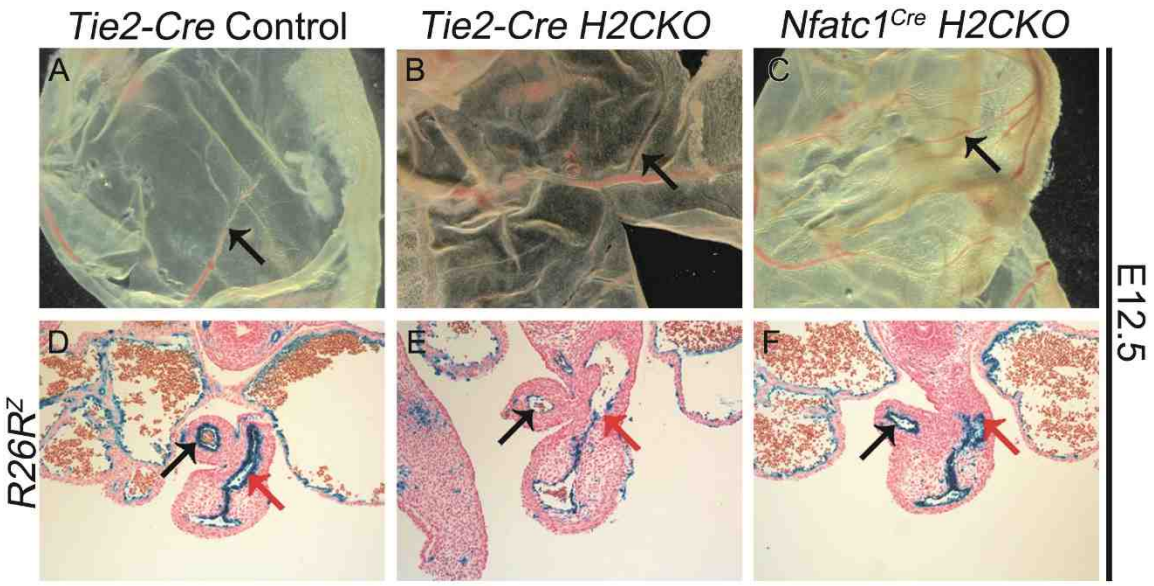

Figure 6: Development of the yolk sac vasculature and septation of the OFT occur normally in *H2CKOs*.

H2CKOs lack yolk sac vasculature defects (A-C) which have been reported in systemic *Hand2* knock outs. Black arrows denote large yolk sac vessels. *H2CKOs* do not exhibit PTA (D-F), which has been reported in other conditional *Hand2* loss of function models. Black arrows denote aorta; red arrows denote pulmonary trunk.

In addition to cardiac defects, systemic deletion of Hand2 in mice results in severe yolk sac vasculature defects by E9.5. We show that yolk sac vascularization occurs normally in endocardial *H2CKOs* (Fig. 6A-C), supporting previous conclusions that Hand2 is required only within smooth muscle of the yolk sac vasculature (Yamagishi et al., 2000). Similarly, a key feature distinguishing endocardial-*H2CKO* embryos from *Mef2c-Cre* or other SHF-*H2CKO* embryos is the absence of outflow tract (OFT) defects. The OFTs of *Mef2c-Cre H2CKOs* fail to septate by E12.5 (Tsuchihashi et al., 2011), whereas OFT septation is clearly evident in endocardial-*H2CKOs* at this stage (Fig. 6D-F). This is a significant observation, as it suggests that SHF progenitor cell death is not causative of the TA phenotype, as we would also expect to see OFT defects if this was the case. To confirm this hypothesis we tested for apoptosis in the pharyngeal mesoderm by immunostaining for activated Caspase-3. Results show no significant changes in apoptosis within the SHF progenitors of *H2CKOs* and controls (P-value = 0.498, Fig. 7A) suggesting further that a specific endocardial Hand2 function causes the observed TA phenotype.

While it is clear that endocardial *H2CKO* embryos develop a hypoplastic RV, we sought to determine at which stage this phenotype becomes apparent. *Tie2-Cre* control and *H2CKO* littermates were collected at E10.5, and direct RV cell counts using DAPI stained nuclei were performed. DAPI(+) nuclei from every sixth section of the RV were counted, and a p-value of 0.003 was calculated, indicating a significantly smaller RV (by ~23%) in *H2CKOs* (Fig. 7B). Having ruled out a loss of progenitor cell contribution from the E9.5 pharyngeal mesoderm, two possible

explanations for this reduction in RV size in *H2CKOs* are apparent: either an increase in the rate of RV cell death, or a decrease in the rate of RV cardiomyocyte proliferation. To address the possibility of an increase in cell death in developing *H2CKO* mutant hearts, we immunostained E10.5 frozen sections with α-activated Caspase-3 and α-GFP antibodies to identify cells of the *Cre*-lineage undergoing apoptosis. A total of 20 pairs of comparative RV sections were counted, and neither a cell-autonomous effect on apoptosis (p-value: 0.705, Fig. 7C), nor a non cell-autonomous effect (P-value: 0.734, data not shown) was observed. Cell proliferation was analyzed in a similar fashion with an α-phospho-histone H3 (PHH3) antibody. No difference in proliferation was observed (P-value: 0.654, Fig. 7D).

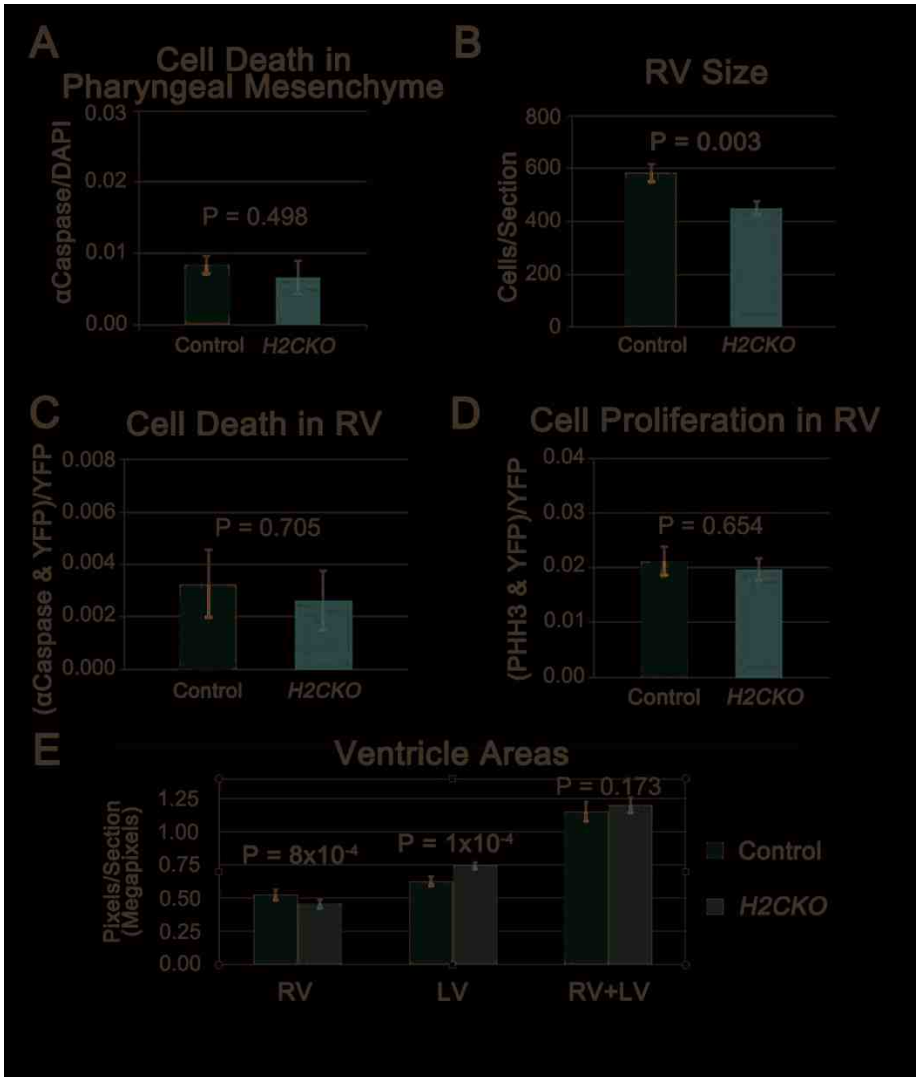

Figure 7: *H2CKOs* develop a hypoplastic RV and larger LV, but do not show significant differences in cell death or proliferation.

Cell death in control and *Tie2-Cre H2CKO* E9.5 pharyngeal mesoderm was measured by quantification of active-Caspase-3(+) cells. No difference was detected (A). Hypoplastic RV at E10.5 in *Tie2-Cre H2CKOs* was confirmed by counting DAPI(+) RV nuclei (B). Cell death was measured in control and *Tie2-Cre H2CKO* E10.5 RV by quantification of active-Caspase-3(+) cells. No difference was detected

(C). Cell proliferation in the E10.5 RV was determined by counting PHH3(+) cells. No difference was detected between control and H2CKO hearts (D). Ventricle area measurements revealed a smaller RV and larger LV in *Tie2-Cre H2CKOs* (E).

Loss of Hand2 alters the position of the IVS, blocking connection between the RA and RV

Given these data, and the observation that both *Tie2-Cre* and *Nfatc1*^{Cre} *H2CKOs* exhibit abnormalities of IVS position, we investigated whether an aberrant rightward positioning of the IVS simply reduces RV size, and thus would increase LV size. To test this hypothesis, we measured ventricular areas from four sections from each of three *H2CKO* embryos, and matched control sections. All sections were from E10.5 littermates, and area measurements were obtained using Adobe Photoshop. Results show that the area of *H2CKO* RVs is significantly smaller (P-value = $8*10^{-4}$) by approximately 13%, while LVs are significantly larger (P-value = $1*10^{-4}$) by approximately 19%. There is no significant difference in total ventricular area (P-value = 0.1730, Fig. 7E). Thus, *H2CKO* TA phenotypes appear to be the result of abnormal growth and positioning of the IVS.

Hand2 controls *Nrg1* expression within the endocardium

We next investigated the changes in gene expression within *H2CKOs* using *ISH*. First we analyzed myocardial gene expression. The stress sensor gene *Anf*, and bHLH Twist family member *Hand1* showed no observable change in expression (Fig. 8A-D). The AV canal marker *Bmp2*, cushion mesenchyme markers *Pdgfra*, *Twist1,* the T-box transcription factor *Tbx20,* and *Gata4* also show no change in expression between mutants and controls suggesting that endothelial cushion EMT is largely unaffected (Fig. 8E-N). In addition to these markers, expression analysis of *Fog2* was of interest, as *Fog2* deficient mice also display a tricuspid atresia

phenotype (Svensson et al., 2000). However, no change in *Fog2* expression was observed (Fig. 9A, B). Deletion of *TgfβR2* from the endothelium results in DILV (Jiao et al., 2006). Analysis of *TgfβR2* expression revealed no differences between *H2CKO* and controls (Fig. 9C, D). Although not comprehensive, these analyses suggest that cell growth, cell death, myocardial, and endocardial EMT transcriptional programs are not significantly affected in *H2CKOs,* and that Hand2 is not regulating *Fog2*.

Notch signaling is known to be essential for proper trabeculation (Grego-Bessa et al., 2007). To better ascertain the etiology of the hypotrabeculation phenotype observed in *H2CKOs* we examined Notch pathway gene expression. We first looked at the expression of the Notch-regulated bHLH transcriptional repressors (and potential Hand2 dimer partners; Firulli et al., 2000) *Hey1* (Fig. 9E, F) and *Hey2* (Fig. 9G, H) finding that endocardial expression was not significantly changed. Next we examined expression of the direct Notch1 target *EphrinB2* (*EfnB2; Grego-Bessa et al., 2007). EfnB2* ISH showed no change in expression between *H2CKOs* and control embryos (Fig. 10A-D). However, EGF family member Neuregulin1 (*Nrg1)* is markedly downregulated at E10.5 within the endocardium of *H2CKOs* (Fig. 10E-H). *Nrg1* is a growth factor that is produced in the endocardium and is known to be a major mediator of trabeculation in the developing ventricles. *Nrg1* is dramatically downregulated in *Tie2-Cre Notch1* CKOs, and *EfnB2* systemic null embryos (Grego-Bessa et al., 2007). The maintenance of *EfnB2* and loss of *Nrg1* in *H2CKOs* suggests that Hand2 may act downstream of *EfnB2*, but upstream of *Nrg1*,

representing a novel step of the *Notch1* trabeculation and septation signaling pathway.

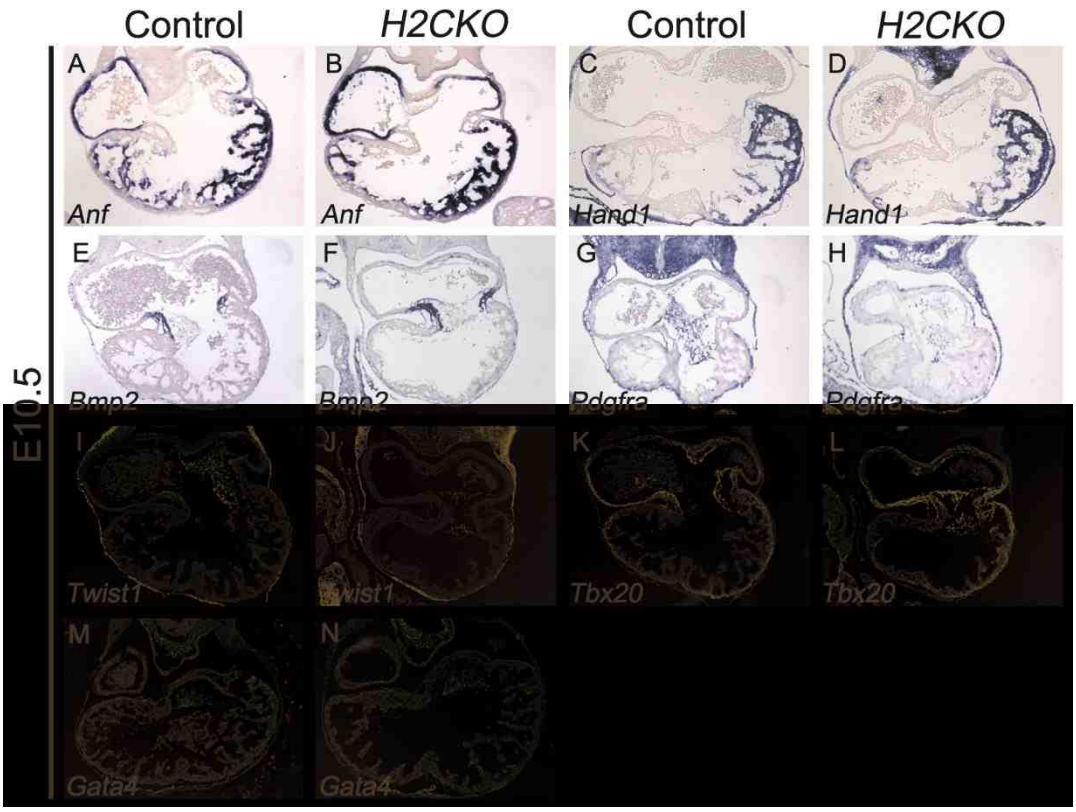

Figure 8: Additional markers analyzed in *Tie2-Cre H2CKOs*

Unchanged *Anf* (A, B) and *Hand1* (C, D) expression indicates normal patterning of the left ventricle in *H2CKOs*. Unchanged *Bmp2* (E, F) expression indicates proper formation of AVC myocardium. Unchanged *Pdgfra* (G, H), *Twist1* (I, J), *Tbx20* (K, L), and *Gata4* (M, N) expression indicates that EMT and early endocardial cushion formation occur normally in *H2CKOs*.

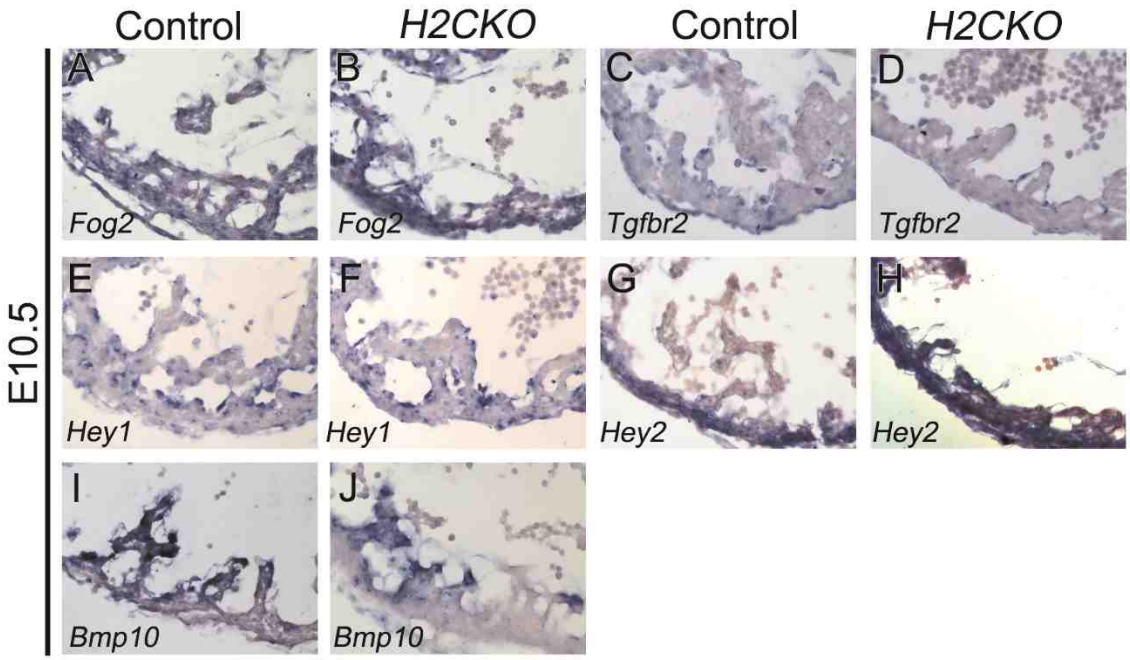

Figure 9: ISH RV images of tricuspid atresia and *Notch1* related marker expression in *Tie2-Cre H2CKOs* at E10.5.

Unchanged expression of *Fog2* (A, B) and *TgfβR2* (C, D) in *H2CKOs* indicates that endocardial loss of *Hand2* function is a novel cause of tricuspid atresia. Unchanged expression of Notch1 targets *Hey1* (E, F), *Hey2 (*G, H), indicate normal Notch1 function in *H2CKOs*. *Bmp10* expression is not altered in *H2CKOs* (I, J).

We next analyzed *Bmp10* expression, as Bmp10 is also crucial for proper trabeculation, is independently downstream of Notch1 signaling (Grego-Bessa et al., 2007), and represents a clear link to myocardial communication from the endothelium (Chen et al., 2004; Chen et al., 2006). *BMP10* ISH at E10.5 suggested a small downregulation in *H2CKOs* (Fig. 9I, J) while E12.5 ISH showed a near complete loss of *Bmp10* expressing trabecular tissue within the RV (Fig. 10I, J). To confirm that *Bmp10* expression is reduced, we then dissected out ventricles from E10.5 hearts, and isolated RNA for qRT-PCR. As expected, qRT-PCR analysis confirms that both *Hand2* and *Nrg1* are significantly downregulated in *H2CKOs* (Fig. 10K). However, the decrease in *Bmp10* expression is not statistically significant (Fig. 10K). The more dramatic loss of *Bmp10* within the RV of E12.5 *H2CKOs* reflects well the absence of RV trabeculation (Fig. 10J). In addition to trabeculation, we further hypothesize that the formation and positioning of the IVS is regulated by this Hand2-dependent endocardium to myocardium signaling, which is necessary for the formation of a patent connection between the RA and RV via the tricuspid valve.

Endocardial Hand2 functions downstream of Notch1 and the direct Notch1 target *EfnB2*

The transmembrane receptor Notch1 is a crucial factor during cardiogenesis. Upon interaction with an extracellular ligand the Notch1 intracellular domain (NICD) is proteolytically released. NICD translocates to the nucleus where it dimerizes with

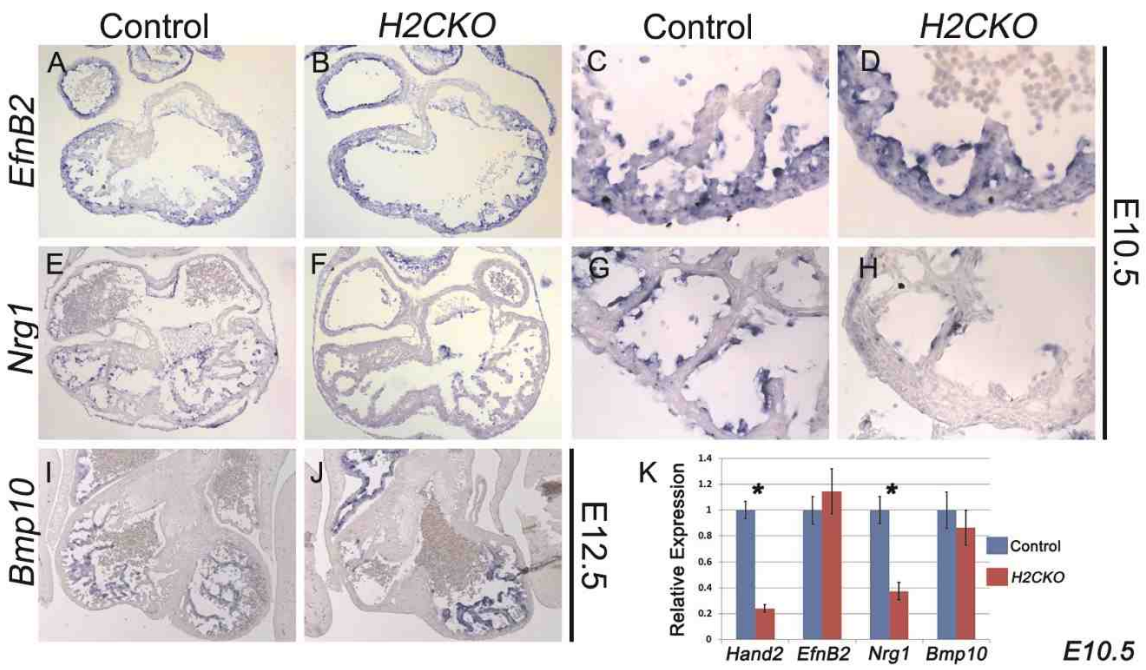

Figure 10: *H2CKOs* exhibit down-regulation of *Nrg1*, followed by loss of *Bmp10* expressing trabecular tissue.

Expression of the Notch1 target *EfnB2* is unchanged in *H2CKOs* at E10.5 when compared to controls (A-D). *Nrg1* expression at E10.5 is decreased in *H2CKOs* when compared to controls (E-H). *H2CKOs* have less *Bmp10* expressing trabecular myocardium in the RV at E12.5 (I, J). qRT-PCR on isolated ventricles confirms the reduction of *Nrg1* in E10.5 *H2CKOs,* as well as demonstrates that the majority of ventricular *Hand2* expression at E10.5 is endocardial. *EfnB2* and *Bmp10* expression is unaltered at E10.5 (K).

its partner RBPJk to activate transcription of target genes. Previous studies have shown that deletion of *Notch1* or *RBPJk* results in hypotrabeculation due to loss of *EfnB2* and *Nrg1* (Grego-Bessa et al., 2007). To confirm that *Hand2* lies within the *Notch1* signaling pathway, we assayed *Hand2* expression in E9.5 *RBPJk*$^{-/-}$ (Oka et al., 1995) embryos. Whole-mount analyses reveal a loss of cardiac *Hand2*, while expression within the OFT and pharyngeal mesenchyme is unaffected (Fig. 11A, B). Sectioned embryos revealed a specific loss of *Hand2* within mutant endocardium (Fig. 11C, D), definitively establishing its role as a Notch1 signaling effector.

During trabeculation *NICD* directly transactivates *EfnB2*, which acts through its EphB2/EphB4 tyrosine kinase receptors to upregulate *Nrg1* (Grego-Bessa et al., 2007). While our data clearly show *Hand2* to be upstream of *Nrg1* in the Notch1 trabeculation pathway, it was not clear if *Hand2* lies downstream of *EphrinB2* signaling, or if *Hand2* represents an *EfnB2* independent parallel Notch signaling pathway. To address this problem we acquired *EfnB2*$^{fx/fx}$ mice (kindly provided by Dr. Thomas Coate), and assayed *Hand2* expression in E9.5 *Tie2-Cre(+);EfnB2*$^{fx/fx}$ embryos. ISH shows that *Hand2* is downregulated in endocardial cells of *Tie2-Cre(+);EfnB2*$^{fx/fx}$ embryos (Fig. 11F arrow), while *Hand2* expression in pharyngeal mesenchyme and the proepicardial organ is unaffected when compared to *Tie2-Cre(-);EfnB2*$^{fx/+}$ control hearts (Fig. 11E). qRT-PCR analysis at E10.5 confirms *Hand2* downregulation within *Tie2-Cre(+);EfnB2*$^{fx/fx}$ isolated hearts (n = 3, Fig. 11G). Together, these data show that Hand2 is a Notch-dependent endocardial factor positioned between *EfnB2* and *Nrg1* in the transcriptional pathway controlling differentiation of the myocardium.

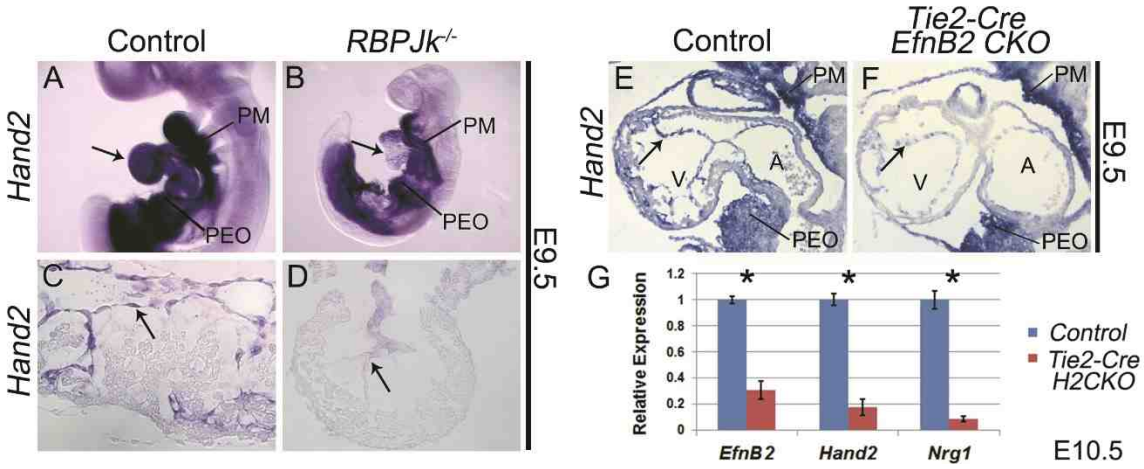

Figure 11: Hand2 functions downstream of Notch1 and the direct Notch1 target *EphrinB2* during trabeculation.

Wholemount *Hand2* ISH in wild type (A) and *RBPJk* systemic knockout embryos (B). Arrows indicate cardiac *Hand2* expression (A) and loss of expression (B). Section *Hand2* ISH (C) revealed a downregulation of Hand2 within endocardium (arrows) of RBPJk systemic knockout hearts (D). Section *Hand2* ISH (E) revealed a downregulation of *Hand2* in *Tie2-Cre EfnB2 CKO* hearts (F). Arrows indicate endocardium; PM, pharyngeal mesenchyme; PEO, proepicardial organ. qRT-PCR on isolated ventricles confirmed that endocardial ablation of *EfnB2* results in a loss of *Hand2* and *Nrg1* (G).

Hand2 regulation of *Nrg1* is direct via a 250bp *Nrg1* promoter sequence

ISH and qRT-PCR data clearly shows that Hand2 functions upstream of *Nrg1* (Fig. 10K). As *Hand2* encodes a transcription factor with a similar expression profile to *Nrg1*, we sought to determine if Hand2 regulation of *Nrg1* is direct. Although there are three distinct isoforms of *Nrg1*, *Nrg1* type one has been shown to be the predominant Neuregulin in cardiovascular development (Meyer et al., 1997), and was the focus of our analysis. Sequence corresponding to the *Nrg1* promoter was downloaded from Ensemble Genome Browser for several mammalian species, and aligned using ClustalW. As Hand2 binds the consensus sequence CANNTG, termed an E-box, or alternatively CGNNTG, a D-box, we searched the aligned promoter for conserved E-boxes and D-boxes. Three were found within 500bp of the *Nrg1* translation start site (Fig. 12A), a region previously identified as part of an 850bp promoter necessary for high *Nrg1* transcriptional activity *in vitro* (Frensing et al., 2008). To test if Hand2 directly interacts with this region of the *Nrg1* promoter, we conducted ChIP assays in HeLa cells. As antibodies to endogenous Hand2 have proven to be problematic, we employed a Myc-tagged Hand2 cotransfected with a plasmid encoding an untagged version of the Hand2 dimerization partner E12. Negative controls included Myc-Hand2 + E12 immunoprecipitated with beads only (no αMyc added), and *Pcs2+Myc* samples immunoprecipated with αMyc. Enrichment of the *Nrg1* promoter region was assessed by semiquantitative PCR using primers corresponding to a 103bp region from -426 to -324 of the human *Nrg1* promoter. This amplicon, which showed robust enrichment within Myc-Hand2 + E12 immunoprecipitated samples (Fig. 12B), is within 70bp or less

of all three conserved consensus sites. To confirm that Hand2 E12 heterodimers are capable of binding the conserved consensus sequences, radio-labeled oligos corresponding to these sites were used in electrophoretic mobility shift assays with *in vitro* translated Hand2 and E12. Hand2 E12 heterodimers were found to interact with oligos corresponding to sites 1 and 3, and this interaction could be considerably decreased by addition of excess unlabeled WT oligo (Fig. 12C, D). In contrast, addition of an excess of unlabeled mutant oligo had no effect on the interaction. No interaction was observed between Hand2 E12 complexes and an oligo corresponding to site 2. To test if Hand2 is capable of trans-activating the *Nrg1* promoter, *Hand2* and *E12* expression constructs were transfected into HeLa cells along with a *Nrg1* luciferase reporter containing the 1000bp upstream of the murine *Nrg1* translation start site. A *pGL4.74* renilla reporter was used as an internal control. Co-transfection of *Hand2* and *E12* resulted in reporter activation of approximately 7 fold. Furthermore, subsequent assays utilizing truncated 500bp (-500/0) and 250bp (-500/-250) promoters demonstrated even greater activation (~18 fold and 16 fold respectively; Fig. 12E). Transactivation data from the 500bp promoter reveal that E12 alone is not sufficient for activation, while Hand2 alone results in only mild transactivation. Consistent with EMSA results, co-transfection of Hand2 and E12 results in robust transactivation, which a DNA binding deficient Hand2 clone was unable to reproduce (Fig. 12F).

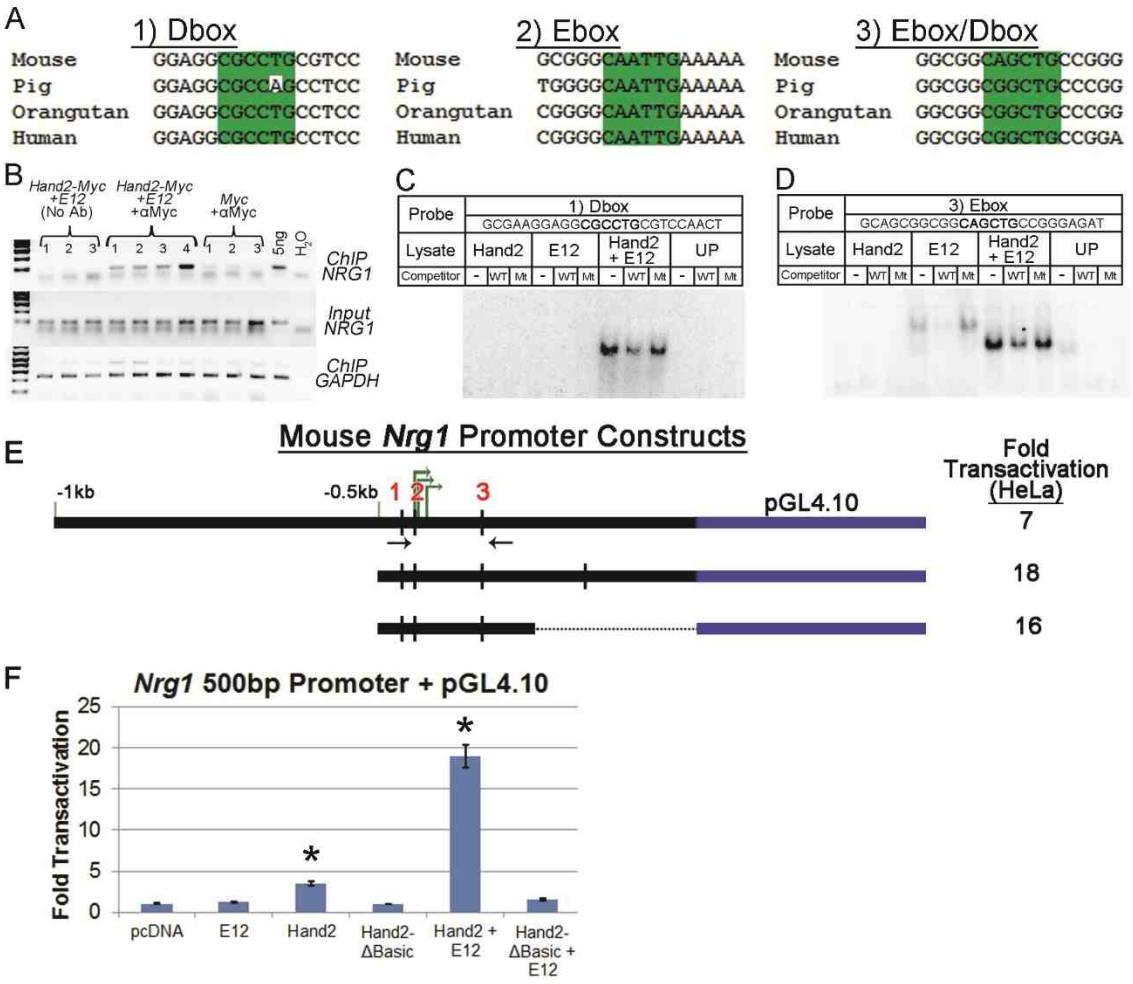

Figure 12: Hand2 directly regulates *Nrg1* via the 500bp *Nrg1* promoter

Sequence alignments reveal three Hand2 consensus sites (E-boxes and D-boxes) that are highly conserved among mammals (A). ChIP of the *NRG1* promoter. H2 indicates Hand2 transfection (B). EMSAs for sites 1 (C) and 3 (D) show robust and specific binding of Hand2 E12 heterodimers. No binding observed for site 2. Luciferase reporter assays with *Nrg1* promoters of varying length. Red numbers indicate Hand2 consensus sites, green arrows indicate transcription start sites, and black arrows indicate approximate location of human ChIP primers (E). Transactivation of luciferase reporter containing the 500bp *Nrg1* promoter. Error bars denote standard error; asterisks denote significant difference from control. (F).

Replacement of *Hand2* within *EfnB2* deficient endocardium results in a rescue of cardiac trabeculation

EfnB2 mutant embryos display hypotrabeculation accompanied by loss of *Hand2* and *Nrg1* expression. The aforementioned analyses establish that Hand2 directly regulates *Nrg1*. Therefore, if Hand2 is both necessary and sufficient for regulation of *Nrg1*, we reasoned that *Hand2* replacement in *Nfatc1^{Cre} EfnB2 CKOs* would restore *Nrg1* expression and improve the level of ventricular trabeculation. To this end, we generated a Cre-activatable *Hand2* transgene (*CAG-CAT-Hand2*). This allele was generated by replacing the *Twist1* cDNA of the *CAG-CAT-Twist1* vector (Connerney et al., 2006) with a *Hand2* cDNA. In the unrecombined state, the CMV enhancer/chicken beta-actin (*CAG*) promoter drives expression of chloramphenicol acetyltransferase (*CAT*). *CAT* and a downstream stop codon are flanked by loxP sites in such a way that recombination removes *CAT*, resulting in *CAG* promoter driven expression of the *Hand2* transgene. In this way, Cre-dependent tissue specific overexpression of *Hand2* can be achieved (Fig. 13A).

Established models of limb development have demonstrated that ectopic expression of Hand2 in limb mesenchyme results in preaxial polydactyly (Firulli et al., 2005). As predicted, *Prx1-Cre* mediated activation of *CAG-CAT-Hand2* within limb mesenchyme results in polydactyly, indicating that the transgene can be efficiently and specifically activated by Cre (Fig. 13B). Similarly, αMyc immunohistochemistry on sections of *Wnt1-Cre(+); CAG-CAT-Hand2(+)* embryos reveals activation of the *Hand2* transgene in the expected neural crest cell

populations (Fig. 13C), and *Nfatc1*^{Cre} efficiently activates *CAG-CAT-Hand2* in the endocardium (Fig. 13D). E13.5 *Nfatc1*^{Cre}*; CAG-CAT-Hand2(+)* embryos are present at Mendelian ratios and do not display any obvious cardiac phenotypes (data not shown). Subsequently, *CAG-CAT-Hand2(+)* males were crossed with *EfnB2*$^{fx/fx}$ females to generate *CAG-CAT-Hand2(+); EfnB2*$^{fx/+}$ females. These females were then crossed with *Nfatc1*^{Cre}*; EfnB2*$^{fx/+}$ males to generate *Nfatc1*^{Cre}*; CAG-CAT-Hand2(+); EfnB2 CKOs* (n = 3). *CAG-CAT-Hand2(-) EfnB2 CKOs* die by E11.5, with severe pericardial edema, hemorrhaging, and defects in cardiac looping and chamber development (Fig. 14). These phenotypes closely resemble the defects previously observed in *Tie2-Cre EfnB2 CKOs* (Gerety and Anderson, 2002), indicating that while EfnB2 function within extracardiac vasculature is likely important, loss of endocardial *EfnB2* is causative of the observed mid-gestation lethality. *Hand2* ISH at E10.5 confirms robust endocardial *Hand2* expression in controls (Fig. 15E, and F), and loss of *Hand2* in *EfnB2 CKOs* (Fig. 15G arrow). The presence of the *CAG-CAT-Hand2* allele restores *Hand2* expression within the *EfnB2 CKOs* (Fig. 15H arrow). *Nrg1* ISH reveals robust expression in controls (Fig. 15I, and J), and loss of *Nrg1* expression in *EfnB2 CKOs* (Fig. 15K arrow). *CAG-CAT-Hand2(+) EfnB2 CKOs* display an increase in *Nrg1* expression (Fig. 15L, arrow), while assessment of trabeculation by *Bmp10* ISH reveals an increase in *Bmp10* expressing trabecular myocardium (Fig. 15P arrow) when compared to un-rescued *EfnB2 CKOs* (Fig. 15 O arrow).

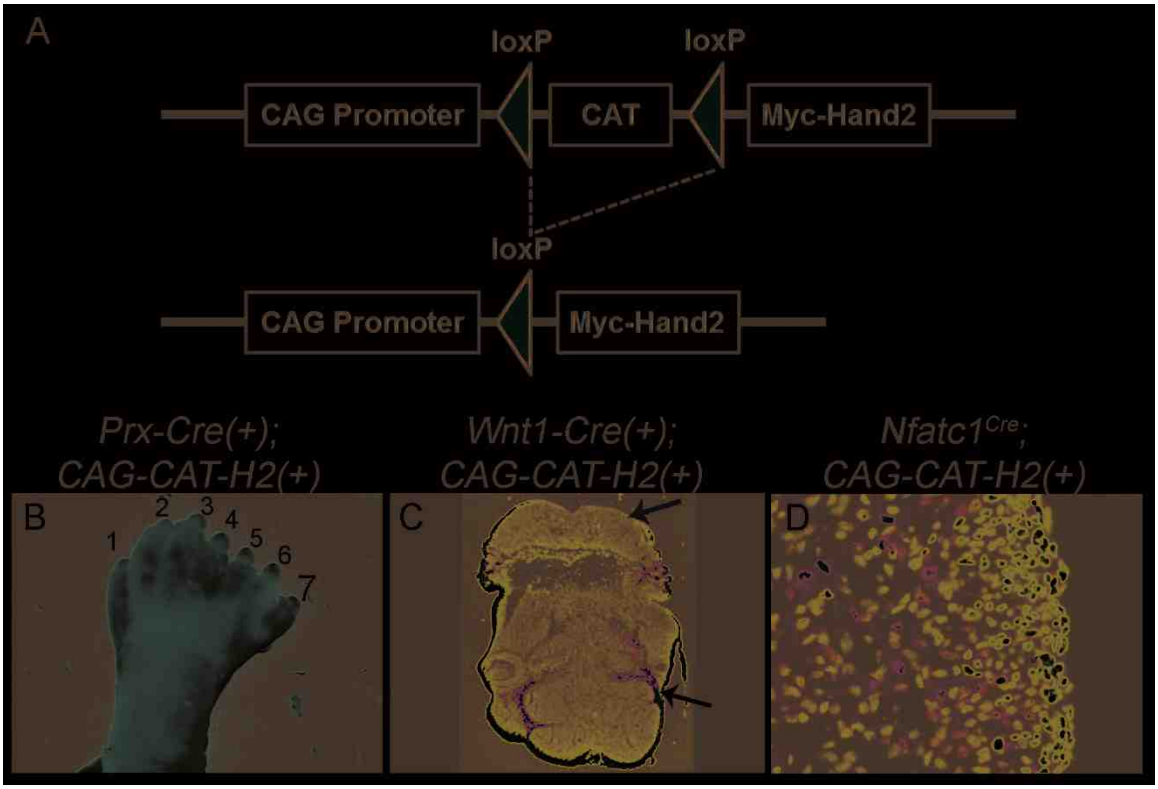

Figure 13: Construction and validation of *CAG-CAT-Hand2* allele

Schematic of CAG-CAT-Hand2 transgenic allele (A). Activation of *CAG-CAT-Hand2* with *Prx-Cre* results in polydactyly. Toes are numbered (B). Rostral section from E11.5 *Wnt1-Cre(+); CAG-CAT-Hand2(+)* embryo that exhibits exencephaly (yellow arrow). αMyc immunohistochemistry marks Hand2 transgene expressing neural crest cells in green (C; white arrow). Transverse section of E14.5 *Nfatc1^{Cre}*; *CAG-CAT-Hand2(+)* heart. αMyc immunohistochemistry marks Hand2 transgene expressing endocardial cells in green (D). *CAG-CAT-H2; CAG-CAT-Hand2*.

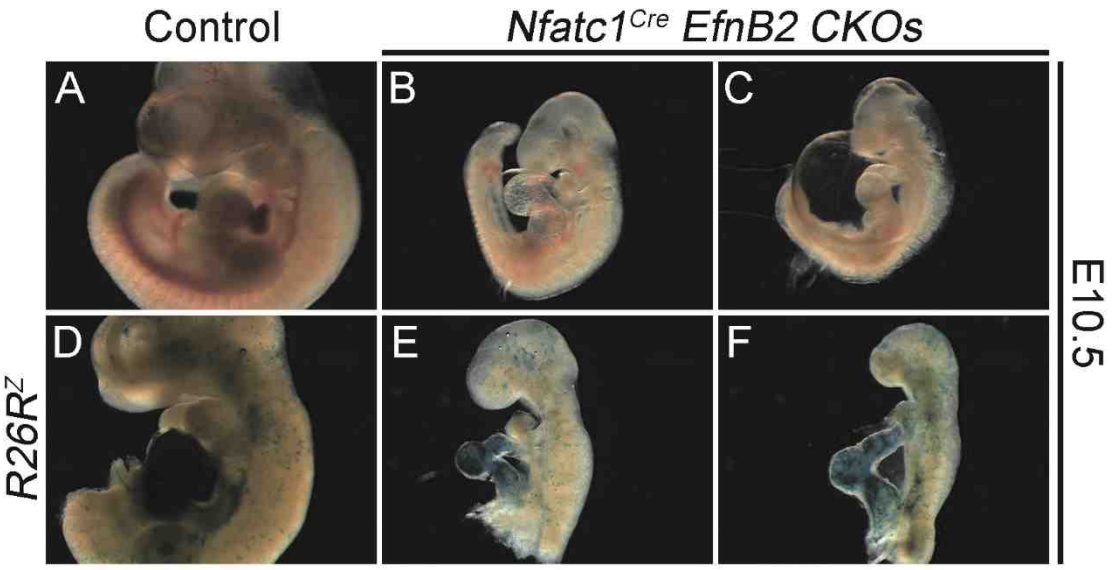

Figure 14: *Nfatc1*^{Cre} *H2CKOs* die by E11.5 with severe cardiac defects

Control embryo (A). *Nfatc1*^{Cre} *EfnB2 CKO* embryos are smaller than controls, and display severe pericardial edema and heart looping defects (B, C). *R26R* lacZ stained control and mutant embryos (D-F).

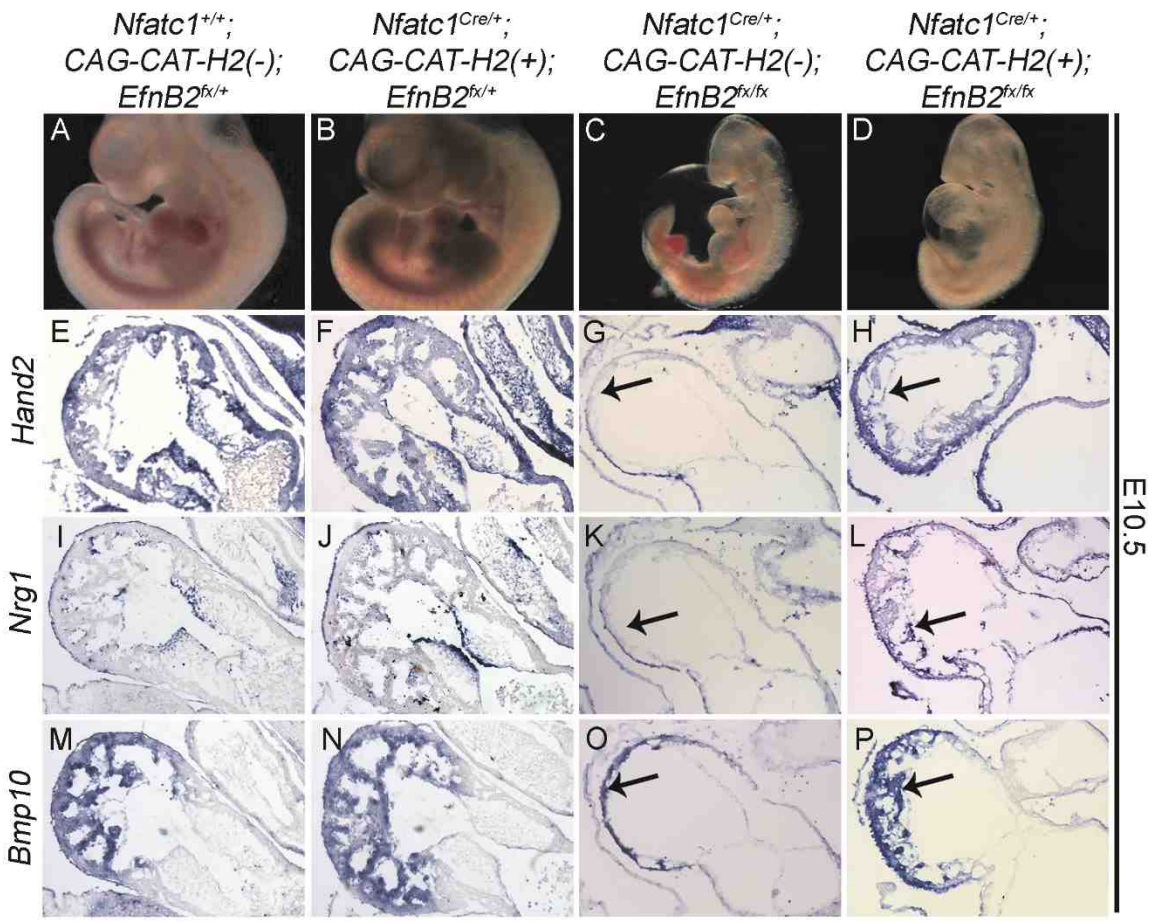

Figure 15: Activation of a *CAG-CAT-Hand2* transgene in *Nfatc1^{Cre} EfnB2 CKOs* partially rescues phenotype and *Nrg1* expression.

Wholemount images of E10.5 control, *CAG-CAT-Hand2(+)* control, mutant, and rescued mutant embryos (A-D). Section *Hand2* ISH (E-H). Arrow in G indicates loss of *Hand2*, arrow in H indicates endocardial activation of *CAG-CAT-Hand2*. Section Nrg1 ISH (I-L). Arrow in K indicates loss of *Nrg1*; arrow in L indicates increased *Nrg1* expression. Section Bmp10 ISH (M-P). Arrow in O indicates Bmp10 expressing myocardium and lack of trabeculation; arrow in P indicates restoration of *Bmp10* expressing trabeculations. *CAG-CAT-H2; CAG-CAT-Hand2.*

Notch signaling regulates coronary angiogenesis

Early embryonic lethality in genetic models of dysfunctional notch signaling has precluded an *in vivo* assessment of the role of Notch signaling in formation of the coronary arteries. As we have established Hand2 as an integral component of endocardial Notch signaling, and as coronary endothelium has recently been reported to be derived at least in part from the endocardium (Wu et al., 2012), the survival of *H2CKOs* to E14.5 allows us a unique opportunity to assess Notch function in early coronary development. Analysis of hearts at E13.5, one day after initiation of intramyocardial coronary formation (Tian et al., 2013), shows that *Nfatc1^{Cre} H2CKO* hearts (Fig. 16B, magnification D) have an increased density of primitive coronary vessels when compared to control ventricles (Fig. 16A, magnification C). To ascertain the underlying mechanism of this hypervascularization, we analyzed genes associated with vascular development in E10.5 and E13.5 isolated ventricles by qRT-PCR (n = 4, Fig. 16E and F respectively). As expected, expression levels of *Hand2* and *Nrg1* are down at both time points. Has2, which encodes an enzyme responsible for the production of hyaluronan, an ECM component necessary for trabeculation, was also downregulated at both E10.5 and E13.5 (down 33%, P-value = 0.004; down 54%, P-value = $8*10^{-4}$ respectively). Analysis of vascular markers at E10.5 reveals dysregulation of select components of Vegf signaling (Fig. 16E). *VegfR2* and the VegfR2 co-receptor *Nrp1* are downregulated by 30% and 14% respectively (P-value: 0.001 and 0.048, respectively), while *VegfD*, which encodes a VegfR3 specific ligand, is downregulated by 25% (P-value = 0.029).

By E13.5 expression levels of *VegfR2* and *VegfD* have recovered (Fig. 7F), while *Nrp1* remains modestly downregulated (P-value = $1.0*10^{-4}$). Surprisingly, expression of *VegfA*, which encodes the primary Vegf ligand that regulates vascular development (Ferrara et al., 1996), is upregulated by over 200% (P-value: 0.013). Similarly, expression of *VegfR3* is upregulated by 120% (P-value = 0.044), while expression of *Dll4*, which encodes a notch ligand regulated by VegfRs (Wythe et al., 2013), is upregulated by approximately 85% (P-value = 0.039). Differential regulation of several additional key vascular factors was also observed at E13.5. The venous markers *CouptfII* and *EphB4* are downregulated by 21 and 24% respectively (P-value = 0.022, and 0.001 respectively), while the arterial marker *EfnB2* is downregulated by 33% (P-value = 0.002). Surprisingly, *Sox18* and *Lyve1*, which encode factors typically associated with endothelium of the lymphatic system (Banerji et al., 1999; François et al., 2008), were upregulated by 45% and 73% respectively (P-value = 0.003 and 0.044 respectively). To determine what cardiac cell populations this additional expression of lymphatic associated factors was originating from, we conducted Lyve-1 immunostaining at E10.5 (Fig. 16G, H) and E13.5 (Fig. 16I-N) in control and *H2CKO* hearts. Sections were co-stained with VegfR2 to mark cardiac endothelium. E10.5 immunostaining reveals that Lyve-1 is expressed throughout the ventricular endocardium of both control and *H2CKO* hearts. In contrast, by E13.5 Lyve-1 immunostaining in control hearts is restricted to peripheral endothelium which will give rise to the cardiac lymphatic system (Fig. 16I), while robust Lyve-1 immunostaining persists in the ventricular endocardium of

H2CKOs (Fig. 16J, L). However, while Lyve-1 marks E13.5 ventricular endocardium of *H2CKOs* (Fig. 16N white arrow), Lyve-1 expression does not mark coronary endothelium (Fig. 16N yellow arrow).

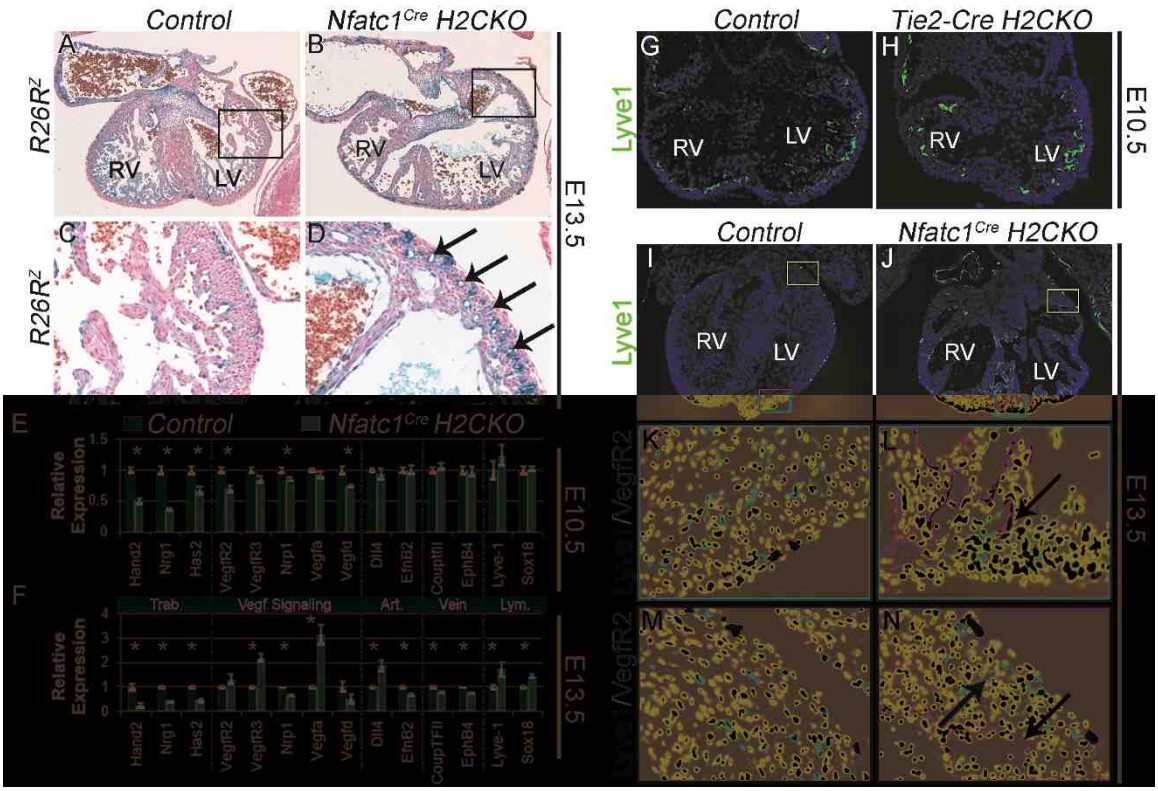

Figure 16: Hand2 controls coronary development and endocardial maturation via regulation of vegf signaling

R26R lacZ stained E13.5 hearts (A, B). LV outer curvature of *R26R* lacZ stained hearts (C, D). *Nfatc1*^{Cre} *H2CKOs* display hypervascularization. qRT-PCR analysis of E10.5 and E13.5 gene expression in *Nfatc1*^{Cre} *H2CKOs* (E, F). Asterisks denote a statistically significant difference between control and *H2CKO* expression levels (n = 4). Lyve-1 immunostaining in E10.5 Control and *Tie2-Cre H2CKO* hearts (G, H). Lyve-1 immunostaining in E13.5 Control and *Nfatc1*^{Cre} *H2CKO* hearts (I-N). In control hearts Lyve-1 expression is restricted to endothelial lymphatic precursors by E13.5 (K), while *H2CKOs* continue to express Lvye-1 within ventricular endocardium (white arrow in L). Persistent Lyve-1 expression marks ventricular endocardium (white arrow in N) but not coronary endothelium (yellow arrow in N).

Ablation of Hand2 in endocardium derived cushion mesenchyme

During cardiac development a subset of *Hand2* expressing endocardial cells undergo EMT and populate the AV cushions. *Hand2* expression is initially maintained in these mesenchymal cells, which will remodel to form the mature valves. However, Hand2 function in AV cushion mesenchyme has not been investigated. As both *Nfatc1*^{Cre} and *Tie2-Cre H2CKOs* die before the organization of the mature valves can be evaluated, an alternative Cre recombinase is needed. The enhancer controlling Periostin Cre (*Postn-Cre*) activity is reportedly induced at approximately E10.5 within mesenchymal cells of the AV cushions, but not within ventricular endocardium (Lindsley et al., 2007), making the *Postn-Cre* ideal for this experiment. Therefore, the *Postn-Cre* was utilized to selectively ablate *Hand2* from valve mesenchyme. Timed matings between *Postn-Cre(+)*;*Hand2*$^{fx/+}$ males and *Hand2*$^{fx/fx}$*;R26R*$^{z/z}$ females were conducted and the embryos collected at various time points from mid-gestation to birth. As *Postn-Cre* activity was evident by E11.5, hearts from E12.5 embryos were used to compare Cre lineage to *Hand2* expression. As expected, β-galactosidase staining within the E12.5 heart robustly marks the AV cushion mesenchyme (black arrow Fig. 17A), as well as a small population of cells within the epicardium from which a population of cardiac myofibroblasts are derived. *Hand2 in situ* hybridizations (ISH) similarly confirm that *Hand2* expression overlaps with *Postn-Cre* lineage within AV valve mesenchyme, but *Postn-Cre* lineage does not overlap with *Hand2* expression within the endocardium (Fig. 17A-C). *Hand2* ISH of *H2CKO* embryos shows significant *Postn-Cre*-mediated deletion of *Hand2*

within AV cushions (asterisks in Fig. 17C), in contrast to unaffected *Hand2* expression within the endocardium.

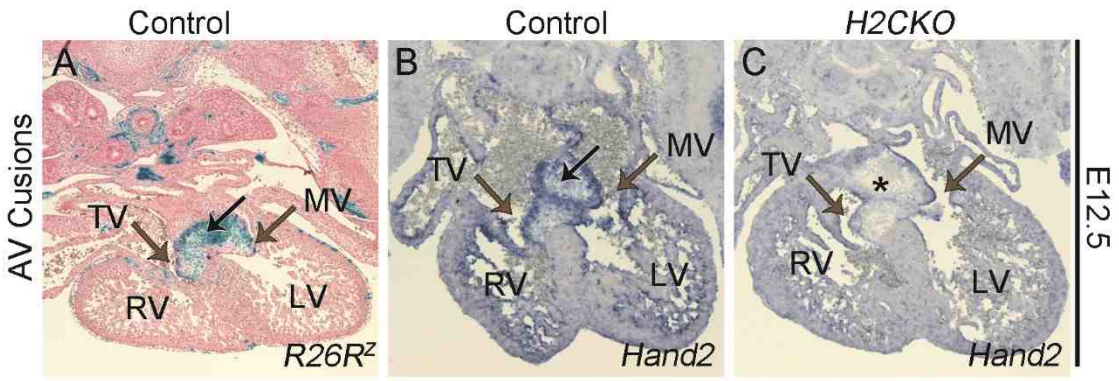

Figure 17: *Postn-Cre* mediated deletion of *Hand2* from AV cushions.

Transverse section of *Postn-Cre(+)* lacZ stained control AV cushion at E12.5 (A). *Hand2* ISH of control (B) and *H2CKO* (C) AV cushion. Black arrows indicate cushion mesenchyme; brown arrows indicate tricuspid and mitral valves. Asterisk indicates deletion of *Hand2*; right ventricle, RV; left ventricle, LV.

	Postn-Cre(-)	*Postn-Cre(+); Hand2fx/+*	*Postn-Cre(+); Hand2fx/fx*
E12.5	21 (22)	11 (11)	13 (11)
E14.5	7 (5)	1 (3)	3 (3)
E16.5	9 (7)	4 (4)	1 (4)
E18.5	30 (29)	15 (15)	13 (15)
P10	29 (23)	16 (11)	0 (11)

Table 2: *Postn-Cre H2CKOs* die shortly after birth

Genotypes and numbers of embryos collected at various stages of development. Expected number in parentheses.

Postn-Cre H2CKOs are viable at birth, but die within the first 10 days of life (Table 2). A small portion of *Hand2*$^{fx/fx}$ pups die from cleft palate (Fig. 18); however, the occurrence of the palate defect is independent of the presence of the *Cre* allele, and results from hypomorphic expression, which has been previously reported with this *Hand2* conditional allele (Morikawa et al., 2007). To determine whether *H2CKOs* exhibit AV valve phenotypes, E18.5 hearts were sectioned and analyzed by alcian blue staining, which marks proteoglycans within the heart valves (Fig. 19A, B). No significant differences in size or shape between control and *H2CKO* AV valves are observed. Furthermore, alcian blue staining reveals comparable proteoglycan levels and distribution in control (Fig. 19A) and *H2CKO* valves (Fig. 19B). E18.5 *Hand2* ISH reveals that *Hand2* expression is restricted to the endocardium overlying AV canal valves, and is not detectable within the valve mesenchyme of either control (Fig. 19C) or *H2CKO* (Fig. 19D) leaflets. ISH shows no significant difference in expression of the ECM component *Postn* within the mesenchymal cells of the cushions of control (Fig. 19E) and *H2CKO* (Fig. 19F) embryos. These data indicate that Hand2 has no obvious cell-autonomous role in AV cushion remodeling.

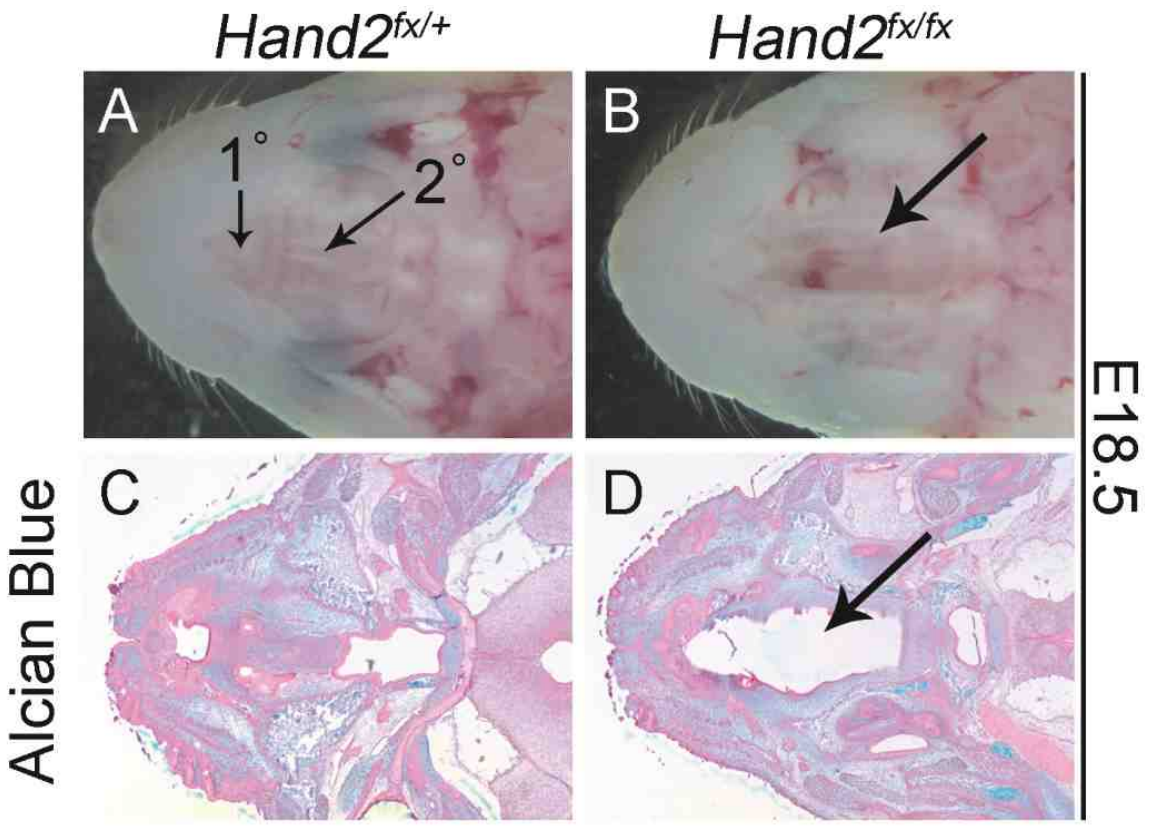

Figure 18: *Hand2*$^{fx/fx}$ mice have low penetrance cleft palate.

Wholemount picture of *Hand2*$^{fx/+}$ (A) and *Hand2*$^{fx/fx}$ (B) palate with lower jaw dissected away. Alcian blue stained transverse sections of *Hand2*$^{fx/+}$ (C) and *Hand2*$^{fx/fx}$ (D) palate. Arrows in (B) and (D) indicate cleft. Primary palate, 1˚; Secondary palate, 2˚.

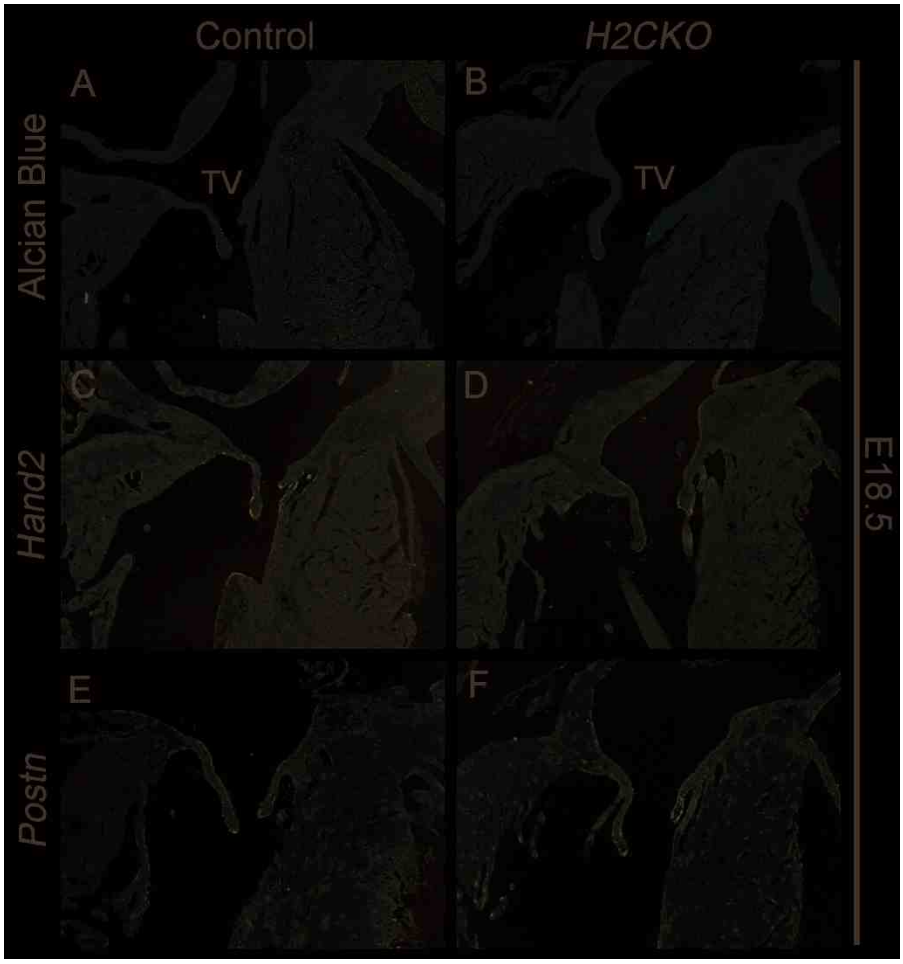

Figure 19: *Postn-Cre H2CKO* AV valves are normal at E18.5.

Alcian blue stained section of E18.5 control (A) and *H2CKO* (B) tricuspid valve (TV). *Hand2* ISH of control (C) and *H2CKO* (D) tricuspid valve. *Postn* ISH of control (E) and *H2CKO* (F) tricuspid valve.

D. Discussion

Loss of *Hand2* within a pool of progenitors that originate in the pharyngeal mesenchyme and give rise to both endocardium and myocardium has been associated with TA (Tsuchihashi et al., 2011). In this study we show that loss of *Hand2* specifically in the endocardium, a cell population where robust *Hand2* expression has previously gone uninvestigated, also results in TA. While we cannot rule out the possibility that loss of *Hand2* within a subpopulation of SHF derived myocardium would also result in a TA phenotype, the absence of TA in the myocardial *cTnT-Cre H2CKOs* (Morikawa and Cserjesi, 2008), as well as SHF *Islet1-Cre* and *Tbx20-Cre H2CKOs* (Tsuchihashi et al., 2011) suggests this is unlikely. In addition, our data show that *Hand2* plays an important role in Notch dependent endocardium to myocardium signaling, and this signaling regulates trabeculation as well as septal position and morphogenesis. Indeed, severe myocardial abnormalities in E13.5 *H2CKOs* include large muscular protrusions that resemble multiple septums. These myocardial protrusions express the septal marker *Irx2* and compact zone/septal marker *Hey2*, while excluding expression of the trabecular marker *Anf* (Fig. 20). These data suggest that Hand2 balances the specification of trabecular and septal myocardium from primitive myocardium. Our results indicate that Hand2 influences myocardial identity through regulation of the secreted factor Nrg1. These results are consistent with previous reports that mice lacking either Nrg1 or the Nrg1 receptor ErbB2 do not develop trabecular myocardium (Lee et al., 1995; Meyer and Birchmeier, 1995). Furthermore, E12.5 embryonic hearts homozygous for an allele encoding a DNA

binding deficient form of Hand2 are reported to be hypotrabeculated with a smaller RV and dilated LV (Liu et al., 2009).

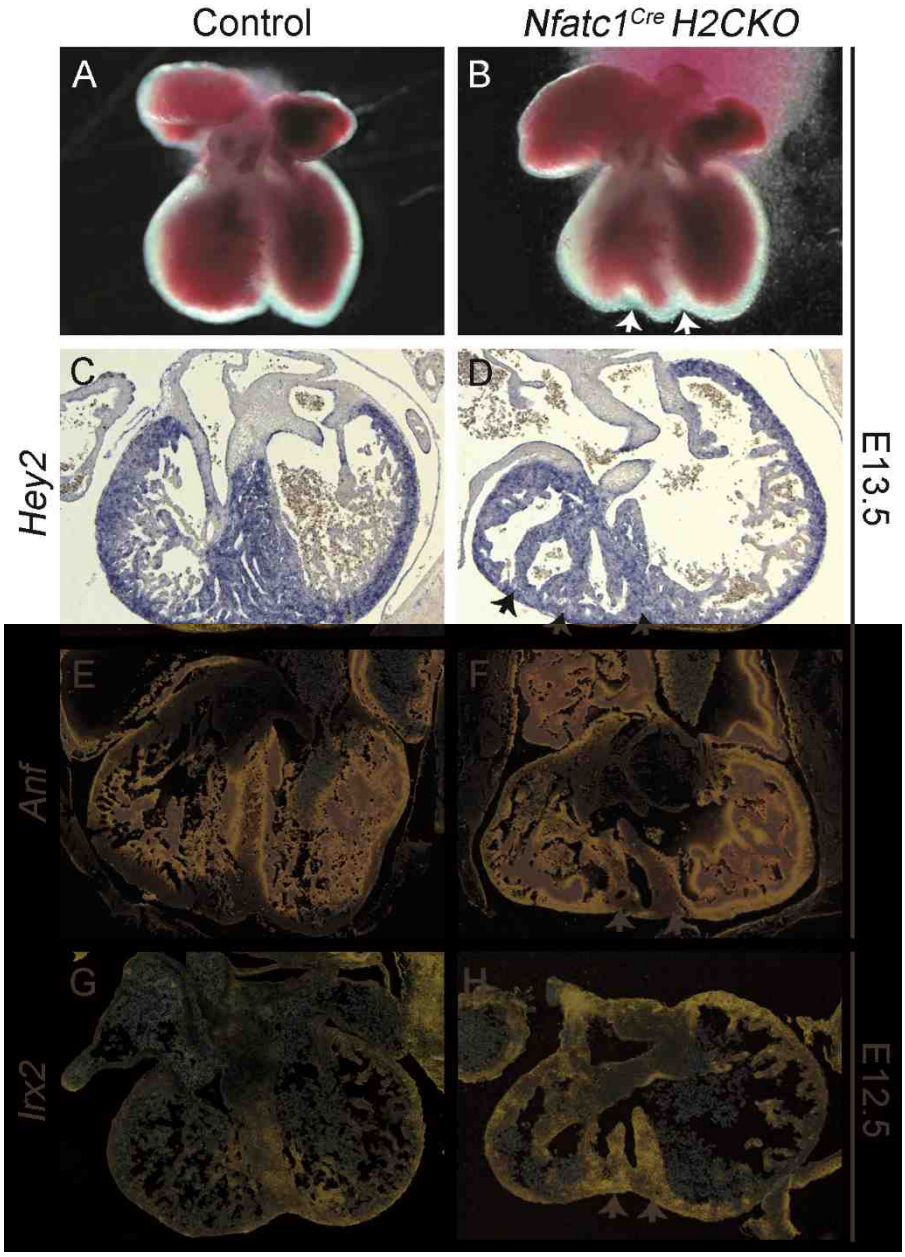

Figure 20: A subset of *Nfatc1^{Cre} H2CKOs* displays multiple septums, which are marked by *Hey2* and *Irx2.*

Wholemount images of E13.5 control and *Nfatc1^{Cre} H2CKO* hearts (A-B). *Hey2* section ISH of control and *Nfatc1^{Cre} H2CKO* at E13.5 (C-D). *Anf* section ISH of control and *Nfatc1^{Cre} H2CKO* at E13.5 (E-F). *Irx2* section ISH of control and *Nfatc1^{Cre} H2CKO* at E12.5 (G-H). Arrow heads denote septal tissue.

While it is clear that endocardial loss of *Hand2* impairs the Notch dependent processes of trabeculation and septal development, it is less clear how this impairment results in TA. It is possible that multiple morphogenic factors contribute to the TA observed in *H2CKOs*. Previous studies have concluded that TA occurs when the atrial connection to the AV canal expands rightward, but the ventricular inner curvature fails to remodel (Kim et al., 2001). Given the dramatic myocardial defects observed in *H2CKOs*, Hand2 dependent endocardial to myocardial signaling almost certainly regulates the remodeling of AV canal myocardium at some level; however, histological analysis of *H2CKOs* suggests that a rightward shifted septum fuses with cushion and RV myocardium in such a way that further development of the primitive right AV canal is blocked. Regardless, this study conclusively shows for the first time that endocardial dysfunction resulting from ablation of *Hand2* can result in TA.

In addition to identifying *Nrg1* as a downstream target of Hand2, we also identify two upstream regulators. By demonstrating a loss of *Hand2* in endocardium lacking *RBPJk* or *EfnB2* we identify Hand2 as a crucial downstream effector of endocardial Notch signaling. While *EfnB2* is reported to be directly activated by Notch1, it is not clear how EfnB2 and its receptor tyrosine kinase EphB4 regulate *Hand2* expression. To address this mystery, an attempt to locate the Hand2 endocardial enhancer and characterize its responsiveness to Ephrin signaling is underway. Our finding that endocardial Hand2 is a Notch effector correlates well with previous reports that TA is among the range of phenotypes observed in the Notch effector Hey2 systemic mutants (Donovan et al., 2002;

Sarkozy et al., 2005). Interestingly, while we show *Hey2* expression to be unaffected in E10.5 *H2CKOs*, *Hand2* is reported to be markedly downregulated in *Hey1/Hey2* double knockout embryos (Kokubo et al., 2005). Furthermore, as E-box binding bHLH factors co-expressed within the endocardium, the additional possibility that Hand2 and Hey factors are dimerization partners further complicates data interpretation. In fact, a recent ChIP-Seq study of Hey binding sites within transduced HEK-293s indicated that both Hey1 and Hey2 interact with the 500bp *Nrg1* promoter (Heisig et al., 2012). Furthermore, assessment of *Nrg1* expression in *Hey2* knockout and *Hey1/3* double knockout E14.5 ventricles revealed approximately 3 fold and 2.5 fold increases, respectively. While we do not observe any synergy or antagonism between Hand2 and Hey factors in *Nrg1* trans-activation assays (data not shown), the possibility that these factors act in a complex combinatorial fashion *in vivo* cannot be ruled out.

During development *Nrg1* is expressed throughout the arterial vasculature, while *Hand2* expression in extracardiac endothelial cells has not been reported. Interestingly, *Hand2* ISH at E10.5 does reveal expression within endothelium of the dorsal aorta, while expression within the cardinal vein is absent (Fig. 21B, C). This expression profile closely resembles that of *Nrg1* (Fig. 21D, E), and is consistent with reports that *Notch* is expressed in arterial endothelium, but not venous endothelium (Villa et al., 2001). These data suggest that Hand2 may play an important role in *Nrg1* regulation within an arterial subset of extracardiac endothelium as well as the endocardium.

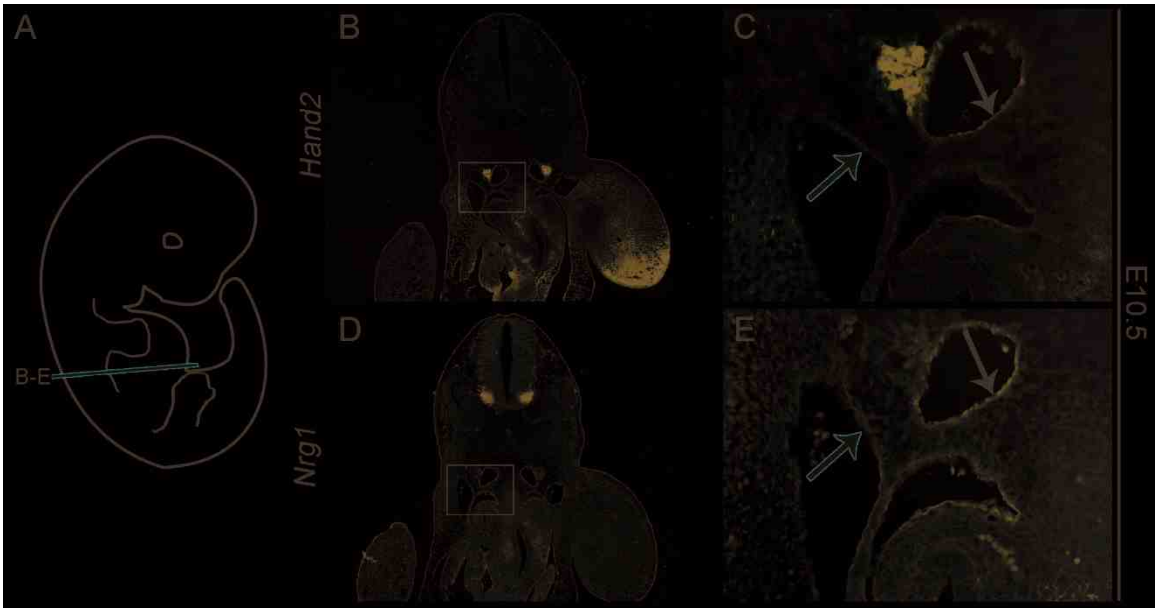

Figure 21: *Hand2* and *Nrg1* are co-expressed within the dorsal aorta.

Schematic showing plane of section for panels B-E (A). Hand2 ISH in wild-type E10.5 embryo (B); box represents panel (C). Black arrow indicates Hand2 expression in endothelium of the dorsal aorta, red arrow indicates lack of expression within endothelium of the cardinal vein. Nrg1 ISH in wild-type E10.5 embryo (D). Box represents panel (E). Black arrow indicates *Nrg1* expression in endothelium of the dorsal aorta, red arrow indicates lack of expression within endothelium of the cardinal vein.

To determine if Hand2 is independently sufficient to drive *Nrg1* expression, or if Ephrin signaling utilizes additional downstream effectors to cooperatively regulate *Nrg1*, we attempted to rescue *Nrg1* expression and trabeculation in *Nfatc1^{Cre} EfnB2 CKOs* using a Cre activatable *Hand2* transgene (*CAG-CAT-Hand2*). *CAG-CAT-Hand2(+) EfnB2 CKOs* displayed markedly improved trabeculation, as visualized by *Bmp10* ISH, and increased expression of *Nrg1*. However, while *Nrg1* expression was increased, it was not restored to control levels, and rescued mutants still displayed hallmarks of cardiovascular failure such as pericardial edema. These results indicate that Hand2 is a crucial component of *Nrg1* regulation that is sufficient to drive at least low levels of *Nrg1* expression; however, Ephrin signaling appears have additional inputs into *Nrg1* expression, and almost certainly modulates cardiovascular development via mechanisms independent of both *Hand2* and *Nrg1*. Our observation that approximately 37% of *Nrg1* expression remains in *Tie2-Cre H2CKOs* (Fig. 10K) while less than 10% remains in *Tie2-Cre EfnB2 CKOs* (Fig. 11G), supports this notion.

While Hand2 has long been appreciated as a regulator of ventricular morphogenesis, we demonstrate for the first time that proper development of the primitive coronary vasculature is dependent on endocardial *Hand2* expression. The exact origins of the coronary endothelium are still being debated (see Zhang and Pu, 2013 for review), but recent data indicate that the coronary plexus forms by angiogenesis (Red-Horse et al., 2010; Wu et al., 2012), and the endocardium makes an important contribution (Wu et al., 2012). Although dramatic defects in

myocardial morphogenesis can be observed in *H2CKOs*, histological analyses at E13.5 also reveal endocardial phenotypes. *H2CKOs* display precocious and disorganized development of the coronary vascular plexus. Analysis of vascular related gene expression in E10.5 and E13.5 *H2CKOs* by qRT-PCR surprisingly reveals that nearly all of the major components of cardiac Vegf signaling are differentially expressed. *VegfR2* and *VegfD* are downregulated at E10.5, while *VegfR3* and *VegfA* are significantly upregulated by E13.5. Additionally, VegfR2 co-receptor *Nrp1* is downregulated at both E10.5 and E13.5, while expression of the notch ligand *Dll4* is increased at E13.5. Other genes differentially expressed in E13.5 *H2CKOs* include the venous markers *CouptfII* and *EphB4* (downregulated), as well the lymphatic associated marker *Sox18* (upregulated). Interestingly, *EfnB2* is moderately downregulated at E13.5, possibly indicating the presence of a Hand2 feedback loop. *VegfA* is the most upregulated gene in our dataset, and as VegfA is well known for its pro-angiogenic qualities (Ferrara et al., 2003; Gerhardt et al., 2003), these molecular analyses correlate well with the observed hyper-vascularization phenotype. Furthermore, qRT-PCR and immunostaining reveals elevated expression of the receptor Lyve-1 within endocardium of E13.5 *H2CKOs*. Analysis at E10.5 demonstrates that Lyve-1 is initially expressed throughout the endocardium, and is subsequently suppressed, such that by E13.5 strong expression is no longer visible within ventricular endocardium, but only within inflow tract derived peripheral endothelial cells that will give rise to the cardiac lymphatic system. Given the early endocardial expression of Lyve-1, this persistence within *H2CKOs* most likely represents a

defect in endocardial maturation, rather than ectopic activation of the lymphatic gene program. Of the genes we observed to be differentially expressed in E13.5 *H2CKOs*, only *Nrp1* is also downregulated at E10.5. *Nrp1* encodes an isoform specific VegfA receptor that acts in concert with VegfR2 (Soker et al., 1998). Interestingly, an RNA subtractive hybridization screen previously identified *Nrp1* as being downregulated in Hand2 systemic null embryos (Yamagishi et al., 2000). Our data demonstrate that *Nrp1* is an endocardial target of Hand2, although regulation may also occur in additional tissues such as smooth muscle. Expression of *VegfR3* is upregulated in E13.5 *H2CKOs* by over 100%. VegfR3 is capable of functioning as both a homo-dimer and VegfR3-VegfR2 hetero-dimer, and distinct functions have been associated with different interactions (Dixelius et al., 2003). VegfR3 has been demonstrated to play crucial roles in angiongenic sprouting and development of the lymphatic system (Benedito et al., 2012; Veikkola et al., 2001). Given that we have established Hand2 as a downstream effector of Notch signaling, and Notch reportedly regulates expression of *VegfRs* (Herbert and Stainier, 2011), we considered the possibility that Hand2 directly regulates *VegfR3* expression. Using the previously described HeLa ChIP samples, we show that immunoprecipitation of *Hand2-Myc/E12* transfected cell lysates results in selective enrichment of a region within the *VegfR3* promoter that has been reported to have regulatory activity (Fig. 22A; Shawber et al., 2007). Furthermore, by EMSA we show that Hand2 E12 heterodimers can specifically bind an oligo corresponding to one of the two E-boxes within this promoter region (Fig. 22B), which consists of the 500bp upstream of the *VegfR3*

translation start site. Finally, a luciferase reporter containing the mouse *VegfR3* promoter (-500/0), was repressed by Hand2 E12 heterodimers (~ 50% repression, Fig. 22C). Collectively these data indicate that Hand2 directly represses *VegfR3* expression within cardiac endothelium.

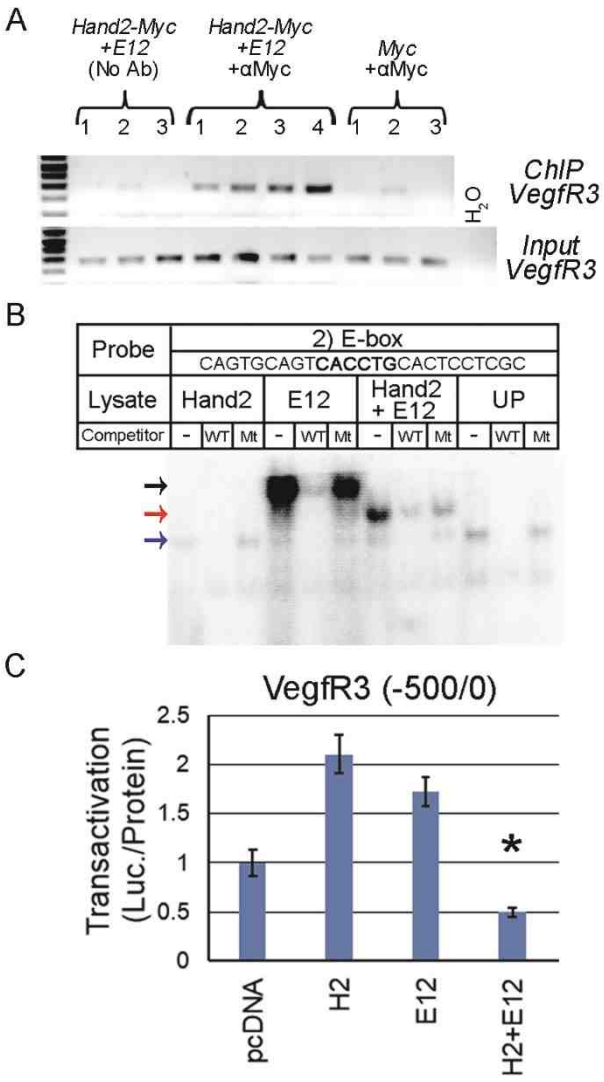

Figure 22: Hand2 directly regulates *VegfR3*

ChIP of a region within the 500bp *VegfR3* promoter (A). EMSA demonstrates Hand2 E12 heterodimers can specifically bind an oligo corresponding to an E-box within the human *VegfR3* promoter (B). Black arrow indicates E12 binding, red arrow indicates Hand2 E12 heterodimer binding, and blue arrow indicates nonspecific binding. Hand2 E12 heterodimers repress a luciferase reporter containing the homologous mouse 500bp *VegfR3* promoter (C). Error bars denote standard error; asterisk denotes significant difference from pcDNA control.

Similar to several extracardiac angiogenic models of Notch signaling obstruction (Benedito et al., 2012; Hellstrom et al., 2007; Larrivee et al., 2012; Tammela et al., 2008), we show that endocardial *Hand2* ablation results in a hyper-vascularization phenotype featuring the formation of an excessive number of new vessels. Furthermore, we show that this phenotype is accompanied by broad dysregulation of Vegf signaling. Homeostasis of Vegf signaling is crucial during embryonic development, as mice heterozygous for a *VegfA* null mutation die at E9.5, while an increase in *VegfA* expression (~3 fold) results in lethality at approximately E13.5 (Miquerol et al., 2000). Given the alterations observed in expression of *VegfA*, *VegfD*, *VegfR2*, *VegfR3*, and *Nrp1* within *H2CKOs*, dysregulation of Vegf signaling and a consequential defect in endocardial maturation most likely account for the observed coronary phenotype. These data not only provide insight into a second novel function of Hand2 within the endocardium, but also reveal a wider role of Notch signaling during coronary vessel development. Coronary heart disease is a major cause of mortality in developed nations, being responsible for approximately one of every six deaths in the United States (Go et al., 2013). As such, there is great interest in better understanding the molecular processes that regulate coronary formation and function. While much remains to be done, the results of this study bring us one step closer to the depth of understanding that will be necessary if we are to engineer efficacious treatments.

Collectively, our data reveal multiple novel roles for Hand2 in the endocardium where loss-of-function results in a TA phenotype. Histological analyses

indicate that the observed TA is a direct result of aberrant septal morphogenesis. We show that Hand2 participates in both endocardium-to-myocardium and endocardium-to-endocardium based Notch signaling, with striking phenotypes associated with dysfunction. Endocardial *Hand2* expression is regulated by Notch1 via EfnB2, and directly activates production of the crucial secreted growth factor Nrg1. In addition, Hand2 mediates proper development of the coronary vasculature by modulating Vegf signaling. Importantly, these studies suggest that mutations in the *HAND2* locus, as well as additional components of endocardial Notch signaling, are a possible cause of TA in humans. Additional studies will be necessary to fully elucidate the contribution of endocardial Hand2 dysfunction to disease.

Deletion of *Hand2* from mesenchymal cells of the cardiac cushions at E11.5, well after initiation of *Hand2* expression in endocardial precursors, does not result in any cardiac valve phenotypic abnormalities. This data supports a model in which essential Hand2 function lies within the ventricular endocardium. *Hand2* expression within the early stage cushion mesenchyme is gradually downregulated, and by E18.5, *Hand2* expression within the valves is restricted to only the *Postn-Cre*-negative endothelium covering the valve surface. We conclude that *Hand2* does not play a critical role in endocardium derived cushion cells post EMT. However, it is interesting that *Hand2* expression is robustly sustained in overlying valve endocardium, particularly on the backside of valves (ventricular side of AV canal). These data do not rule out a possible non cell-autonomous role in cushion remodeling, through endothelial to mesenchymal signaling.

Chapter III

Hand2 Function in Neural Crest Cells

A. Introduction

From early to mid-gestation *Hand2* is expressed within most cardiac cell populations, including the cNCC. Developmental analyses demonstrate that Hand2 regulates a large number of important processes in cNCCs. Targeted deletion of *Hand2* in NCC derived tissues via the *Wnt1-Cre* results in embryonic lethality at E12.5 (Morikawa et al., 2007). However, pharmacological rescue with the β-agonist isoproterenol allows for analysis of cardiovascular development to birth, as the primary cause of death is a reduction in catecholamine production within the sympathetic nervous system. In pharmacologically rescued embryos conditional ablation of *Hand2* in NCC derived tissues results in alignment defects of the aortic arch arteries and OFT, resulting in DORV with associated VSD (Holler et al., 2010; Morikawa and Cserjesi, 2008). These phenotypic abnormalities are thought to be the result of defects in cell migration, cell-cell communication/adhesion, and cell cycle regulation. Histological analysis shows that fewer cNCC reach the OFT in mutants, and that more of the migrating cells travel independently, whereas cNCC of the control embryos seem to migrate as a coherent sheet. Interestingly, Hand2 function in zebrafish development is required for proper ECM remodeling and the subsequent migration of lateral plate mesodermal cells. Hand2 is thought to regulate this migratory event by maintaining matrix metalloproteinase (MMP) activity, resulting in the diminishment of laminin deposition and proper gut looping (Yin et al., 2010).

While it is not currently clear if Hand2 regulates ECM remodeling during NCC migration, a microarray screen of RNA collected from murine E10.5 *Wnt1-Cre Hand2* conditional knockout whole hearts revealed a set of over 300 differentially regulated genes in the NCC specific *Hand2* deletion embryos, and included *Mmp14* (Holler et al., 2010). Other candidates related to cell migration included *Pdgf*, *Itga9*, *Itgα4*, *Adam19* and *Cx40*. *Cx40* was of particular interest since it is a component of cardiac gap junctions, which are major mediators of cell-cell communication in the developing heart. Interestingly, *Cx40* was strongly expressed in wild-type cNCC, but was dramatically down-regulated in *Hand2* CKO cNCC. To determine if Hand2 directly binds the *Cx40* putative promoter, chromatin immunoprecipitation assays were conducted on a *Hand2* expressing rat cardiomyocyte cell line. This pull-down showed that Hand2 binds the proximal E-box-containing regions of the *Cx40* promoter *in vitro*. Furthermore, a luciferase transactivation assay demonstrated that when co-transfected, *Hand2* and its dimer partner *E12* can modestly up-regulate *Cx40-luciferase* expression, suggesting that Hand2 regulates chemical and electrical cell-cell communication through transcriptional control of gap junction components.

In addition to cNCC migration related factors, many cell cycle related genes are differentially expressed in *Wnt1-Cre Hand2* CKOs (Holler et al., 2010). The most highly regulated of these genes (up 37 fold) was cyclin B1 interacting protein 1 (*Ccnb1ip1*), which is an ubiquitin ligase that promotes the degradation of cyclin B. While the details of its function during development remain unclear, recent malignancy related research suggests that *Ccnb1ip1* plays a role in

coordinating the cell cycle with cell migration and invasion (Singh et al., 2007) – functions required for OFT septation and valve formation. Others included *cdk6*, a serine/threonine kinase that regulates the G0 to G1 transition by phosphorylating retinoblastoma protein (Malumbres and Barbacid, 2005), *Insm1*, a regulator of NCC derived sympathetic neuron development which also interacts with cyclin D1 in the heart (Liu et al., 2006; Pellegrino et al., 2011), and several histones. Interestingly, a number of genes already associated with various aspects of cardiovascular development were found to be differentially regulated in the *Wnt1-Cre Hand2* CKO mice. One down-regulated candidate that was particularly interesting was *Sox11*, since *Sox11* null embryos develop DORV and associated VSDs as well as other OFT defects (Sock et al., 2004). Additional differentially regulated genes include the transcription factor *Foxc1*, the Notch downstream bHLH affecter and potential Hand dimer partner Hey1 (Firulli et al., 2000; Firulli et al., 2007; Kokubo et al., 2005), the metalloproteinases *MMP14* and *Adam19*, which are critical for tissue remodeling, and *NF-ATc2* which induces *NF-ATc1.* NF-ATc1 has key functions within the endocardium where Hand2 is also expressed *(Zhou et al., 2002)*. Collagen type XI a1 (*Col11a1*), which is expressed in non-cartilaginous heart tissue, has been implicated in valve development (Peacock et al., 2008), while the latent transforming growth factor beta binding protein 1 (*Ltbp1*), has also been implicated in various aspects of cardiogenesis, including OFT septation, endocardial cushion EMT, and valve remodeling (Todorovic et al., 2011). Significantly, both *Col11a1* and *Ltbp1* are down-regulated in the *Wnt1-Cre Hand2* CKOs. The Sonic Hedgehog (Shh)

signaling repressor *Gli3* was also down-regulated. *GLI3* mutations in humans are associated with isolated VSDs (Qiu et al., 2006). Interestingly, Gli3 is downstream of *Hand2* within the developing limb (Charite et al., 2000). During limb morphogenesis, Hand2 restricts *Gli3* expression to anterior mesenchyme, while Gli3 restricts *Hand2* to the posterior limb mesenchyme. This genetic interaction establishes a Shh/FGF signaling feedback loop that is essential for proper limb patterning (te Welscher et al., 2002). Since *Shh* has been demonstrated to be necessary for normal OFT development (Washington Smoak et al., 2005), it is possible that Hand2 plays a similar role within cNCC. Given the number of transcripts regulated and the range of developmental processes they are known to function in, it is clear that *Hand2* plays an important role in cNCC development. In order to more precisely define this role, additional experiments, such as Hand2 ChIP-seq, are required to determine which genes are regulated directly by *Hand2,* and which are regulated by as of yet unidentified intermediates.

Hand2 function within NCC derived components of the ANS

In addition to cNCCs, *Hand2* is widely expressed in NCC derived components of the ANS. The ANS consists of the sympathetic, parasympathetic, and enteric nervous systems. In the past decade several loss of function genetic models have been employed to identify Hand2 functions within the ANS, with critical roles being identified within both the sympathetic nervous system and the enteric nervous system. Zebrafish *Hand2* deletion mutants (*hands off*) display

appropriate generic neuronal differentiation, but noradrenergic differentiation of sympathetic ganglia is impaired (Lucas et al., 2006). In this model mutant sympathetic ganglia express *Th* and *Dbh*, two crucial catecholaminergic enzymes, at much lower levels than control ganglia. These results were recapitulated in a series of murine based studies which utilized the *Wnt1-Cre* to conditionally ablate *Hand2* from NCCs (Hendershot et al., 2008; Morikawa and Cserjesi, 2008; Morikawa et al., 2007). As was previously mentioned, early ablation of *Hand2* within the NCC lineage via the *Wnt1-Cre* results in embryonic lethality at E12.5. These studies conclude that Hand2 expression permits sympathetic neurons to acquire a catecholaminergic phenotype (Morikawa et al., 2007), and this is accomplished by regulating the expression of transcription factors necessary for noradrenergic neuronal differentiation (Hendershot et al., 2008). Furthermore, pharmacological rescue to birth with the β-agonist isoproterenol convincingly demonstrates that early embryonic lethality can be attributed to noradrenergic deficiency (Morikawa and Cserjesi, 2008). However, these studies only identify ganglia of the sympathetic chain as sites of Hand2 dependent catecholamine production. Catecholamines are synthesized at multiple additional sites, while *Hand2* is expressed within a wide range of NCC derived structures. Given the aforementioned studies, it was not clear if catecholamine production at these additional sites is also Hand2 dependent.

Murine studies utilizing *Wnt1-Cre* and the enteric specific *Nestin-Cre* demonstrate that Hand2 function is required for many aspects of proper enteric development including neurogenesis, cell type specification, proliferation of

enteric precursor cells, and gangliogenesis (D'Autreaux et al., 2011; Hendershot et al., 2007; Lei and Howard, 2011). Enteric neurons do not produce catecholamines, but are essential for proper digestion. Ablation of *Hand2* within enteric neural precursors via the *Nestin-Cre*, results in a severe bowel distention and death by approximately P20 (Lei and Howard, 2011). As *Postn-Cre H2CKO* mice die soon after birth (Table 2, Chapter 2), and the enhancer driving *Postn-Cre* expression is known to be active in NCC derived components of the PNS (Lindsley et al., 2007), we sought to determine if enteric neurons, sympathetic ganglia, or additional sites of catecholamine synthesis were compromised in *Postn-Cre H2CKOs*.

B. Methods

Mice

Generation of *Postn-Cre(+)*; *Hand2*$^{fx/fx}$ embryos and genotyping was conducted as described in Chapter II.

Section RNA *In Situ* Hybridization, quantitative RT-PCR, and Histological Preparations

In situ hybridizations, qRT-PCR, and histology were conducted as described in Chapter II.

Electrocardiograms

ECGs were recorded and processed as described previously (Shen et al., 2008). P3 pups were anesthetized with four percent isoflurane before electrode placement. Four percent isoflurane was continuously supplied via facemask and

environmental temperature was controlled via heat lamp. Electrodes were placed in both front legs and the left rear leg. Two ECG traces of approximately one minute in length were recorded for each pup, and the average heart rate was calculated. Results reflect n = 4; as previous studies have established that catecholamine insufficiency would only be expected to result in a decreased heart rate, p-value was calculated using a student's one tailed t-test.

C. Results

In addition to AV valve mesenchyme, the *Postn-Cre* lineage includes NCC derived mesenchyme of the OFT valves. X-gal staining of embryos carrying a lacZ reporter confirmed that the *Postn-Cre* lineage overlaps with Hand2 expression in OFT mesenchyme (Fig. 23A, B). Furthermore, *Hand2* ISH demonstrated that *Postn-Cre* can effectively ablate this expression in E12.5 *H2CKO* embryos (Fig. 23C). However, as with the endocardium-derived AV valves, analysis of OFT valves at E18.5 failed to reveal any remodeling defects. No differences in alcian blue staining were observed between control (Fig. 24A) and *H2CKO* (Fig. 24B) hearts, indicating that proteoglycan deposition is not impaired. *Hand2* ISH once again demonstrates that *Hand2* expression is restricted to endothelium overlying the valves (non-ventricular side of OFT valves) at late stages of embryogenesis (Fig. 24C, D). Furthermore, expression of *Postn* is unaltered in *H2CKOs* (Fig. 24E, F).

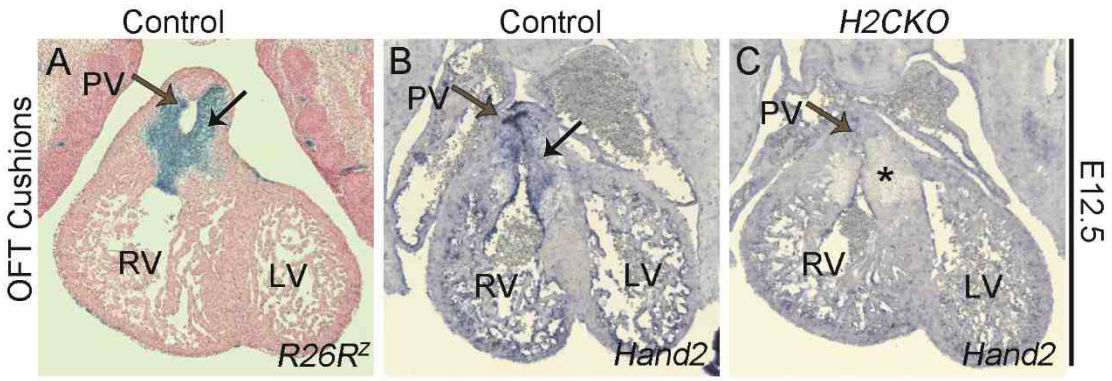

Figure 23: *Postn-Cre* mediated deletion of *Hand2* from OFT cushions.

Transverse section of *Postn-Cre(+)* lacZ stained control OFT cushion at E12.5 (A). *Hand2* ISH of control (B) and *H2CKO* (C) OFT cushion. Black arrows indicate cushion mesenchyme; brown arrows indicate primitive pulmonary valve. Asterisk indicates deletion of *Hand2*; right ventricle, RV; left ventricle, LV.

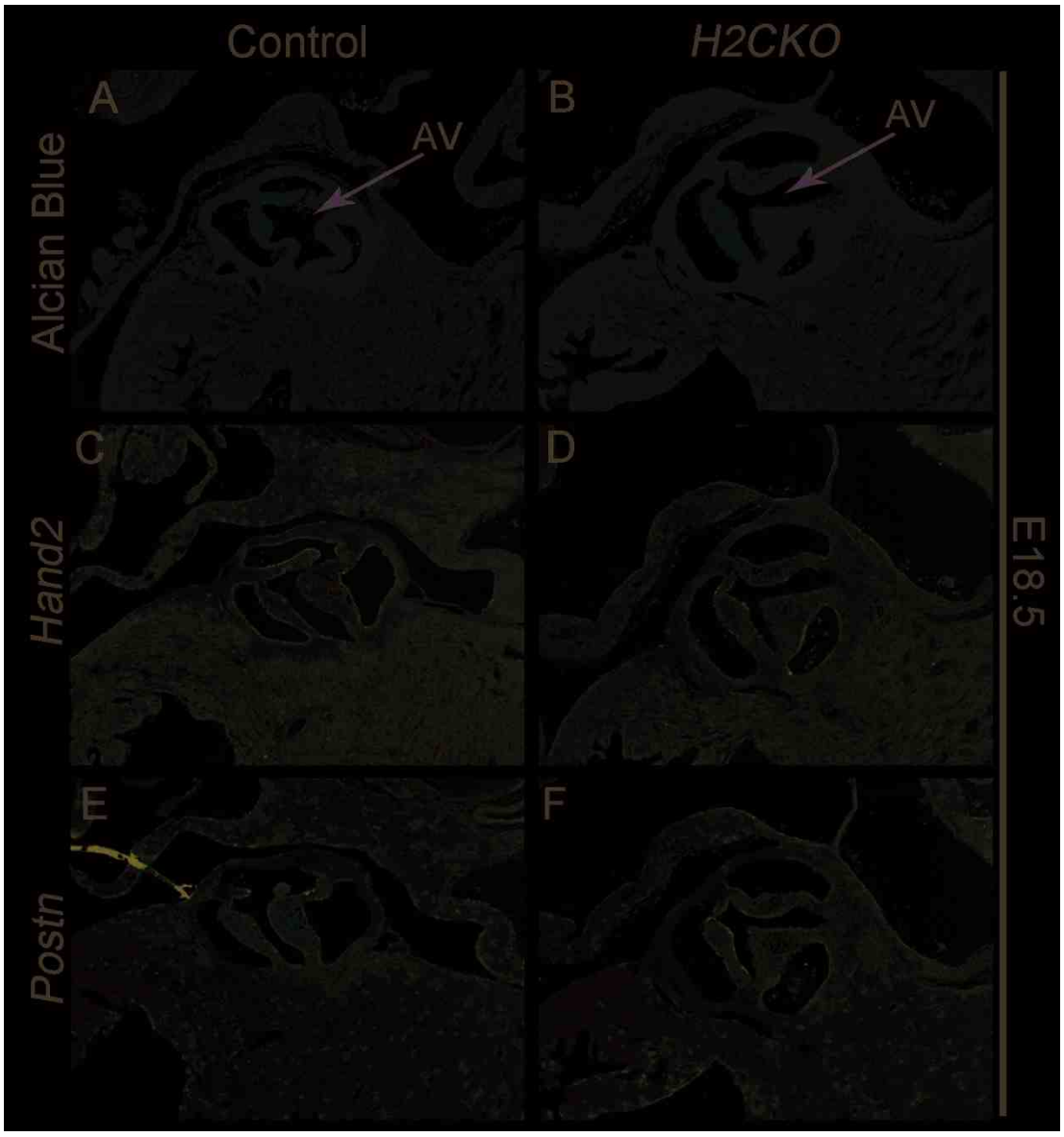

Figure 24: *Postn-Cre H2CKO* OFT valves are normal at E18.5.

Alcian blue stained section of E18.5 control (A) and *H2CKO* (B) Aortic valve (AV). *Hand2* ISH of control (C) and *H2CKO* (D) aortic valve. *Postn* ISH of control (E) and *H2CKO* (F) aortic valve.

Postn-Cre ablates *Hand2* from neurons of the enteric nervous system

As *Postn-Cre H2CKOs* die soon after birth with a failure to thrive phenotype, similar to *Nestin-Cre H2CKOs*, we first looked for defects within the developing gut. Lineage tracing at E12.5 and E16.5 shows that *Postn-Cre* indeed marks the myenteric plexus in the stomachs and intestines of control (Fig. 25A, C) and *H2CKO* embryos (Fig. 25B, D). Similarly, ISH at E16.5 confirms previous reports (Hendershot et al., 2008; Lei and Howard, 2011; Wu and Howard, 2002) that *Hand2* is also expressed within these enteric neurons (Fig. 25E). Furthermore, this expression is ablated in *H2CKOs* (Fig. 25F). To determine if this loss of *Hand2* affects viability, we dissected out and visually assessed the gastrointestinal tracts of P3 pups (Fig. 25G). While deletion of *Hand2* in enteric neural precursor cells results in gut obstruction and severe bowel distention by P20 (Lei and Howard, 2011), P3 *Postn-Cre H2CKOs* displayed a lack of fecal matter posterior to the cecal appendages (arrow Fig. 25G). This is indicative of impaired bowel motility and may contribute to the observed early neonatal death in *H2CKOs*.

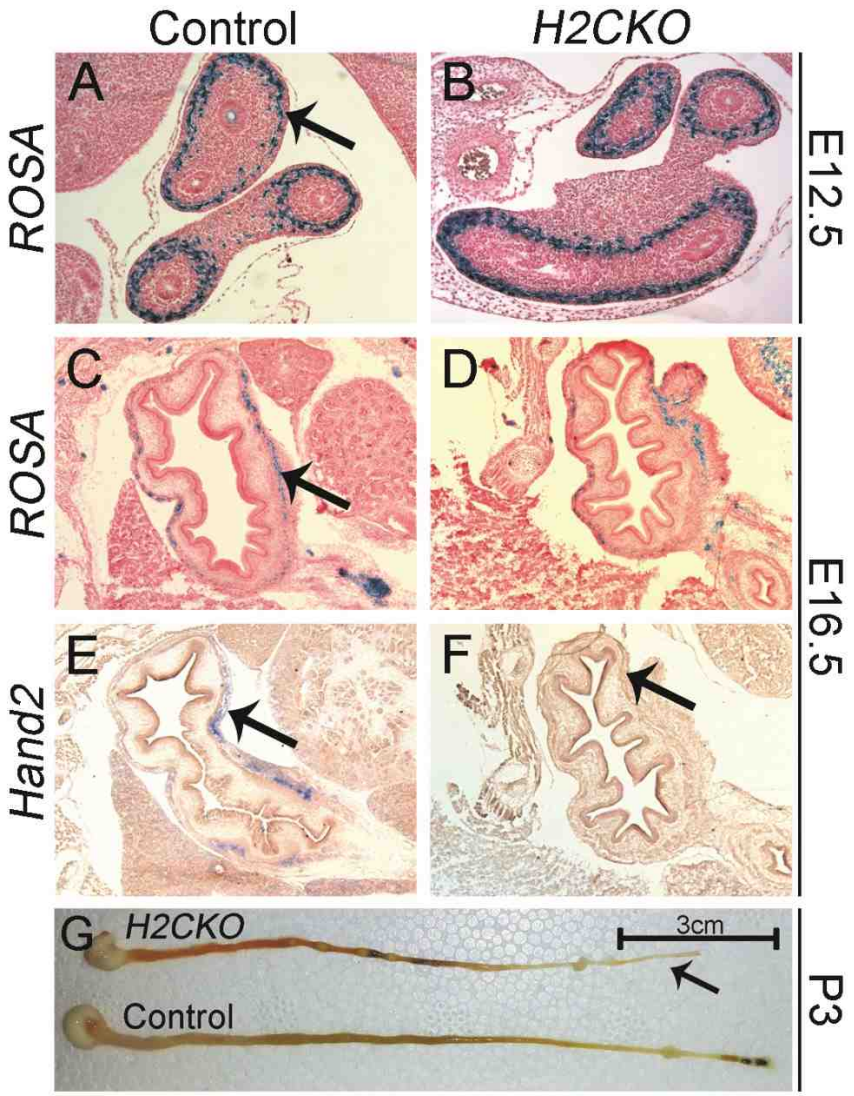

Figure 25: *Postn-Cre* is co-expressed with *Hand2* within the enteric nervous system.

β-galactosidase stained sections of control and *H2CKO* stomachs at E12.5 (A, B), and E16.5 (C, D). *Hand2* section ISH of control (E) and *H2CKO* (F) stomachs at E16.5. Dissected out gastrointestinal tract of control and *H2CKO* P3 pups (G). Arrows in (A,C) indicate myenteric plexus, arrow in (E) indicates *Hand2* expression within the myenteric plexus, (F) indicates deletion of *Hand2*.

H2CKOs display a loss of *Dbh* expression within sphenopalatine ganglia

We next carefully compared *Postn-Cre* lineage with *Hand2* expression in the sympathetic chain. Analysis of E12.5 embryos reveals robust *Cre* activity in components of the peripheral nervous system, as well as in and around the developing nasal cavity and maxilla (data not shown). As the *Postn-Cre* lineage is reported to include Schwann cells surrounding the sympathetic ganglia (Lindsley et al., 2007), we examined the sympathetic ganglia of *H2CKOs* at E12.5, when *Wnt1-Cre* generated *H2CKOs* die from lack of catecholamines (Hendershot, Liu et al. 2008). *Postn*-lineage analysis in transverse sections at the level of the heart confirms activation of the *R26R* reporter within the cells surrounding the sympathetic ganglia (Fig. 26B, C). Although the cells enveloping the trunk sympathetic ganglia were clearly marked, ISH demonstrates that expression of *Hand2* (Fig. 26D, E) as well as *Dbh* (Fig. 26F, G), a gene known to be directly regulated by Hand2 (Rychlik et al., 2003; Xu et al., 2003), is unaffected when control and *H2CKO* embryos are compared.

Interestingly, more detailed analyses of E12.5 heads reveal that the *Postn-Cre* lineage is not restricted to cells on the outer surface, but also marks the neurons within sphenopalatine ganglia (arrow; Fig. 26H). Despite being commonly considered parasympathetic and having a parasympathetic root, the sphenopalatine ganglia have an additional sympathetic root derived from the cervical sympathetic ganglia (Coppola et al., 2010). The sphenopalatine ganglia are known to express *Dbh,* with levels peaking at E12.5 and gradually being downregulated (Hirsch et al., 1998). In the rat, at least a subpopulation of

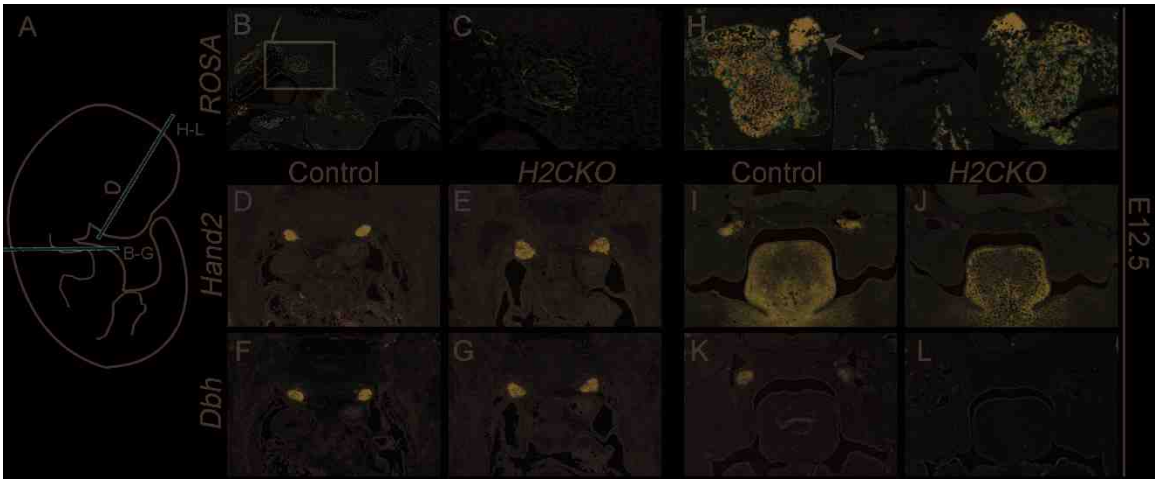

Figure 26: *Postn-Cre* mediates deletion of Hand2 within schwann cells of the sympathetic trunk and within the sphenopalatine ganglia at E12.5

Schematic showing planes of section (A). β-galactosidase stained sections of control sympathetic ganglia (B, C). *Hand2* ISH sections of control (D) and *H2CKO* (E) sympathetic ganglia. *Dbh* section ISH of control (F) and *H2CKO* (G) sympathetic ganglia. β-galactosidase stained frontal sections of sphenopalatine ganglia (arrow, H). *Hand2* ISH of sphenopalatine ganglia in control (I), and *H2CKO* (J) embryos. *Dbh* ISH in control (K), and *H2CKO* (L) embryos. β-galactosidase staining and ISH was conducted at E12.5.

sphenopalatine cells express TH and produce catecholamines, while most of the cells produce low levels of TH but do not produce catecholamines (Leblanc and Landis, 1989). Projections from the sphenopalatine ganglia are known to innervate the lacrimal gland, and regulate blood flow to the nasal mucosa, while additional evidence suggests a role in regulating cerebral blood flow (Suzuki et al., 1990; Ter Laan et al., 2013). ISH of frontal sections reveals that *Hand2* is robustly expressed within the sphenopalatine ganglia of control embryos (Fig. 26I), and its expression is ablated in *H2CKOs* (Fig. 26J). This loss of *Hand2* is accompanied by a loss of *Dbh*, which is likely dependent on Hand2 function (Fig. 26K, L). This data suggested that, despite normal *Hand2* expression within the mid-gestation sympathetic trunk, neonatal *H2CKOs* may exhibit a reduction in catecholamine biosynthesis outside the sympathetic chain, or possibly within trunk ganglia due to a later stage deletion. We thus sought to examine additional tissues at later embryonic time points, to better define all of the sources of norepinephrine and epinephrine that might be compromised in *H2CKOs*.

Late-stage Cre activity does not affect the sympathetic chain, but mediates deletion of *Hand2* from the adrenal medulla

To determine whether the *Postn-Cre* lineage, which is initially restricted to cells surrounding the trunk ganglia, later expands expression to include the ganglia neurons, *ROSA* reporter staining was conducted at E16.5. β-galactosidase staining indicates that the *Postn-Cre* lineage includes only a small subpopulation of neurons within sympathetic trunk ganglia (Fig. 27A, B).

Importantly, *Hand2* (data not shown) and *Dbh* (Fig. 27C, D) expression within the sympathetic trunk remains robust in *H2CKOs*. In the neonate and the adult, the adrenal medulla is the primary site for synthesis of circulating catecholamines (Malmejac, 1964). *ROSA* reporter staining at E16.5 indicates that *Postn-Cre* lineage includes cells of control (Fig. 27E) and *H2CKO* (Fig. 27F) adrenal medulla. Control and *H2CKO* adrenal glands were then collected from P3 pups, and analyzed by ISH. *Hand2* (Fig. 27G) and *Dbh* (Fig. 27I) are both robustly expressed within control adrenal medulla at P3, whereas *Postn-Cre* efficiently ablates *Hand2* (Fig. 27H), resulting in downregulation of *Dbh* (Fig. 27J), which would be expected to reduce catecholamine biosynthesis in *H2CKOs*. Furthermore, we confirmed these results by collecting additional P3 adrenal glands, isolating RNA, and conducting qRT-PCR. In *H2CKOs Hand2* expression was reduced to approximately 7% of control levels (p-value = 0.004), while *Dbh* levels were reduced to approximately 11% (p-value = 0.023). Expression of *Th*, which encodes the enzyme responsible for conversion of L-tyrosine to a dopamine precursor, and *Pnmt*, which encodes the enzyme responsible for converting norepinephrine to epinephrine, was reduced to approximately 23% (p-value = 0.001) and 9% (p-value = 0.016), respectively (Fig. 27K).

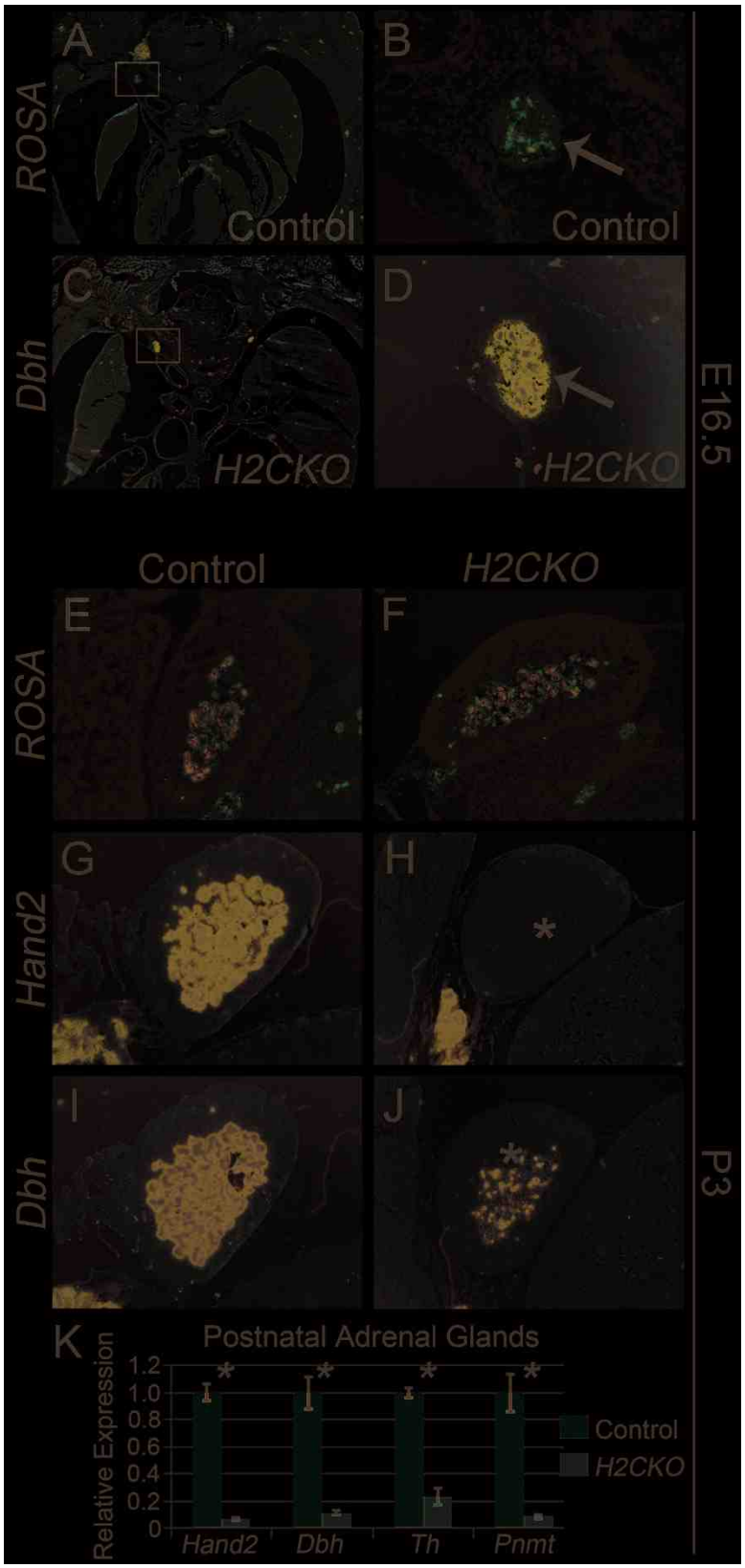
A
B
ROSA
Control
Control
C
D
Dbh
H2CKO
H2CKO
E16.5
Control
H2CKO
E
F
ROSA
G
H
Hand2
*
I
J
Dbh
*
P3
K
Postnatal Adrenal Glands
Relative Expression
1.2
1.0
0.8
0.6
0.4
0.2
0
*
*
*
*
Control
H2CKO
Hand2
Dbh
Th
Pnmt

Figure 27: Expression of *Dbh* within sympathetic ganglia of *H2CKOs* is maintained at late stages of embryonic development, but *Postn-Cre* does ablate *Hand2* expression within the adrenal medulla, resulting in downregulation of *Dbh, Th, and Pnmt*.

β-galactosidase stained sections of control sympathetic trunk ganglia (A) and magnification (B) at E16.5. *Dbh* ISH of *H2CKO* sympathetic trunk ganglia (C), and magnification (D) at E16.5. Arrows in (B, D) indicate ganglia. β-galactosidase stained sections of control (E), and *H2CKO* (F) adrenal medulla at E16.5. *Hand2* ISH of control (G) and *H2CKO* (H) adrenal medulla at P3. *Dbh* ISH of control (I) and *H2CKO* (J) adrenal medulla at P3. qRT-PCR of *Hand2*, *Dbh*, *Th*, and *Pnmt* in isolated P3 adrenal glands (K). Asterisks in (H, J) indicate reduction of *Hand2* and *Dbh* respectively. Asterisks in (K) indicate p-values less than 0.05.

Postn-Cre H2CKO Pups exhibit bradycardia

When observing *H2CKO* pups, it is clear that the animals are significantly smaller by P3 and exhibit a failure to thrive (Fig. 28A). Given the lack of cardiac structural defects, and the identification of multiple catecholaminergic *Hand2*-expressing cell populations that overlap with the *Postn-Cre* lineage, a catecholamine deficiency in conjunction with gastrointestinal dysfunction is the most likely cause of the lethal failure to thrive phenotype. As catecholaminergic stimulation is essential for proper cardiac function, we tested this hypothesis by conducting electrocardiograms (ECGs) on P3 pups, and thereby assessing heart rates. After assessing four mutants, and an equal number of littermate controls (Fig. 28B, C), we determined that *Postn-Cre H2CKOs* had significantly slower sinus node rates (P-value = 0.019, Fig. 28D), a condition commonly referred to as bradycardia. Control pups averaged 466 beats per minute (bpm), while *Postn-Cre H2CKOs* averaged only 337 bpm. In addition to heart rate, the ECG traces were used to calculate the average amount of time between the start of atrial activation and the start of ventricular activation (PR interval), but no significant difference was noted (Fig. 28E). Similarly, the duration of atrial depolarization (P-wave duration), and duration of ventricular depolarization (QRS complex duration) were measured, with no significant difference found between controls and *H2CKOs* (Fig. 28E). To determine if *H2CKOs* were experiencing heart failure we examined expression of *Nppa* (*atrial natriuretic factor*; *Anf*), which becomes upregulated in ventricular muscle when undergoing stress (Edwards et al., 1988). Compared to the highly restricted atrial expression of *Anf* in control hearts (Fig.

28F) a clear marked increase in ventricular *Anf* expression is observed in *H2CKO* hearts (Fig. 28G), supporting heart failure as a cause of *H2CKO* neonatal lethality.

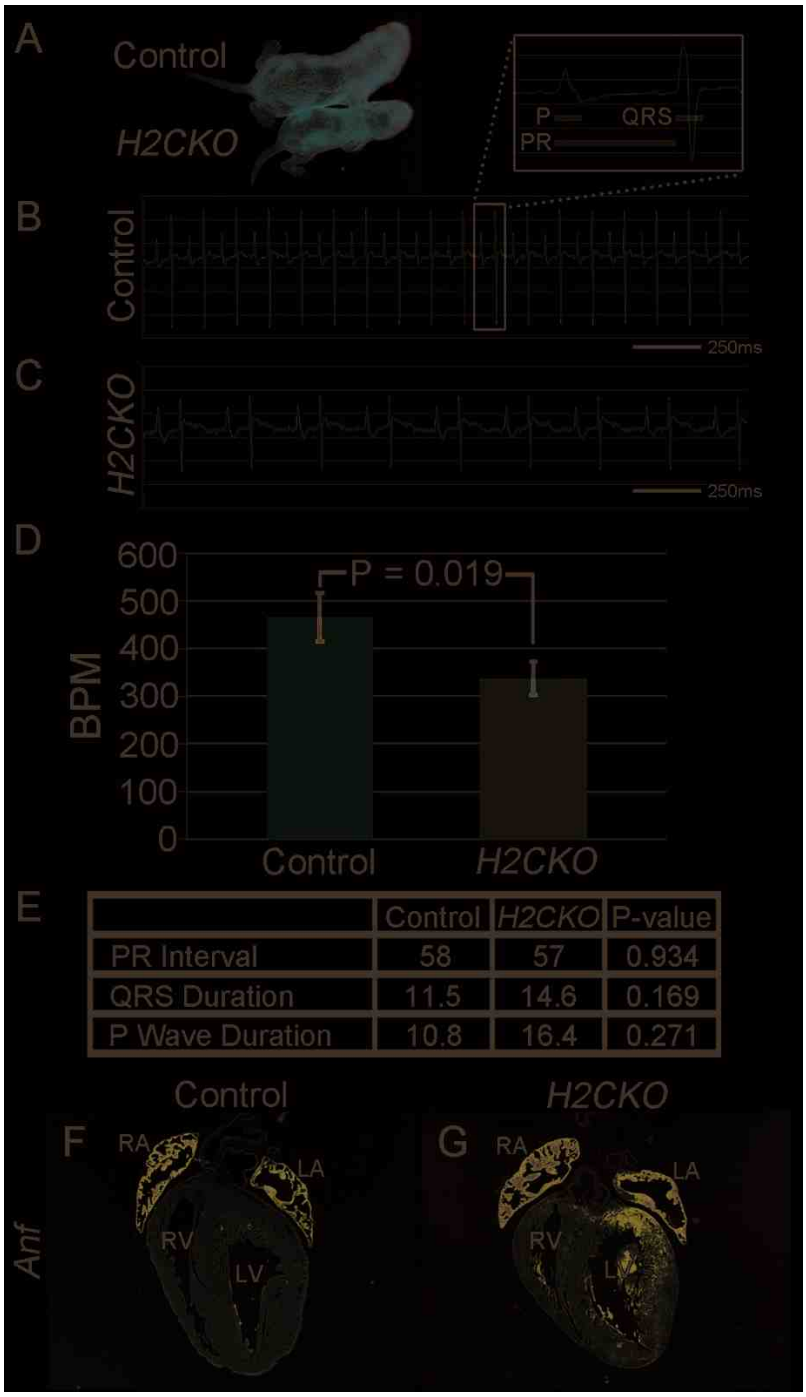

Figure 28: ***Postn-Cre H2CKO*** **pups have significantly slower heart rates and expanded *Anf* expression.**

H2CKO pups that survive to P3 are noticeably smaller than littermates (A). Representative ECG trace for P3 control (B) and *H2CKO* (C) pups. Panel (B) insert represents one cycle of cardiac contraction. Red bars denote the portion of the trace measured for P-wave duration, PR interval, and QRS complex duration as labeled. Control pups averaged 466 bpm, while *H2CKO* pups averaged 337 bpm (D). P = p-value. Differences in average PR interval (ms), QRS complex duration (ms), and P wave duration (ms) between control and *H2CKO* P3 pups were not statistically significant (E). *Anf* ISH in P3 control (F) and *H2CKO* (G) hearts.

D. Discussion

Hand2 expression and *Postn-Cre* lineage overlap within components of the enteric nervous system. Previous studies of enteric function show that ablation of *Hand2* within enteric neural precursors via the *Nestin-Cre*, which is initiated by E11.5, results in a severe bowel distention by P20 (Lei and Howard, 2011). The data in the current study show that *Postn-Cre* is initiated by E12.5, making it possible that *Postn-Cre H2CKOs* share the same gastrointestinal dysfunction as *Nestin-Cre H2CKOs*. Indeed, a lack of fecal matter posterior to cecal appendages of *Postn-Cre H2CKOs* indicates that decreased gastrointestinal motility could be contributing to neonatal lethality. Interestingly, this lack of motility resembles a human congenital motility disorder called Hirschsprung's disease, which is pathologically characterized by a lack of enteric ganglia in a variable stretch of the distal bowel wall. While *Postn-Cre H2CKOs* do not appear to suffer from a complete loss of enteric ganglia (Fig. 25D), it is possible that a reduction in gangliogenesis within specific regions of the gut has evaded our detection. Indeed, as *Nestin-Cre H2CKOs* suffer from a functional aganglionosis (Lei and Howard, 2011), and the *Postn-Cre* enteric lineage closely resembles that of the *Nestin-Cre*, this would not be surprising; however, as the *Nestin-Cre H2CKOs* survive until P20, while *H2CKOs* generated by the *Postn-Cre* do not, the involvement of additional non-enteric phenotypes is likely.

This study demonstrates that, in addition to the established early embryonic roles Hand2 plays in cardiac morphogenesis and the development and function of the sympathetic ganglia, Hand2 plays important homeostatic

post-embryonic functions in the production of catecholamines. It is well established that *Hand2* expression within the sympathetic chain is required for neurons to acquire and maintain a catecholaminergic phenotype (Hendershot et al., 2008; Schmidt et al., 2009). Loss of *Hand2* within the sympathetic chain results in downregulation of the crucial biosynthetic enzymes Tyrosine Hydroxylase and Dbh (Hendershot et al., 2008). For a more complete description of Hand2's role within the sympathetic nervous system, as established by various manipulations of *Hand2* expression within multiple genetic systems, see (Table 3). Our results confirm previous data showing that *Postn-Cre* expression is restricted to the cells surrounding sympathetic chain ganglia at E12.5 (Lindsley et al., 2007). As expected, *Hand2* expression within the trunk sympathetic ganglia is unaffected in *H2CKOs*, at both E12.5 and E16.5. *Dbh* expression is similarly unaffected, indicating that trunk sympathetic ganglia in *Postn-Cre H2CKOs* produce sufficient concentrations of norepinephrine and epinephrine for embryonic survival to birth. However, we observed that *Hand2* expression and the *Postn-Cre* lineage overlap within the sphenopalatine ganglia at E12.5, and ablation of *Hand2* results in a dramatic decrease in *Dbh* expression in these ganglia. Given that the sphenopalatine ganglia is reported to have a sympathetic root derived from the superior cervical sympathetic ganglion, in addition to parasympathetic and sensory roots, the observation of *Dbh* downregulation is not surprising, and suggests that dysfunction within these ganglia could be contributing to the early neonatal death in *H2CKOs*.

Study	Model	Phenotype/Results	Conclusions
(Morikawa et al., 2005)	P19-embryonic carcinoma (P19-EC) cells stably expressing *Hand2* (P19-H2)	Retinoic acid treated P19-H2 cells but not P19-EC cells express peripherin (a peripheral nervous system marker), and a subset of these co-express Th.	Ectopic Hand2 expression is able to activate the sympathetic nervous system developmental program within P19-EC cells.
(Lucas et al., 2006)	Zebrafish *hand2* deletion mutant (*hands off*)	Sympathetic precursor cells aggregate to form normal sympathetic ganglion primordial, but *th* and *dbh* expression is strongly reduced	Generic neuronal differentiation is unaffected, but noradrenergic differentiation of sympathetic neurons is impaired
(Morikawa et al., 2007)	Mouse Wnt1-Cre Hand2 CKO	Death at E12.5 with cardiovascular and craniofacial defects. Sites of sympathetic development are populated by neural crest cells, which express pan-neuronal markers. *Th* and *Dbh* expression is dramatically reduced.	Hand2 permits sympathetic neurons to acquire a catecholaminergic phenotype
(Hendershot et al., 2008)	Mouse *Wnt1-Cre Hand2 CKO*	See above; *H2CKOs* exhibit a significant and progressive loss of sympathetic neurons.	Hand2 affects generation of the neural precursor pool by affecting proliferative capacity of progenitors and by regulating expression of transcription factors necessary for noradrenergic neuronal differentiation
(Morikawa and Cserjesi, 2008)	Mouse *Wnt1-Cre Hand2 CKO*	See above; early embryonic lethality could be rescued by administration of isoproterenol, a β-adrenoceptor agonist	Noradrenergic deficiency alone accounts for early embryonic lethality of *Wnt1-Cre H2CKOs*
(Schmidt et al., 2009)	Reduction/ablation of *Hand2* within differentiated sympathetic neurons by siRNA in cultured chick sympathetic neurons, and *Dbh-Cre* in *Hand2* conditional mice	Large decrease in *Th* and *Dbh* expression within *Hand2* siRNA treated chick sympathetic neurons. Pan-neuronal genes were not affected, while expression of cholinergic marker genes was enhanced. *Dbh-Cre H2CKO* mice showed decreased numbers of sympathetic neurons, and large reduction in Th expression	Hand2 plays a key role in maintaining noradrenergic properties in differentiated neurons

Table 3: **Hand2 function within the sympathetic nervous system.**

Interestingly, *Hand2* expression and the *Postn-Cre* lineage overlap within the catecholaminergic cells of the adrenal medulla. Similar to what is observed in sphenopalatine ganglia, ablation of *Hand2* within the adrenal medulla also results in a dramatic reduction of *Dbh*. ISH of *H2CKO* adrenal glands indicates that a small population of cells maintains *Dbh* expression, while the vast majority of expression within the adrenal medulla is lost. This is consistent with *Hand2* loss of function studies within the sympathetic chain, where *Dbh* is known to be a direct Hand2 target (Rychlik et al., 2003; Vincentz et al., 2013; Xu et al., 2003). Furthermore, qRT-PCR shows that *H2CKO* adrenal glands exhibit significant decreases in *Th* and *Pnmt*, which like *Dbh*, encode enzymes that catalyze essential steps in the synthesis of the catecholamine adrenalin. In a study of $Dbh^{-/-}$ embryos, it was stated that while most die in utero, approximately 12% survive until birth. The 12% survival was attributed to a flow of catecholamines across the placenta, thus also explaining why of those that survive to birth, 40% die by P2 (Thomas et al., 1995). These data make it tempting to consider that *Postn-Cre H2CKOs* may have enough catecholaminergic biosynthetic capability to survive to birth as a result of unaffected sympathetic chain ganglia and supplementation from the mother, but at birth this supplementation ceases, leading to lethal catecholamine deficiency. It is well established that the adrenal medulla is a particularly important source of catecholamines that regulate heart rate, blood pressure, blood vessel constriction, and other critical aspects of cardiovascular function (Axelrod and Reisine, 1984; Fung et al., 2008). These data suggest that catecholamine deficiency, in conjunction with an enteric

phenotype, causes *H2CKO* postnatal lethality. Heart rates in *H2CKOs* are significantly slower than control littermates. This phenotype is consistent with previous publications on genetic models of catecholamine deficiency, such as *Epas1* null mice, which are reported to have low catecholamine levels and a pronounced bradycardia (Tian et al., 1998), as well as *Th* null embryos, which are reported to have a 28% reduction in heart rate (Ream et al., 2008). In contrast, no difference in PR interval was observed between controls and *H2CKOs*, and while P-wave duration and QRS complex duration both trended toward an increase, no significant differences were observed, indicating that conditional ablation of *Hand2* does not alter dromotropic properties of the P3 heart. The reason for the differential effects of *Hand2* deficiency on chronotropy versus dromotropy is unclear. It may involve differential expression of beta-adrenergic receptors and/or their downstream targets in sinoatrial nodal cells versus cells of the cardiac specific conduction system. The decreased heart rates observed in P3 *H2CKOs* support the conclusion that a catecholaminergic insufficiency, in addition to enteric dysfunction, results in the neonatal *H2CKO* failure to thrive. In further support of this conclusion, upregulation of ventricular *Anf* expression in *H2CKO* hearts indicates pathological changes within these cardiomyocytes that ultimately lead to cardiac failure.

Chapter IV

Conclusions and Future Directions

The bHLH transcription factor Hand2 is widely expressed during embryonic development, and systemic deletion has convincingly demonstrated its essential nature. However, *Hand2* expression is not ubiquitous, and the tissue specific nature of Hand2 function is only just beginning to be understood. This dissertation project addresses novel tissue specific loss- and gain-of-function experiments that are necessary to fully understand the dynamic and essential role for Hand2 in the developing heart. A firm understanding of the lineage specific roles that Hand2, as well as other Twist family transcription factors, play during embryonic development will be indispensable when analyzing how transcription factor dysfunction leads to congenital disease.

Hand2 is robustly expressed within the embryonic endocardium, and its role within this tissue has not been previously studied. The data presented above establishes a functional requirement for Hand2 within the endocardium via a Notch-dependent mechanism. *Hand2* conditional knockout within the endothelium (*Tie2-Cre*) or endocardium ($Nfatc1^{Cre}$) results in embryonic lethality by E14.5 due to severe cardiac defects. *H2CKO* hearts display pronounced hypotrabeculation, aberrant septation, and absence of a direct connection between the RA and RV, closely phenocopying the human congenital disease TA. *Nrg1* encodes a secreted signaling ligand, which is crucial for proper cardiac trabeculation and, in the endocardium, is regulated through Notch signaling via the ligand EfnB2. *Nrg1* expression is greatly reduced in *H2CKO* endocardium;

however, *EfnB2* expression is unaffected. DNA-binding and trans-activation assays demonstrate that Hand2 regulation of *Nrg1* is direct, via interaction with the *Nrg1* promoter. Additional genetic studies reveal that Hand2 functions directly within the Notch signaling pathway. The endocardium of embryos lacking either the Notch pathway effector *RBPJk*, or *EfnB2* fails to express *Hand2* and *Nrg1*. Collectively, these data establish Hand2 as an integral component of endocardial-myocardial Notch signaling, functioning downstream of EfnB2, and upstream of Nrg1 to regulate trabeculation and septal morphogenesis.

We have established endocardial Hand2 as a downstream effector of Notch signaling. As the coronary endothelium derives at least in part from the endocardium via angiogenesis, and as Notch signaling is a known potent regulator of angiogenesis, we analyzed coronary angiogenesis and vascular gene expression in *H2CKOs*. *H2CKO* embryos display precocious formation of the coronary angiogenic plexus. Interestingly, gene expression analyses of *H2CKO* hearts at E10.5, prior to plexus formation, reveals that *VegfR2*, its co-receptor *Nrp1*, and *VegfD* are all downregulated. In addition, analysis of E13.5 hearts reveals that *H2CKOs* fail to downregulate Lyve-1 within the ventricular endocardium, indicating that dysregulated Vegf signaling results in defective endocardial maturation. Likewise, increased expression of *VegfA* and *VegfR3* within E13.5 *H2CKOs* may reflect a failure to downregulate expression from elevated levels present during earlier stages of cardiac development. VegfA is strongly pro-angiogenic, and likely accounts for the precocious coronary development observed in *H2CKOs*.

Postn-Cre H2CKOs survive till birth, but fail to thrive and die soon after. While our analyses reveal an absence of cardiac or sympathetic chain phenotypes, *Hand2* is clearly ablated from the adrenal medulla and sphenopalatine ganglia where, similar to the sympathetic trunk, *Hand2* plays an important role in regulating *Dbh* expression. The reduction of *Dbh*, *Th*, and *Pnmt* in *H2CKOs* indicates that pups likely have a decreased ability to synthesize catecholamines, resulting in the observed postnatal lethality. As catecholaminergic sympathetic stimulation is essential for proper cardiac function, ECG data showing that P3 *H2CKOs* have slower heart rates than control littermates, and upregulation of *Anf* within the ventricles of *H2CKOs*, supports this conclusion.

This dissertation project has revealed several novel aspects of Hand2 function, however, many interesting questions remain, particularly in regards to Hand2 function within the endocardium. Hand2 is commonly considered to primarily function within the myocardium, but in this study we conclusively demonstrate that Hand2 plays crucial functions within embryonic endocardium. However, Hand2 expression and function within the endocardium after birth has not been assessed. In chapter II we demonstrate that by E18.5 endocardial *Hand2* expression is restricted to endothelium overlying the cardiac valves. It is unknown whether this expression persists into adulthood, or is gradually lost after birth. Even if this expression is lost, an interesting question remains: what function, if any, does Hand2 carry out within valve endothelial cells during late stages of embryonic development? The preferential expression of *Hand2* on the

back side of OFT and AV valves suggests that Hand2 may be involved in setting up the distinct layers (ventricularis/atrialis, spongiosa, fibrosa) observed in mature valves. However, due to embryonic lethality in *Tie2-Cre* and *Nfatc1*^{Cre} *H2CKOs*, alternative avenues such as utilization of the inducible endothelial specific *VE-cadherin-CreERT2* recombinase (Monvoisin et al., 2006) will need to be explored. Also of interest, Notch signaling is reportedly activated within adult mouse hearts in response to injury (Gude et al., 2008; Øie et al., 2010). While myocardial Hand2 expression is also induced in failing hearts (Dirkx et al., 2013), a careful examination of endocardial Hand2 expression has not been conducted. If endocardial Hand2 is activated, it would be interesting to determine what role, if any, it plays in the response of the vasculature to ischemic injury.

The data presented in the current study conclusively demonstrate dysregulation of Vegf signaling in endocardial *H2CKOs*. However, the complex interconnected nature of Vegf signaling makes determining which effects are primary and which are secondary extremely challenging. Solving this puzzle will require a combination of approaches, including genome wide analysis of Hand2 transcriptional targets via ChIP-Seq, and analysis of protein-protein interactions with other endothelial related bHLH factors such as Hey proteins and Hif1α. This work is currently underway. Another key to sorting out primary and secondary effects will be improving our understanding of the expression profiles of genes dysregulated in *H2CKOs*. The expression profiles of many vascular related genes are poorly characterized within the heart, complicating data interpretation. Furthermore, upregulated genes may be ectopically expressed within cardiac

tissues that would not otherwise express them. In the current study we have analyzed the expression profiles of the most compelling genes discovered to be differentially expressed at the relevant time-points, but additional work remains. These experiments are also underway, and together with unbiased sequencing based assays will provide additional mechanistic insight into Hand2 regulation of endocardial maturation and development of the coronary vasculature.

Appendix I: Hand2 Function in the Epicardium

In contrast to *Hand1*, *Hand2* is robustly expressed within the PEO and epicardium during cardiovascular development but is undetectable within epicardial precursors that reside in the septum transversum, placing Hand1 temporally upstream of *Hand2* in this tissue. Recently, *Hand1*^{eGFPCre} was used to conditionally delete *Hand2* from *Hand1* expressing cells within the septum transversum, as well as their derivatives (Barnes et al., 2011). *H2CKOs* display defects in epicardial EMT, a deficiency of cardiac fibroblasts, and increased epicardial apoptosis which results in an incompetent coronary vasculature that leads to embryonic lethality by E14.5 (Barnes et al., 2011). This phenotype is recapitulated by E9.5 deletion of Hand2 using the tamoxifen-inducible *WT1*^{ERT2Cre} allele, which mediates ablation of *Hand2* from the septum transversum, PEO, and lateral mesoderm (Barnes et al., 2011; Zhou et al., 2008). Gene expression analysis of primary epicardial cell cultures from *Hand1*^{eGFPCre} *H2CKOs* revealed increased levels of the fibronectin receptor *Itgα4* (also shown to be effected in NCC *Hand2* ablation studies) and a greatly lowered ratio of *PDGFRα* to *PDGFRβ*. Interestingly, platelet derived growth factor receptors have been previously shown to function in cell fate and specification of the epicardium after secondary EMT. Epicardial cells expressing *PDGFRα* derive into cardiac fibroblasts where *PDGFRβ* is associated with differentiation into coronary smooth muscle (Smith et al., 2011) *H2CKOs* show marked reduction in *PDGFRα* expression as well as reduced numbers of cardiac fibroblasts. Hand2 regulation of *PDGFRα* regulation is direct, as luciferase assays demonstrated that *Hand2*

was able to transactivate the *PDGFRα* promoter (Barnes et al., 2011). These data support a novel role for Hand2 in specification of epicardial cell fates post-secondary EMT.

In addition to modified PDGFR signaling and cell fate, Hand2 plays a role in the ECM by modulating fibronectin assembly. Fibronectin is normally assembled into a complex structural network, which anchors cell and ECM adhesion molecules such as integrins (Pae et al., 2008). In wild type epicardial explants fibronectin is organized into neat bundles that facilitate these interactions, influencing actin dynamics, EMT, and the cell cycle. In addition, fibronectin regulates the stability and availability of extracellular matrix related factors, such as Tgfβ proteins and growth factors (Leiss et al., 2008; Sottile et al., 1998). Although transcriptional and protein levels of fibronectin are unaltered in *Hand2* epicardial CKO mice, fibronectin organization in mutant explants is abnormally uniform and sheet-like (Barnes et al., 2011). Furthermore, the fibronectin cell surface receptor *Itgα4* is significantly upregulated in *H2CKO* explant cultures. Itgα4 is thought to play a role in adhesion of the epicardium to the underlying myocardium via interaction with vascular cell adhesion molecule 1 (VCAM-1), which is reciprocally expressed with *Itgα4* during cardiogenesis (Kwee et al., 1995; Pinco et al., 2001; Yang et al., 1995). This suggests that the combination of fibronectin disarray and transcriptional dysregulation of downstream signaling and adhesion components could be a key mediator of the *Hand2* epicardial CKO phenotype. Studies in zebrafish have complemented these observations. In wild type zebrafish embryos, fibronectin deposition is

restricted to the basal surface of myocardial precursors, while in *Hand2* mutants, fibronectin assembly is disorganized and no longer localized to a single surface (Trinh et al., 2005). Unfortunately, how *Hand2* regulates fibronectin assembly is not yet known. Recent research in zebrafish demonstrated that fibronectin deposition at the midline is initially required for temporally correct migration of myocardial precursors (Trinh and Stainier, 2004), and that Hand2 transcriptionally downregulates *fibronectin* expression, to create an environment conducive to fusion of these precursors at the midline (Garavito-Aguilar et al., 2010). These studies indicate that Hand2 plays an important non-cell autonomous role in zebrafish cardiac development by transcriptionally modulating fibronectin expression and deposition.

Ablation of *Hand2* from the epicardium via *Wt1-Cre*

In mice, early deletion of Hand2 from epicardial precursors via either the tamoxifen-inducible $WT1^{ERT2Cre}$ allele or $Hand1^{eGFPCre}$ results in several distinct phenotypes. These data, in addition to the reported zebrafish phenotypes, suggest that Hand2 may play both an early role in epicardial precursors, and a later role in the maturation of epicardial derivatives. To further temporally define when Hand2 function is required within the epicardial lineage, and to avoid potential confounding effects associated with tamoxifen injections, we utilized a transgenic non-inducible *WT1-Cre* allele (Kolander et al., 2014). In contrast to the $Hand1^{eGFPCre}$, this Cre allele does not activate within the septum transversum. Furthermore, it marks only a subpopulation of the PEO, and all cells of the

epicardium. Upon crossing *Wt1-Cre(+); Hand2*$^{fx/+}$ males with *Hand2*$^{fx/fx}$*; R26R*$^{z/z}$ females, embryos were collected and Xgal stained at E9.5 and E11.5. At E9.5 we observed recombination within a subpopulation of the PEO (Fig. 29A-D), and by E11.5 all epicardial cells were marked (Fig. 29E-H). Surprisingly, unlike *Hand1*^{eGFPCre} and *WT1*^{ERT2Cre} *H2CKOs, Wt1-Cre H2CKOs* were viable and present at expected ratios (data not shown).

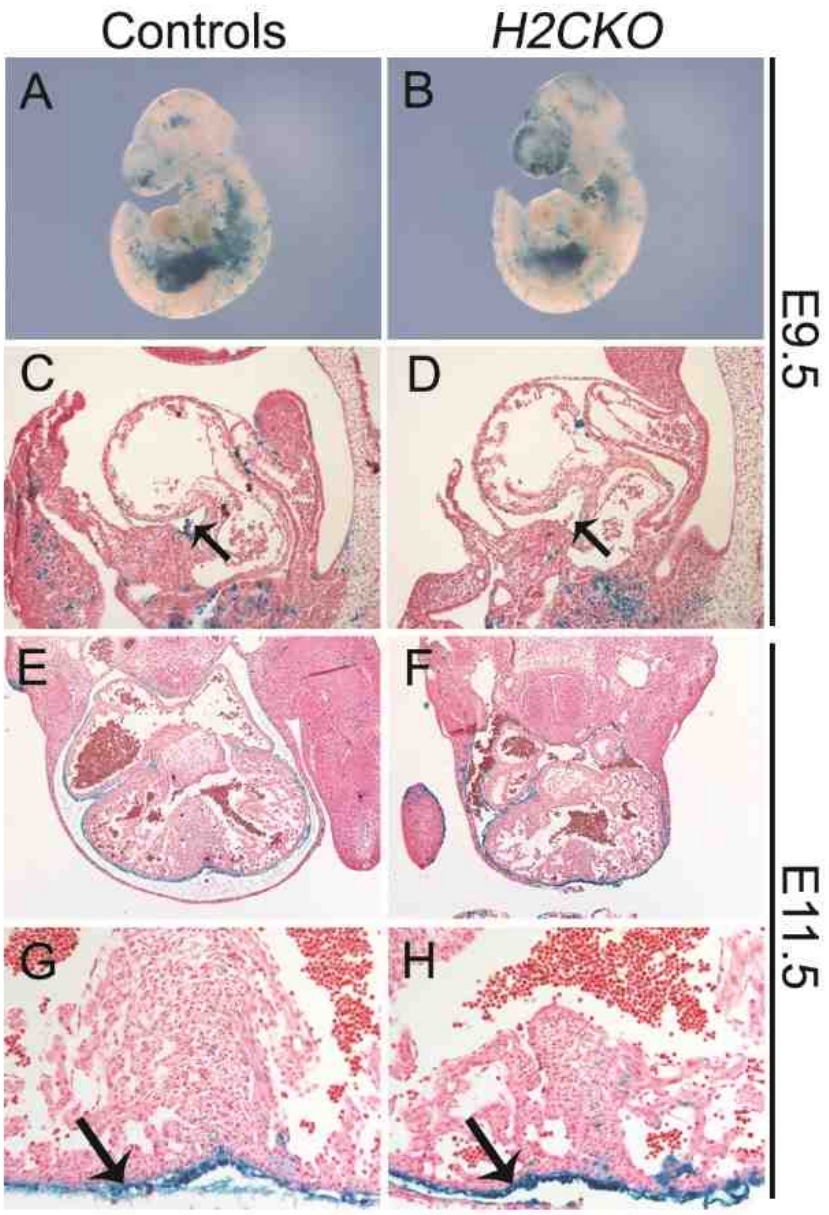

Figure 29: WT1-Cre transgene mediates recombination in a PEO subpopulation and the epicardium

R26R lacZ stained E9.5 control and *H2CKO* embryos (A, B). Sagittal sections of lacZ stained control and *H2CKO* E9.5 hearts (C, D). Black arrows indicate PEO. *R26R* lacZ stained E11.5 control and *H2CKO* embryos (E, F). Transverse sections of lacZ stained control and *H2CKO* E11.5 hearts (G, H).

Discussion

Both *Hand1*^{eGFPCre} and *WT1*^{ERT2Cre} mediated deletion of *Hand2* results in severe morphogenetic defects and early embryonic lethality. Surprisingly *Wt1-Cre H2CKOs* do not recapitulate these defects. As both the *Hand1*^{eGFPCre} and *WT1*^{ERT2Cre} lineages mark early epicardial precursors within the septum transversum, while the *Wt1-Cre* does not, this may indicate that Hand2 function is required earlier in the process of epicardialization than was previously thought. While ISH does not readily reveal *Hand2* expression within the septum transversum, a low but biologically essential level of expression cannot be ruled out. Alternatively, or perhaps in addition to this possibility, the *Wt1-Cre H2CKOs* contained two floxed *Hand2* alleles (*Wt1-Cre(+); Hand2*$^{fx/fx}$), while *Hand1*^{eGFPCre} and *WT1*^{ERT2Cre} *H2CKOs* contained only one (*Cre*$^{+}$*; Hand2*$^{fx/-}$). The requirement for *Wt1-Cre* to recombine both alleles may have temporally delayed the reduction in *Hand2* gene dosage, thus alleviating the effects. Regardless, *Hand2* does not appear to play essential roles in the epicardium after E11.5, when the *R26R*^{Z} reporter is robustly activated.

References

Allwork, S., Anderson, R., 1978. Remodeling of the membranous septum throughout life and its relevance to defective ventricular septation. British Heart Journal 40, 463.

Armstrong, E.J., 2004. Heart Valve Development: Endothelial Cell Signaling and Differentiation. Circulation Research 95, 459-470.

Atchley, W.R., Fitch, W.M., 1997. A natural classification of the basic helix-loop-helix class of transcription factors. Proc Natl Acad Sci U S A 94, 5172-5176.

Axelrod, J., Reisine, T.D., 1984. Stress hormones: their interaction and regulation. Science 224, 452-459.

Banerji, S., Ni, J., Wang, S.-X., Clasper, S., Su, J., Tammi, R., Jones, M., Jackson, D.G., 1999. LYVE-1, a new homologue of the CD44 glycoprotein, is a lymph-specific receptor for hyaluronan. The Journal of cell biology 144, 789-801.

Barbosa, A.C., Funato, N., Chapman, S., McKee, M.D., Richardson, J.A., Olson, E.N., Yanagisawa, H., 2007. Hand transcription factors cooperatively regulate development of the distal midline mesenchyme. Dev Biol 310, 154-168.

Barnes, R.M., Firulli, A.B., 2009. A twist of insight - the role of Twist-family bHLH factors in development. The International Journal of Developmental Biology 53, 909-924.

Barnes, R.M., Firulli, B.A., Conway, S.J., Vincentz, J.W., Firulli, A.B., 2010. Analysis of the Hand1 cell lineage reveals novel contributions to cardiovascular, neural crest, extra-embryonic, and lateral mesoderm derivatives. Developmental Dynamics 239, 3086-3097.

Barnes, R.M., Firulli, B.A., VanDusen, N.J., Morikawa, Y., Conway, S.J., Cserjesi, P., Vincentz, J.W., Firulli, A.B., 2011. Hand2 Loss-of-Function in Hand1-Expressing Cells Reveals Distinct Roles in Epicardial and Coronary Vessel Development. Circulation Research 108, 940-949.

Barnett, J.V., Desgrosellier, J.S., 2003. Early events in valvulogenesis: a signaling perspective. Birth Defects Res C Embryo Today 69, 58-72.

Barnette, D.N., Hulin, A., Ahmed, A.S., Colige, A.C., Azhar, M., Lincoln, J., 2013. Tgfbeta-Smad and MAPK signaling mediate scleraxis and proteoglycan expression in heart valves. J Mol Cell Cardiol 65, 137-146.

Benedito, R., Rocha, S.F., Woeste, M., Zamykal, M., Radtke, F., Casanovas, O., Duarte, A., Pytowski, B., Adams, R.H., 2012. Notch-dependent VEGFR3

upregulation allows angiogenesis without VEGF-VEGFR2 signalling. Nature 484, 110-114.

Brand, T., 2003. Heart development: molecular insights into cardiac specification and early morphogenesis. Dev Biol 258, 1-19.

Brown, C.B., Feiner, L., Lu, M.M., Li, J., Ma, X., Webber, A.L., Jia, L., Raper, J.A., Epstein, J.A., 2001. PlexinA2 and semaphorin signaling during cardiac neural crest development. Development 128, 3071-3080.

Burgess, R., Cserjesi, P., Ligon, K.L., Olson, E.N., 1995. Paraxis: a basic helix-loop-helix protein expressed in paraxial mesoderm and developing somites. Dev Biol 168, 296-306.

Cai, C.L., Zhou, W., Yang, L., Bu, L., Qyang, Y., Zhang, X., Li, X., Rosenfeld, M.G., Chen, J., Evans, S., 2005. T-box genes coordinate regional rates of proliferation and regional specification during cardiogenesis. Development 132, 2475-2487.

Castanon, I., Baylies, M.K., 2002. A Twist in fate: evolutionary comparison of Twist structure and function. Gene 287, 11-22.

Castanon, I., Von Stetina, S., Kass, J., Baylies, M.K., 2001. Dimerization partners determine the activity of the Twist bHLH protein during Drosophila mesoderm development. Development 128, 3145-3159.

Chakraborty, S., Wirrig, E.E., Hinton, R.B., Merrill, W.H., Spicer, D.B., Yutzey, K.E., 2010. Twist1 promotes heart valve cell proliferation and extracellular matrix gene expression during development in vivo and is expressed in human diseased aortic valves. Dev Biol 347, 167-179.

Charite, J., McFadden, D.G., Olson, E.N., 2000. The bHLH transcription factor dHAND controls Sonic hedgehog expression and establishment of the zone of polarizing activity during limb development. Development 127, 2461-2470.

Chen, H., Shi, S., Acosta, L., Li, W., Lu, J., Bao, S., Chen, Z., Yang, Z., Schneider, M.D., Chien, K.R., Conway, S.J., Yoder, M.C., Haneline, L.S., Franco, D., Shou, W., 2004. BMP10 is essential for maintaining cardiac growth during murine cardiogenesis. Development 131, 2219-2231.

Chen, H., Yong, W., Ren, S., Shen, W., He, Y., Cox, K.A., Zhu, W., Li, W., Soonpaa, M., Payne, R.M., Franco, D., Field, L.J., Rosen, V., Wang, Y., Shou, W., 2006. Overexpression of bone morphogenetic protein 10 in myocardium disrupts cardiac postnatal hypertrophic growth. J Biol Chem 281, 27481-27491.

Chen, Z.F., Behringer, R.R., 1995. twist is required in head mesenchyme for cranial neural tube morphogenesis. Genes Dev 9, 686-699.

Combs, M.D., Yutzey, K.E., 2009. Heart valve development: regulatory networks in development and disease. Circ Res 105, 408-421.

Connerney, J., Andreeva, V., Leshem, Y., Muentener, C., Mercado, M.A., Spicer, D.B., 2006. Twist1 dimer selection regulates cranial suture patterning and fusion. Dev Dyn 235, 1345-1357.

Coppola, E., Rallu, M., Richard, J., Dufour, S., Riethmacher, D., Guillemot, F., Goridis, C., Brunet, J.F., 2010. Epibranchial ganglia orchestrate the development of the cranial neurogenic crest. Proc Natl Acad Sci U S A 107, 2066-2071.

Creazzo, T.L., Godt, R.E., Leatherbury, L., Conway, S.J., Kirby, M.L., 1998. Role of cardiac neural crest cells in cardiovascular development. Annu Rev Physiol 60, 267-286.

Creuzet, S.E., 2009. Neural crest contribution to forebrain development. Semin Cell Dev Biol 20, 751-759.

Cserjesi, P., Brown, D., Ligon, K.L., Lyons, G.E., Copeland, N.G., Gilbert, D.J., Jenkins, N.A., Olson, E.N., 1995a. Scleraxis: a basic helix-loop-helix protein that prefigures skeletal formation during mouse embryogenesis. Development 121, 1099-1110.

Cserjesi, P., Brown, D., Lyons, G.E., Olson, E.N., 1995b. Expression of the novel basic helix-loop-helix gene eHAND in neural crest derivatives and extraembryonic membranes during mouse development. Dev Biol 170, 664-678.

D'Autreaux, F., Margolis, K.G., Roberts, J., Stevanovic, K., Mawe, G., Li, Z., Karamooz, N., Ahuja, A., Morikawa, Y., Cserjesi, P., Setlick, W., Gershon, M.D., 2011. Expression level of Hand2 affects specification of enteric neurons and gastrointestinal function in mice. Gastroenterology 141, 576-587, 587 e571-576.

de Lange, W.J., Halabi, C.M., Beyer, A.M., Sigmund, C.D., 2008. Germ line activation of the Tie2 and SMMHC promoters causes noncell-specific deletion of floxed alleles. Physiol Genomics 35, 1-4.

DeLaughter, D.M., Saint-Jean, L., Baldwin, H.S., Barnett, J.V., 2011. What chick and mouse models have taught us about the role of the endocardium in congenital heart disease. Birth Defects Res A Clin Mol Teratol 91, 511-525.

Dirkx, E., Gladka, M.M., Philippen, L.E., Armand, A.-S., Kinet, V., Leptidis, S., el Azzouzi, H., Salic, K., Bourajjaj, M., da Silva, G.J., 2013. Nfat and miR-25

cooperate to reactivate the transcription factor Hand2 in heart failure. Nature cell biology.

Dixelius, J., Mäkinen, T., Wirzenius, M., Karkkainen, M.J., Wernstedt, C., Alitalo, K., Claesson-Welsh, L., 2003. Ligand-induced vascular endothelial growth factor receptor-3 (VEGFR-3) heterodimerization with VEGFR-2 in primary lymphatic endothelial cells regulates tyrosine phosphorylation sites. Journal of Biological Chemistry 278, 40973-40979.

Donovan, J., Kordylewska, A., Jan, Y.N., Utset, M.F., 2002. Tetralogy of fallot and other congenital heart defects in Hey2 mutant mice. Curr Biol 12, 1605-1610.

Duband, J.L., Monier, F., Delannet, M., Newgreen, D., 1995. Epithelium-mesenchyme transition during neural crest development. Acta Anat (Basel) 154, 63-78.

Edwards, B.S., Ackermann, D.M., Lee, M.E., Reeder, G.S., Wold, L.E., Burnett, J.C., Jr., 1988. Identification of atrial natriuretic factor within ventricular tissue in hamsters and humans with congestive heart failure. J Clin Invest 81, 82-86.

Espira, L., Lamoureux, L., Jones, S.C., Gerard, R.D., Dixon, I.M., Czubryt, M.P., 2009. The basic helix-loop-helix transcription factor scleraxis regulates fibroblast collagen synthesis. J Mol Cell Cardiol 47, 188-195.

Feiner, L., Webber, A.L., Brown, C.B., Lu, M.M., Jia, L., Feinstein, P., Mombaerts, P., Epstein, J.A., Raper, J.A., 2001. Targeted disruption of semaphorin 3C leads to persistent truncus arteriosus and aortic arch interruption. Development 128, 3061-3070.

Ferrara, N., Carver Moore, K., Chen, H., Dowd, M., Lu, L., O'Shea, K.S., Powell Braxton, L., Hillan, K.J., Moore, M.W., 1996. Heterozygous embryonic lethality induced by targeted inactivation of the VEGF gene.

Ferrara, N., Gerber, H.-P., LeCouter, J., 2003. The biology of VEGF and its receptors. Nature medicine 9, 669-676.

Firulli, A.B., McFadden, D.G., Lin, Q., Srivastava, D., Olson, E.N., 1998. Heart and extra-embryonic mesodermal defects in mouse embryos lacking the bHLH transcription factor Hand1. Nat Genet 18, 266-270.

Firulli, B.A., Hadzic, D.B., McDaid, J.R., Firulli, A.B., 2000. The basic helix-loop-helix transcription factors dHAND and eHAND exhibit dimerization characteristics that suggest complex regulation of function. J Biol Chem 275, 33567-33573.

Firulli, B.A., Howard, M.J., McDaid, J.R., McIlreavey, L., Dionne, K.M., Centonze, V.E., Cserjesi, P., Virshup, D.M., Firulli, A.B., 2003. PKA, PKC, and the protein

phosphatase 2A influence HAND factor function: a mechanism for tissue-specific transcriptional regulation. Mol Cell 12, 1225-1237.

Firulli, B.A., Krawchuk, D., Centonze, V.E., Vargesson, N., Virshup, D.M., Conway, S.J., Cserjesi, P., Laufer, E., Firulli, A.B., 2005. Altered Twist1 and Hand2 dimerization is associated with Saethre-Chotzen syndrome and limb abnormalities. Nat Genet 37, 373-381.

Firulli, B.A., Redick, B.A., Conway, S.J., Firulli, A.B., 2007. Mutations within helix I of Twist1 result in distinct limb defects and variation of DNA binding affinities. J Biol Chem 282, 27536-27546.

François, M., Caprini, A., Hosking, B., Orsenigo, F., Wilhelm, D., Browne, C., Paavonen, K., Karnezis, T., Shayan, R., Downes, M., 2008. Sox18 induces development of the lymphatic vasculature in mice. Nature 456, 643-647.

Frensing, T., Kaltschmidt, C., Schmitt-John, T., 2008. Characterization of a neuregulin-1 gene promoter: positive regulation of type I isoforms by NF-kappaB. Biochim Biophys Acta 1779, 139-144.

Fuchtbauer, E.M., 1995. Expression of M-twist during postimplantation development of the mouse. Dev Dyn 204, 316-322.

Fung, M.M., Viveros, O.H., O'Connor, D.T., 2008. Diseases of the adrenal medulla. Acta Physiol (Oxf) 192, 325-335.

Gao, Z., Kim, G.H., Mackinnon, A.C., Flagg, A.E., Bassett, B., Earley, J.U., Svensson, E.C., 2010. Ets1 is required for proper migration and differentiation of the cardiac neural crest. Development 137, 1543-1551.

Garavito-Aguilar, Z.V., Riley, H.E., Yelon, D., 2010. Hand2 ensures an appropriate environment for cardiac fusion by limiting Fibronectin function. Development 137, 3215-3220.

Garg, V., Yamagishi, C., Hu, T., Kathiriya, I.S., Yamagishi, H., Srivastava, D., 2001. Tbx1, a DiGeorge syndrome candidate gene, is regulated by sonic hedgehog during pharyngeal arch development. Dev Biol 235, 62-73.

Gerety, S.S., Anderson, D.J., 2002. Cardiovascular ephrinB2 function is essential for embryonic angiogenesis. Development 129, 1397-1410.

Gerhardt, H., Golding, M., Fruttiger, M., Ruhrberg, C., Lundkvist, A., Abramsson, A., Jeltsch, M., Mitchell, C., Alitalo, K., Shima, D., 2003. VEGF guides angiogenic sprouting utilizing endothelial tip cell filopodia. The Journal of cell biology 161, 1163-1177.

Gitelman, I., 2007. Evolution of the vertebrate twist family and synfunctionalization: a mechanism for differential gene loss through merging of expression domains. Mol Biol Evol 24, 1912-1925.

Go, A.S., Mozaffarian, D., Roger, V.L., Benjamin, E.J., Berry, J.D., Borden, W.B., Bravata, D.M., Dai, S., Ford, E.S., Fox, C.S., Franco, S., Fullerton, H.J., Gillespie, C., Hailpern, S.M., Heit, J.A., Howard, V.J., Huffman, M.D., Kissela, B.M., Kittner, S.J., Lackland, D.T., Lichtman, J.H., Lisabeth, L.D., Magid, D., Marcus, G.M., Marelli, A., Matchar, D.B., McGuire, D.K., Mohler, E.R., Moy, C.S., Mussolino, M.E., Nichol, G., Paynter, N.P., Schreiner, P.J., Sorlie, P.D., Stein, J., Turan, T.N., Virani, S.S., Wong, N.D., Woo, D., Turner, M.B., 2013. Heart disease and stroke statistics--2013 update: a report from the American Heart Association. Circulation 127, e6-e245.

Grego-Bessa, J., Luna-Zurita, L., del Monte, G., Bolos, V., Melgar, P., Arandilla, A., Garratt, A.N., Zang, H., Mukouyama, Y.S., Chen, H., Shou, W., Ballestar, E., Esteller, M., Rojas, A., Perez-Pomares, J.M., de la Pompa, J.L., 2007. Notch signaling is essential for ventricular chamber development. Dev Cell 12, 415-429.

Gross, J.B., Hanken, J., 2008. Review of fate-mapping studies of osteogenic cranial neural crest in vertebrates. Dev Biol 317, 389-400.

Gude, N.A., Emmanuel, G., Wu, W., Cottage, C.T., Fischer, K., Quijada, P., Muraski, J.A., Alvarez, R., Rubio, M., Schaefer, E., 2008. Activation of Notch-mediated protective signaling in the myocardium. Circulation research 102, 1025-1035.

Heisig, J., Weber, D., Englberger, E., Winkler, A., Kneitz, S., Sung, W.K., Wolf, E., Eilers, M., Wei, C.L., Gessler, M., 2012. Target gene analysis by microarrays and chromatin immunoprecipitation identifies HEY proteins as highly redundant bHLH repressors. PLoS Genet 8, e1002728.

Hellstrom, M., Phng, L.K., Hofmann, J.J., Wallgard, E., Coultas, L., Lindblom, P., Alva, J., Nilsson, A.K., Karlsson, L., Gaiano, N., Yoon, K., Rossant, J., Iruela-Arispe, M.L., Kalen, M., Gerhardt, H., Betsholtz, C., 2007. Dll4 signalling through Notch1 regulates formation of tip cells during angiogenesis. Nature 445, 776-780.

Hendershot, T.J., Liu, H., Clouthier, D.E., Shepherd, I.T., Coppola, E., Studer, M., Firulli, A.B., Pittman, D.L., Howard, M.J., 2008. Conditional deletion of Hand2 reveals critical functions in neurogenesis and cell type-specific gene expression for development of neural crest-derived noradrenergic sympathetic ganglion neurons. Dev Biol 319, 179-191.

Hendershot, T.J., Liu, H., Sarkar, A.A., Giovannucci, D.R., Clouthier, D.E., Abe, M., Howard, M.J., 2007. Expression of Hand2 is sufficient for neurogenesis and cell type-specific gene expression in the enteric nervous system. Dev Dyn 236, 93-105.

Herbert, S.P., Stainier, D.Y., 2011. Molecular control of endothelial cell behaviour during blood vessel morphogenesis. Nat Rev Mol Cell Biol 12, 551-564.

Heude, E., Bouhali, K., Kurihara, Y., Kurihara, H., Couly, G., Janvier, P., Levi, G., 2010. Jaw muscularization requires Dlx expression by cranial neural crest cells. Proc Natl Acad Sci U S A 107, 11441-11446.

High, F.A., Epstein, J.A., 2008. The multifaceted role of Notch in cardiac development and disease. Nature Reviews Genetics 9, 49-61.

Hirsch, M.R., Tiveron, M.C., Guillemot, F., Brunet, J.F., Goridis, C., 1998. Control of noradrenergic differentiation and Phox2a expression by MASH1 in the central and peripheral nervous system. Development 125, 599-608.

Hoek, K., Rimm, D.L., Williams, K.R., Zhao, H., Ariyan, S., Lin, A., Kluger, H.M., Berger, A.J., Cheng, E., Trombetta, E.S., Wu, T., Niinobe, M., Yoshikawa, K., Hannigan, G.E., Halaban, R., 2004. Expression profiling reveals novel pathways in the transformation of melanocytes to melanomas. Cancer Res 64, 5270-5282.

Holler, K.L., Hendershot, T.J., Troy, S.E., Vincentz, J.W., Firulli, A.B., Howard, M.J., 2010. Targeted deletion of Hand2 in cardiac neural crest-derived cells influences cardiac gene expression and outflow tract development. Dev Biol 341, 291-304.

Howard, T.D., Paznekas, W.A., Green, E.D., Chiang, L.C., Ma, N., Ortiz de Luna, R.I., Garcia Delgado, C., Gonzalez-Ramos, M., Kline, A.D., Jabs, E.W., 1997. Mutations in TWIST, a basic helix-loop-helix transcription factor, in Saethre-Chotzen syndrome. Nat Genet 15, 36-41.

Huang, X., Saint-Jeannet, J.P., 2004. Induction of the neural crest and the opportunities of life on the edge. Dev Biol 275, 1-11.

Hutson, M.R., Kirby, M.L., 2003. Neural crest and cardiovascular development: a 20-year perspective. Birth Defects Res C Embryo Today 69, 2-13.

Jiao, K., Langworthy, M., Batts, L., Brown, C.B., Moses, H.L., Baldwin, H.S., 2006. Tgfbeta signaling is required for atrioventricular cushion mesenchyme remodeling during in vivo cardiac development. Development 133, 4585-4593.

Jones, S., 2004. An overview of the basic helix-loop-helix proteins. GENOME BIOLOGY. 5, 226-226.

Kelly, R.G., 2005. Molecular inroads into the anterior heart field. Trends Cardiovasc Med 15, 51-56.

Kim, J.S., Viragh, S., Moorman, A.F., Anderson, R.H., Lamers, W.H., 2001. Development of the myocardium of the atrioventricular canal and the vestibular spine in the human heart. Circ Res 88, 395-402.

Kioussi, C., Briata, P., Baek, S.H., Rose, D.W., Hamblet, N.S., Herman, T., Ohgi, K.A., Lin, C., Gleiberman, A., Wang, J., Brault, V., Ruiz-Lozano, P., Nguyen, H.D., Kemler, R., Glass, C.K., Wynshaw-Boris, A., Rosenfeld, M.G., 2002. Identification of a Wnt/Dvl/bCatenin - Pitx2 pathway mediating cell-type-specific proliferation during development. Cell 111, 673-685.

Kirby, M.L., Gale, T.F., Stewart, D.E., 1983. Neural crest cells contribute to normal aorticopulmonary septation. Science 220, 1059-1061.

Kirby, M.L., Waldo, K.L., 1995. Neural crest and cardiovascular patterning. Circ Res 77, 211-215.

Kisanuki, Y.Y., Hammer, R.E., Miyazaki, J., Williams, S.C., Richardson, J.A., Yanagisawa, M., 2001. Tie2-Cre transgenic mice: a new model for endothelial cell-lineage analysis in vivo. Dev Biol 230, 230-242.

Kishi, T., 2012. Heart failure as an autonomic nervous system dysfunction. J Cardiol 59, 117-122.

Kokubo, H., Miyagawa-Tomita, S., Nakazawa, M., Saga, Y., Johnson, R.L., 2005. Mouse hesr1 and hesr2 genes are redundantly required to mediate Notch signaling in the developing cardiovascular system. Developmental Biology 278, 301-309.

Kolander, K.D., Holtz, M.L., Cossette, S.M., Duncan, S.A., Misra, R.P., 2014. Epicardial GATA factors regulate early coronary vascular plexus formation. Dev Biol 386, 204-215.

Komiyama, M., Ito, K., Shimada, Y., 1987. Origin and development of the epicardium in the mouse embryo. Anat Embryol (Berl) 176, 183-189.

Kurihara, Y., Kurihara, H., Oda, H., Maemura, K., Nagai, R., Ishikawa, T., Yazaki, Y., 1995. Aortic arch malformations and ventricular septal defect in mice deficient in endothelin-1. J Clin Invest 96, 293-300.

Kwee, L., Baldwin, H.S., Shen, H.M., Stewart, C.L., Buck, C., Buck, C.A., Labow, M.A., 1995. Defective development of the embryonic and extraembryonic circulatory systems in vascular cell adhesion molecule (VCAM-1) deficient mice. Development 121, 489-503.

Larrivee, B., Prahst, C., Gordon, E., del Toro, R., Mathivet, T., Duarte, A., Simons, M., Eichmann, A., 2012. ALK1 signaling inhibits angiogenesis by cooperating with the Notch pathway. Dev Cell 22, 489-500.

Leblanc, G.G., Landis, S.C., 1989. Differentiation of noradrenergic traits in the principal neurons and small intensely fluorescent cells of the parasympathetic sphenopalatine ganglion of the rat. Dev Biol 131, 44-59.

Lee, K.F., Simon, H., Chen, H., Bates, B., Hung, M.C., Hauser, C., 1995. Requirement for neuregulin receptor erbB2 in neural and cardiac development. Nature 378, 394-398.

Lei, J., Howard, M.J., 2011. Targeted deletion of Hand2 in enteric neural precursor cells affects its functions in neurogenesis, neurotransmitter specification and gangliogenesis, causing functional aganglionosis. Development 138, 4789-4800.

Leiss, M., Beckmann, K., Giros, A., Costell, M., Fassler, R., 2008. The role of integrin binding sites in fibronectin matrix assembly in vivo. Curr Opin Cell Biol 20, 502-507.

Levay, A.K., Peacock, J.D., Lu, Y., Koch, M., Hinton, R.B., Jr., Kadler, K.E., Lincoln, J., 2008. Scleraxis is required for cell lineage differentiation and extracellular matrix remodeling during murine heart valve formation in vivo. Circ Res 103, 948-956.

Lie-Venema, H., van den Akker, N.M., Bax, N.A., Winter, E.M., Maas, S., Kekarainen, T., Hoeben, R.C., deRuiter, M.C., Poelmann, R.E., Gittenberger-de Groot, A.C., 2007. Origin, fate, and function of epicardium-derived cells (EPDCs) in normal and abnormal cardiac development. ScientificWorldJournal 7, 1777-1798.

Lindsley, A., Snider, P., Zhou, H., Rogers, R., Wang, J., Olaopa, M., Kruzynska-Frejtag, A., Koushik, S.V., Lilly, B., Burch, J.B., Firulli, A.B., Conway, S.J., 2007. Identification and characterization of a novel Schwann and outflow tract endocardial cushion lineage-restricted periostin enhancer. Dev Biol 307, 340-355.

Liu, N., Barbosa, A.C., Chapman, S.L., Bezprozvannaya, S., Qi, X., Richardson, J.A., Yanagisawa, H., Olson, E.N., 2009. DNA binding-dependent and -independent functions of the Hand2 transcription factor during mouse embryogenesis. Development 136, 933-942.

Liu, W.D., Wang, H.W., Muguira, M., Breslin, M.B., Lan, M.S., 2006. INSM1 functions as a transcriptional repressor of the neuroD/beta2 gene through the recruitment of cyclin D1 and histone deacetylases. Biochem J 397, 169-177.

Liu, Y., Watanabe, H., Nifuji, A., Yamada, Y., Olson, E.N., Noda, M., 1997. Overexpression of a single helix-loop-helix-type transcription factor, scleraxis, enhances aggrecan gene expression in osteoblastic osteosarcoma ROS17/2.8 cells. J Biol Chem 272, 29880-29885.

Lucas, M.E., Muller, F., Rudiger, R., Henion, P.D., Rohrer, H., 2006. The bHLH transcription factor hand2 is essential for noradrenergic differentiation of sympathetic neurons. Development 133, 4015-4024.

Lyons, G.E., 1996. Vertebrate heart development. Curr Opin Genet Dev 6, 454-460.

Ma, L., Lu, M.F., Schwartz, R.J., Martin, J.F., 2005. Bmp2 is essential for cardiac cushion epithelial-mesenchymal transition and myocardial patterning. Development 132, 5601-5611.

Malmejac, J., 1964. Activity of the Adrenal Medulla and its Regulation. Physiol Rev 44, 186-218.

Malumbres, M., Barbacid, M., 2005. Mammalian cyclin-dependent kinases. Trends Biochem Sci 30, 630-641.

Martinsen, B.J., Bronner-Fraser, M., 1998. Neural crest specification regulated by the helix-loop-helix repressor Id2. Science 281, 988-991.

Massari, M.E., Murre, C., 2000. Helix-loop-helix proteins: regulators of transcription in eucaryotic organisms. Mol Cell Biol 20, 429-440.

McFadden, D.G., Barbosa, A.C., Richardson, J.A., Schneider, M.D., Srivastava, D., Olson, E.N., 2005. The Hand1 and Hand2 transcription factors regulate expansion of the embryonic cardiac ventricles in a gene dosage-dependent manner. Development 132, 189-201.

Meyer, D., Birchmeier, C., 1995. Multiple essential functions of neuregulin in development. Nature 378, 386-390.

Meyer, D., Yamaai, T., Garratt, A., Riethmacher-Sonnenberg, E., Kane, D., Theill, L.E., Birchmeier, C., 1997. Isoform-specific expression and function of neuregulin. Development 124, 3575-3586.

Miquerol, L., Langille, B.L., Nagy, A., 2000. Embryonic development is disrupted by modest increases in vascular endothelial growth factor gene expression. Development 127, 3941-3946.

Molin, D.G., DeRuiter, M.C., Wisse, L.J., Azhar, M., Doetschman, T., Poelmann, R.E., Gittenberger-de Groot, A.C., 2002. Altered apoptosis pattern during pharyngeal arch artery remodelling is associated with aortic arch malformations in Tgfbeta2 knock-out mice. Cardiovasc Res 56, 312-322.

Monvoisin, A., Alva, J.A., Hofmann, J.J., Zovein, A.C., Lane, T.F., Iruela-Arispe, M.L., 2006. VE-cadherin-CreERT2 transgenic mouse: A model for inducible recombination in the endothelium. Developmental dynamics 235, 3413-3422.

Morabito, C.J., Dettman, R.W., Kattan, J., Collier, J.M., Bristow, J., 2001. Positive and negative regulation of epicardial-mesenchymal transformation during avian heart development. Dev Biol 234, 204-215.

Morikawa, Y., Cserjesi, P., 2004. Extra-embryonic vasculature development is regulated by the transcription factor HAND1. Development 131, 2195-2204.

Morikawa, Y., Cserjesi, P., 2008. Cardiac neural crest expression of Hand2 regulates outflow and second heart field development. Circ Res 103, 1422-1429.

Morikawa, Y., D'Autreaux, F., Gershon, M.D., Cserjesi, P., 2007. Hand2 determines the noradrenergic phenotype in the mouse sympathetic nervous system. Dev Biol 307, 114-126.

Morikawa, Y., Dai, Y.S., Hao, J., Bonin, C., Hwang, S., Cserjesi, P., 2005. The basic helix-loop-helix factor Hand 2 regulates autonomic nervous system development. Dev Dyn 234, 613-621.

Nakajima, Y., 2010. Second lineage of heart forming region provides new understanding of conotruncal heart defects. Congenit Anom (Kyoto) 50, 8-14.

Nelms, B.L., Labosky, P.A., 2010. Transcriptional Control of Neural Crest Development, 2011/04/01 ed. Morgan & Claypool Life Sciences Publishers.

Øie, E., Sandberg, W.J., Ahmed, M.S., Yndestad, A., Lærum, O.D., Attramadal, H., Aukrust, P., Eiken, H.G., 2010. Activation of Notch signaling in cardiomyocytes during post-infarction remodeling. Scandinavian Cardiovascular Journal 44, 359-366.

Oka, C., Nakano, T., Wakeham, A., de la Pompa, J.L., Mori, C., Sakai, T., Okazaki, S., Kawaichi, M., Shiota, K., Mak, T.W., Honjo, T., 1995. Disruption of the mouse RBP-J kappa gene results in early embryonic death. Development 121, 3291-3301.

Olaopa, M., Zhou, H.M., Snider, P., Wang, J., Schwartz, R.J., Moon, A.M., Conway, S.J., 2011. Pax3 is essential for normal cardiac neural crest

morphogenesis but is not required during migration nor outflow tract septation. Dev Biol 356, 308-322.

Olson, E.N., Srivastava, D., 1996. Molecular pathways controlling heart development. Science 272, 671-676.

Oshima, A., Tanabe, H., Yan, T., Lowe, G.N., Glackin, C.A., Kudo, A., 2002. A novel mechanism for the regulation of osteoblast differentiation: transcription of periostin, a member of the fasciclin I family, is regulated by the bHLH transcription factor, twist. J Cell Biochem 86, 792-804.

Pae, S.H., Dokic, D., Dettman, R.W., 2008. Communication between integrin receptors facilitates epicardial cell adhesion and matrix organization. Dev Dyn 237, 962-978.

Peacock, J.D., Lu, Y., Koch, M., Kadler, K.E., Lincoln, J., 2008. Temporal and spatial expression of collagens during murine atrioventricular heart valve development and maintenance. Dev Dyn 237, 3051-3058.

Pellegrino, M.J., Parrish, D.C., Zigmond, R.E., Habecker, B.A., 2011. Cytokines inhibit norepinephrine transporter expression by decreasing Hand2. Mol Cell Neurosci 46, 671-680.

Perez-Pomares, J.M., Carmona, R., Gonzalez-Iriarte, M., Atencia, G., Wessels, A., Munoz-Chapuli, R., 2002. Origin of coronary endothelial cells from epicardial mesothelium in avian embryos. Int J Dev Biol 46, 1005-1013.

Pinco, K.A., Liu, S., Yang, J.T., 2001. alpha4 integrin is expressed in a subset of cranial neural crest cells and in epicardial progenitor cells during early mouse development. Mech Dev 100, 99-103.

Poelmann, R.E., Gittenberger-de Groot, A.C., 1999. A subpopulation of apoptosis-prone cardiac neural crest cells targets to the venous pole: multiple functions in heart development? Dev Biol 207, 271-286.

Prall, O.W., Menon, M.K., Solloway, M.J., Watanabe, Y., Zaffran, S., Bajolle, F., Biben, C., McBride, J.J., Robertson, B.R., Chaulet, H., Stennard, F.A., Wise, N., Schaft, D., Wolstein, O., Furtado, M.B., Shiratori, H., Chien, K.R., Hamada, H., Black, B.L., Saga, Y., Robertson, E.J., Buckingham, M.E., Harvey, R.P., 2007. An Nkx2-5/Bmp2/Smad1 negative feedback loop controls heart progenitor specification and proliferation. Cell 128, 947-959.

Qiu, G.R., Gong, L.G., He, G., Xu, X.Y., Xin, N., Sun, G.F., Yuan, Y.H., Sun, K.L., 2006. Association of the GLI gene with ventricular septal defect after the susceptibility gene being narrowed to 3.56 cM in 12q13. Chin Med J (Engl) 119, 267-274.

Ream, M.A., Chandra, R., Peavey, M., Ray, A.M., Roffler-Tarlov, S., Kim, H.G., Wetsel, W.C., Rockman, H.A., Chikaraishi, D.M., 2008. High oxygen prevents fetal lethality due to lack of catecholamines. Am J Physiol Regul Integr Comp Physiol 295, R942-953.

Reaume, A.G., de Sousa, P.A., Kulkarni, S., Langille, B.L., Zhu, D., Davies, T.C., Juneja, S.C., Kidder, G.M., Rossant, J., 1995. Cardiac malformation in neonatal mice lacking connexin43. Science 267, 1831-1834.

Red-Horse, K., Ueno, H., Weissman, I.L., Krasnow, M.A., 2010. Coronary arteries form by developmental reprogramming of venous cells. Nature 464, 549-553.

Riley, P., Anson-Cartwright, L., Cross, J.C., 1998. The Hand1 bHLH transcription factor is essential for placentation and cardiac morphogenesis. Nat Genet 18, 271-275.

Rychlik, J.L., Gerbasi, V., Lewis, E.J., 2003. The interaction between dHAND and Arix at the dopamine beta-hydroxylase promoter region is independent of direct dHAND binding to DNA. J Biol Chem 278, 49652-49660.

Saito, D., Takase, Y., Murai, H., Takahashi, Y., 2012. The dorsal aorta initiates a molecular cascade that instructs sympatho-adrenal specification. Science 336, 1578-1581.

Sarkozy, A., Conti, E., D'Agostino, R., Digilio, M.C., Formigari, R., Picchio, F., Marino, B., Pizzuti, A., Dallapiccola, B., 2005. ZFPM2/FOG2 and HEY2 genes analysis in nonsyndromic tricuspid atresia. Am J Med Genet A 133A, 68-70.

Schmidt, M., Lin, S., Pape, M., Ernsberger, U., Stanke, M., Kobayashi, K., Howard, M.J., Rohrer, H., 2009. The bHLH transcription factor Hand2 is essential for the maintenance of noradrenergic properties in differentiated sympathetic neurons. Dev Biol 329, 191-200.

Shawber, C.J., Funahashi, Y., Francisco, E., Vorontchikhina, M., Kitamura, Y., Stowell, S.A., Borisenko, V., Feirt, N., Podgrabinska, S., Shiraishi, K., Chawengsaksophak, K., Rossant, J., Accili, D., Skobe, M., Kitajewski, J., 2007. Notch alters VEGF responsiveness in human and murine endothelial cells by direct regulation of VEGFR-3 expression. J Clin Invest 117, 3369-3382.

Shelton, E.L., Yutzey, K.E., 2008. Twist1 function in endocardial cushion cell proliferation, migration, and differentiation during heart valve development. Dev Biol 317, 282-295.

Shen, W.H., Chen, Z., Shi, S., Chen, H., Zhu, W., Penner, A., Bu, G., Li, W., Boyle, D.W., Rubart, M., Field, L.J., Abraham, R., Liechty, E.A., Shou, W., 2008. Cardiac restricted overexpression of kinase-dead mammalian target of rapamycin (mTOR) mutant impairs the mTOR-mediated signaling and cardiac function. J Biol Chem 283, 13842-13849.

Singh, M.K., Nicolas, E., Gherraby, W., Dadke, D., Lessin, S., Golemis, E.A., 2007. HEI10 negatively regulates cell invasion by inhibiting cyclin B/Cdk1 and other promotility proteins. Oncogene 26, 4825-4832.

Smit, M.A., Peeper, D.S., 2008. Deregulating EMT and senescence: double impact by a single twist. Cancer Cell 14, 5-7.

Smith, C.L., Baek, S.T., Sung, C.Y., Tallquist, M.D., 2011. Epicardial-derived cell epithelial-to-mesenchymal transition and fate specification require PDGF receptor signaling. Circ Res 108, e15-26.

Smith, T.K., Bader, D.M., 2007. Signals from both sides: Control of cardiac development by the endocardium and epicardium. Seminars in Cell & Developmental Biology 18, 84-89.

Snider, P., Olaopa, M., Firulli, A.B., Conway, S.J., 2007. Cardiovascular development and the colonizing cardiac neural crest lineage. ScientificWorldJournal 7, 1090-1113.

Sock, E., Rettig, S.D., Enderich, J., Bosl, M.R., Tamm, E.R., Wegner, M., 2004. Gene targeting reveals a widespread role for the high-mobility-group transcription factor Sox11 in tissue remodeling. Mol Cell Biol 24, 6635-6644.

Soker, S., Takashima, S., Miao, H.Q., Neufeld, G., Klagsbrun, M., 1998. Neuropilin-1 is expressed by endothelial and tumor cells as an isoform-specific receptor for vascular endothelial growth factor. Cell 92, 735-745.

Sottile, J., Hocking, D.C., Swiatek, P.J., 1998. Fibronectin matrix assembly enhances adhesion-dependent cell growth. J Cell Sci 111 (Pt 19), 2933-2943.

Stoller, J.Z., Epstein, J.A., 2005. Cardiac neural crest. Semin Cell Dev Biol 16, 704-715.

Sucov, H.M., 1998. Molecular insights into cardiac development. Annu Rev Physiol 60, 287-308.

Suzuki, N., Hardebo, J.E., Kahrstrom, J., Owman, C., 1990. Selective electrical stimulation of postganglionic cerebrovascular parasympathetic nerve fibers originating from the sphenopalatine ganglion enhances cortical blood flow in the rat. J Cereb Blood Flow Metab 10, 383-391.

Svensson, E.C., Huggins, G.S., Lin, H., Clendenin, C., Jiang, F., Tufts, R., Dardik, F.B., Leiden, J.M., 2000. A syndrome of tricuspid atresia in mice with a targeted mutation of the gene encoding Fog-2. Nat Genet 25, 353-356.

Tammela, T., Zarkada, G., Wallgard, E., Murtomaki, A., Suchting, S., Wirzenius, M., Waltari, M., Hellstrom, M., Schomber, T., Peltonen, R., Freitas, C., Duarte, A., Isoniemi, H., Laakkonen, P., Christofori, G., Yla-Herttuala, S., Shibuya, M., Pytowski, B., Eichmann, A., Betsholtz, C., Alitalo, K., 2008. Blocking VEGFR-3 suppresses angiogenic sprouting and vascular network formation. Nature 454, 656-660.

Tapanes-Castillo, A., Baylies, M.K., 2004. Notch signaling patterns Drosophila mesodermal segments by regulating the bHLH transcription factor twist. Development 131, 2359-2372.

te Welscher, P., Fernandez-Teran, M., Ros, M.A., Zeller, R., 2002. Mutual genetic antagonism involving GLI3 and dHAND prepatterns the vertebrate limb bud mesenchyme prior to SHH signaling. Genes Dev 16, 421-426.

Ter Laan, M., van Dijk, J.M., Elting, J.W., Staal, M.J., Absalom, A.R., 2013. Sympathetic regulation of cerebral blood flow in humans: a review. Br J Anaesth.

Thomas, S.A., Matsumoto, A.M., Palmiter, R.D., 1995. Noradrenaline is essential for mouse fetal development. Nature 374, 643-646.

Tian, H., Hammer, R.E., Matsumoto, A.M., Russell, D.W., McKnight, S.L., 1998. The hypoxia-responsive transcription factor EPAS1 is essential for catecholamine homeostasis and protection against heart failure during embryonic development. Genes Dev 12, 3320-3324.

Tian, X., Hu, T., Zhang, H., He, L., Huang, X., Liu, Q., Yu, W., Yang, Z., Zhang, Z., Zhong, T.P., Yang, X., Yan, Y., Baldini, A., Sun, Y., Lu, J., Schwartz, R.J., Evans, S.M., Gittenberger-de Groot, A.C., Red-Horse, K., Zhou, B., 2013. Subepicardial endothelial cells invade the embryonic ventricle wall to form coronary arteries. Cell Res 23, 1075-1090.

Timmerman, L.A., Grego-Bessa, J., Raya, A., Bertran, E., Perez-Pomares, J.M., Diez, J., Aranda, S., Palomo, S., McCormick, F., Izpisua-Belmonte, J.C., de la Pompa, J.L., 2004. Notch promotes epithelial-mesenchymal transition during cardiac development and oncogenic transformation. Genes Dev 18, 99-115.

Todorovic, V., Finnegan, E., Freyer, L., Zilberberg, L., Ota, M., Rifkin, D.B., 2011. Long form of latent TGF-beta binding protein 1 (Ltbp1L) regulates cardiac valve development. Dev Dyn 240, 176-187.

Trinh, L.A., Stainier, D.Y., 2004. Fibronectin regulates epithelial organization during myocardial migration in zebrafish. Dev Cell 6, 371-382.

Trinh, L.A., Yelon, D., Stainier, D.Y., 2005. Hand2 regulates epithelial formation during myocardial diferentiation. Curr Biol 15, 441-446.

Tsuchihashi, T., Maeda, J., Shin, C.H., Ivey, K.N., Black, B.L., Olson, E.N., Yamagishi, H., Srivastava, D., 2011. Hand2 function in second heart field progenitors is essential for cardiogenesis. Dev Biol 351, 62-69.

Van Mierop, L.H., Kutsche, L.M., 1986. Cardiovascular anomalies in DiGeorge syndrome and importance of neural crest as a possible pathogenetic factor. Am J Cardiol 58, 133-137.

Veikkola, T., Jussila, L., Makinen, T., Karpanen, T., Jeltsch, M., Petrova, T.V., Kubo, H., Thurston, G., McDonald, D.M., Achen, M.G., 2001. Signalling via vascular endothelial growth factor receptor-3 is sufficient for lymphangiogenesis in transgenic mice. The EMBO journal 20, 1223-1231.

Villa, N., Walker, L., Lindsell, C.E., Gasson, J., Iruela-Arispe, M.L., Weinmaster, G., 2001. Vascular expression of Notch pathway receptors and ligands is restricted to arterial vessels. Mech Dev 108, 161-164.

Vincent, S.D., Buckingham, M.E., 2010. How to make a heart: the origin and regulation of cardiac progenitor cells. Curr Top Dev Biol 90, 1-41.

Vincentz, J.W., Barnes, R.M., Firulli, A.B., 2011. Hand factors as regulators of cardiac morphogenesis and implications for congenital heart defects. Birth Defects Res A Clin Mol Teratol 91, 485-494.

Vincentz, J.W., Barnes, R.M., Rodgers, R., Firulli, B.A., Conway, S.J., Firulli, A.B., 2008. An absence of Twist1 results in aberrant cardiac neural crest morphogenesis. Dev Biol 320, 131-139.

Vincentz, J.W., Firulli, B.A., Lin, A., Spicer, D.B., Howard, M.J., Firulli, A.B., 2013. Twist1 controls a cell-specification switch governing cell fate decisions within the cardiac neural crest. PLoS Genet 9, e1003405.

Vincentz, J.W., VanDusen, N.J., Fleming, A.B., Rubart, M., Firulli, B.A., Howard, M.J., Firulli, A.B., 2012. A Phox2- and Hand2-dependent Hand1 cis-regulatory element reveals a unique gene dosage requirement for Hand2 during sympathetic neurogenesis. J Neurosci 32, 2110-2120.

Wang, X., Chan, A.K., Sham, M.H., Burns, A.J., Chan, W.Y., 2011. Analysis of the sacral neural crest cell contribution to the hindgut enteric nervous system in the mouse embryo. Gastroenterology 141, 992-1002 e1001-1006.

Washington Smoak, I., Byrd, N.A., Abu-Issa, R., Goddeeris, M.M., Anderson, R., Morris, J., Yamamura, K., Klingensmith, J., Meyers, E.N., 2005. Sonic hedgehog is required for cardiac outflow tract and neural crest cell development. Dev Biol 283, 357-372.

Wu, B., Zhang, Z., Lui, W., Chen, X., Wang, Y., Chamberlain, A.A., Moreno-Rodriguez, R.A., Markwald, R.R., O'Rourke, B.P., Sharp, D.J., Zheng, D., Lenz, J., Baldwin, H.S., Chang, C.P., Zhou, B., 2012. Endocardial cells form the coronary arteries by angiogenesis through myocardial-endocardial VEGF signaling. Cell 151, 1083-1096.

Wu, X., Howard, M.J., 2002. Transcripts encoding HAND genes are differentially expressed and regulated by BMP4 and GDNF in developing avian gut. Gene Expr 10, 279-293.

Wythe, J.D., Dang, L.T., Devine, W.P., Boudreau, E., Artap, S.T., He, D., Schachterle, W., Stainier, D.Y., Oettgen, P., Black, B.L., Bruneau, B.G., Fish, J.E., 2013. ETS Factors Regulate Vegf-Dependent Arterial Specification. Dev Cell 26, 45-58.

Xu, H., Firulli, A.B., Zhang, X., Howard, M.J., 2003. HAND2 synergistically enhances transcription of dopamine-beta-hydroxylase in the presence of Phox2a. Dev Biol 262, 183-193.

Yamagishi, H., Olson, E.N., Srivastava, D., 2000. The basic helix-loop-helix transcription factor, dHAND, is required for vascular development. J Clin Invest 105, 261-270.

Yang, J.T., Rayburn, H., Hynes, R.O., 1995. Cell adhesion events mediated by alpha 4 integrins are essential in placental and cardiac development. Development 121, 549-560.

Yelbuz, T.M., Waldo, K.L., Kumiski, D.H., Stadt, H.A., Wolfe, R.R., Leatherbury, L., Kirby, M.L., 2002. Shortened outflow tract leads to altered cardiac looping after neural crest ablation. Circulation 106, 504-510.

Yin, C., Kikuchi, K., Hochgreb, T., Poss, K.D., Stainier, D.Y., 2010. Hand2 regulates extracellular matrix remodeling essential for gut-looping morphogenesis in zebrafish. Dev Cell 18, 973-984.

Zhang, B., Pu, W.T., 2013. The mysterious origins of coronary vessels. Cell Res 23, 1063-1064.

Zhou, B., Cron, R.Q., Wu, B., Genin, A., Wang, Z., Liu, S., Robson, P., Baldwin, H.S., 2002. Regulation of the murine Nfatc1 gene by NFATc2. J Biol Chem 277, 10704-10711.

Zhou, B., Ma, Q., Rajagopal, S., Wu, S.M., Domian, I., Rivera-Feliciano, J., Jiang, D., von Gise, A., Ikeda, S., Chien, K.R., Pu, W.T., 2008. Epicardial progenitors contribute to the cardiomyocyte lineage in the developing heart. Nature 454, 109-113.

Zhou, B., von Gise, A., Ma, Q., Hu, Y.W., Pu, W.T., 2010. Genetic fate mapping demonstrates contribution of epicardium-derived cells to the annulus fibrosis of the mammalian heart. Dev Biol 338, 251-261.

CURRICULUM VITAE

Nathan J. VanDusen

Education

2005-2009	Ferris State University, B.S. Biotechnology
2009-2014	Indiana University, Ph.D. Medical and Molecular Genetics

Research and Training Experience

05/08 – 07/08	Research Experience for Undergraduates (REU) intern in the laboratory of Dr. Dale Ramsden, Department of Biochemistry and Biophysics, Lineberger Comprehensive Cancer Center, University of North Carolina at Chapel Hill
05/09 – 08/09	Technician in the laboratory of Dr. Ken Cornetta, Department of Medical and Molecular Genetics, Indiana University, Indianapolis
10/09 – 12/09	Graduate student rotation in the laboratory of Dr. Angelo Cardoso, Department of Pediatrics, Indiana University, Indianapolis
03/10 – 05/10	Graduate student rotation in the laboratory of Dr. Simon Conway, Department of Pediatrics, Wells Center for Pediatric Research, Indiana University, Indianapolis
05/10 – 08/14	Graduate student in the laboratory of Dr. Anthony Firulli, Department of Pediatrics, Wells Center for Pediatric Research, Indiana University, Indianapolis

Honors, Awards, Fellowships

2005 – 2009	Kelso Battle Scholarship
2005 – 2009	Honors Residential Life Scholarship
2005 – 2009	Woodbridge N. Ferris President's Scholarship
2006 – 2009	FSU Dean's Ability Based Biotechnology Scholarship
2009	Indiana University Travel Fellowship
2012 – 2014	American Heart Association Predoctoral Fellowship *Endocardial Dysfunction Causes Tricuspid Atresia, as Revealed through Conditional Ablation of Hand2*

Conferences Attended

2008	University of North Carolina Molecular Biosciences REU Symposium
2008	Van Andel Institute's West Michigan Regional Undergraduate Science Research Conference.

2013	Gave platform presentation at Weinstein Cardiovascular Development Conference and was a Travel Award recipient. *Endocardial Loss of Hand2 Function Disrupts Notch Signaling Causing Hypotrabeculation and Tricuspid Atresia*
2014	Gave platform presentation at Weinstein Cardiovascular Development Conference. *Inhibition of Notch Signaling by Endocardial Ablation of Hand2 Disrupts Coronary Angiogenesis*

Memberships

2005 – 2009	Delta Nu Alpha (professional biotechnology fraternity), president 2008/2009
2010 – 2014	American Association for the Advancement of Science (AAAS)/Science Program for Excellence in Science
2012	American Heart Association

Publications

Barnes RM, Firulli BA, **VanDusen NJ**, Morikawa Y, Conway SJ, Cserjesi P, Vincentz JW, Firulli AB. Hand2 loss-of-function in hand1-expressing cells reveals distinct roles in epicardial and coronary vessel development. Circulation Research. 2011;108:940-949

Vincentz JW, **VanDusen NJ**, Fleming AB, Rubart M, Firulli BA, Howard MJ, Firulli AB. A phox2- and hand2-dependent hand1 cis-regulatory element reveals a unique gene dosage requirement for hand2 during sympathetic neurogenesis. Journal of Neuroscience. 2012;32:2110-2120

VanDusen NJ, Firulli AB. Twist factor regulation of non-cardiomyocyte cell lineages in the developing heart. Differentiation. 2012;84:79-88

Chen H, Zhang W, Sun X, Yoshimoto M, Chen Z, Zhu W, Liu J, Shen Y, Yong W, Li D, Zhang J, Lin Y, Li B, **VanDusen NJ**, Snider P, Schwartz RJ, Conway SJ, Field LJ, Yoder MC, Firulli AB, Carlesso N, Towbin JA, Shou W. Fkbp1a controls ventricular myocardium trabeculation and compaction by regulating endocardial notch1 activity. Development. 2013;140:1946-1957

VanDusen NJ, Vincentz JW, Firulli BA, Howard MJ, Rubart M, Firulli AB. Loss of Hand2 in a population of Periostin lineage cells results in pronounced bradycardia and neonatal death. Developmental Biology. 2014;388:149-158

VanDusen NJ, Vincentz JW, Firulli BA, Zhou B, Grego-Bessa J, de la Pompa JL, Shou W, Firulli AB. Endocardial Loss of Hand2 Function Disrupts Notch

Signaling Causing Hypotrabeculation, Tricuspid Atresia, and Precocious Coronary Development. Manuscript in preparation for Developmental Cell.